INTELLIGENT PLANNING FOR ROBOTIC DISASSEMBLY

by

Soran Parsa

A thesis submitted to
The University of Birmingham
for the degree of
DOCTOR OF PHILOSOPHY

Department of Mechanical Engineering
School of Engineering
College of Engineering and Physical Sciences
The University of Birmingham
September 2020

UNIVERSITY OF
BIRMINGHAM

University of Birmingham Research Archive

e-theses repository

This unpublished thesis/dissertation is copyright of the author and/or third parties. The intellectual property rights of the author or third parties in respect of this work are as defined by The Copyright Designs and Patents Act 1988 or as modified by any successor legislation.

Any use made of information contained in this thesis/dissertation must be in accordance with that legislation and must be properly acknowledged. Further distribution or reproduction in any format is prohibited without the permission of the copyright holder.

Abstract

Environmental concerns and demands, new legislations and rules, and material resource limitations have put pressure on production and manufacturing bodies to seek new strategies and method to meet those criteria. Remanufacturing and reusing of the End-Of-Life (EOL) products has shown a wide potential to deal with production waste and inefficiency. Manual disassembly is not efficient economically and the robotic systems are not reliable in dealing with complex disassembly operations as they have high-level uncertainty. In this research, the geometry of product components and difficulty of disassembly operations were analysed and based on that new optimisation parameters were defined to evaluate the disassemblability of the components. These include Disassembly Handling Index (DHI), Disassembly Operation Index (DOI) and Disassembly Demand Index (DDI). Genetic algorithm optimisation method was modified to find a near-optimal solution. The results using real case study products based on the proposed method shows minimum 10% improvement in manual disassembly time compare with conventional sequence planning methods. In addition, a mathematical model for peg-out-hole disassembly operation in a static equilibrium was developed to determine the relation between peg's depth, and peg and hole diameter mathematically. Then, force/torque sensor mounter on a TM robot arm was employed to produce force and torque maps for peg-out-hole operation experimentally. The maps were analysed using redundancy method to estimate the peg and hole relative position. The results show the average estimation error using proposed method is 6% which can reliable for peg-out-hole operation. Finally, a disassembly planning method based on human-robot collaboration is proposed. This method employs the flexibility and

ability to deal with complex tasks of human, alongside the repeatability and accuracy of the robot. PROMETHEE II method was employed to evaluate disassembly priorities based on the Cleanability, Repairability, and Economy to target the product components based on the remanufacturability criteria. Human-robot collaboration characteristics were defined, and an algorithm was proposed to classify the disassembly task and allocate them to either human or robot. The model encoded using AND/OR method mathematically, and the genetic algorithm was employed to find a near-optimal solution for human-robot collaboration sequence planning. The results compared with Particle Swarm algorithm which shows 8.8% improvement in fitness value. Thus, the developments reported in this thesis have contributed to promoting the efficiency and reliability of the disassembly process as the key step of dealing with EOL products.

Acknowledgements

First and foremost, I want to express my gratitude to my supervisor Dr. Mozafar Saadat, for the amazing support on the project, whose attitude and guidance inspired me for this project. I appreciate all his contributions of time and efforts to make my PhD experience productive and stimulating. Everything represented in this thesis is the result of his guidance and efforts.

I would like to express my deepest appreciation to my second supervisor, Professor Duc Truong Pham, PI of AUTOREMAN project, who without his support the thesis would not have been possible. My gratitude extends to Dr Marco Castellani Whose feedbacks on my project reports helped me improving my research during this project.

The help from my colleagues and friends, Zebang Zhang, Dr Amir Hajiyavand, Dr Yongjing Wang, Ferhat Sadak and Marco Maddalena has been greatly appreciated. I would like to thank all members of the School of Engineering who have been a source of friendships as well as good advice and collaboration.

Finally, I would like to thank Dr Khamis Essa and Professor Farrokh Sassani for their valuable suggestions to enhance my thesis, and Dr Carol Kong for chairing my Viva examination.

Table of Contents

1. Chapter 1- Introduction 1
1.1. Background 1
1.2 Aim and objectives 6
1.3 Thesis outline 7
2. Chapter 2- Literature review 9
2.1 Introduction 9
2.2 Product disassembly representation 11
2.2.1 Graph-based representation 12
2.2.2 Petri Net 15
2.2.3 Matrix-based representation 17
2.2.4 Other methods 19
2.3 Search for optimum solution 20
2.3.1 Disassembly planning 21
2.3.2 Optimisation algorithms 24
2.4 Selective disassembly planning 29
2.5 Automated disassembly planning 34
2.6 Cognitive robotics and collaborative disassembly 38
2.7 Summary 43
3. Chapter 3- Disassembly Planning Based on Disassemblability Characteristics of Product Components 47
3.1 Introduction 47
3.2 Methodology 48
3.2.1 Introducing new parameters for intelligent selective disassembly planning 48
3.2.2 Disassembly Handling Index 50
3.2.3 Disassembly operation Index 51
3.2.4 Disassembly Demand Index 52
3.2.5 Disassembly Cost Index 53
3.3 Improved genetic algorithm optimisation 55
3.3.1 Disassembly representation using Hybrid graph model 55
3.3.2 Disassembly Feasibility and constraint matrices 56
3.3.3 GA Parameters and operators 58
3.4 Case study and performance analysis 62
3.4.1 Case study 1: Turbocharger 62

3.4.2 Case study 2: Water pump 71
3.5 Conclusion 75
4. Chapter 4- Automated Peg-Out-Hole Disassembly planning Using Force/Torque Sensor 77
4.1 Introduction 77
4.2.1 Peg-out-hole mathematical model 78
4.2.2 Disassembly configuration 83
4.2.3 Force-Torque maps 88
4.3 Results and discussions 90
4.3.1 Force and torque maps analysing 92
4.3.2 contact state classification using EM-GMM 95
4.3.3 Position estimation using F/T maps 98
4.4 Conclusion 100
5. Chapter 5- Human-robot collaborative disassembly planning for a reliable and efficient disassembly process 102
5.1 Introduction 102
5.2 Methodology 103
5.2.1 Selective and targeted disassembly 103
5.2.2 Collaborative human-robot disassembly 107
5.2.3 Mathematical model and representation 112
5.2.4 Disassembly sequence optimization algorithm 115
5.3 Experiments and results 123
5.3.1 Validation of the task classification and allocation 123
5.3.2 case study 126
5.3.3 Performance analysis 129
5.4 Conclusion 134
6. Chapter 6- Conclusions 136
6.1 Conclusions 136
6.2 Contributions 140
6.3 Future Works 141
References 143
Apendix A. Publications by the author 157

List of Figures

Figure 1.1 Global resources extraction and their changes between 1980 and 2008 [1]..... 2
Figure 1.2 Traditional manufacturing process [1]. 3
Figure 1.3 product life cycle and each methods that could be used to reduce environment impact [6]..... 4
Figure 1.4 Relationship between disassembly time, disassembly cost and recovery prof-its [10] 5
Figure 1.5 Relationships between overall aim and objective..... 7
Figure 2.1 Disassembly process types and methods 9
Figure 2.2 General steps of disassembly sequence planning [19] 11
Figure 2.3 Different graph representation types. 2.3a, shows a basic graph where R node denotes the main EOL product and Si denotes the components and sub-assemblies. 2.3b, represents a network graph that relationships and constraints are shown using arrows and arcs [21]..... 12
Figure 2.4 Graph-based directed disassembly network where the optimum solution can be seen in bold direction. 14
Figure 2.5 A typical Petri net disassembly model representation where c is the disassembly operation costs and w is a weight function. 16
Figure 2.6 Matrix representation. 2.6a, shows the basic component of a ball pen and 2.6b, represents a matrix-based method, where uses a three-element array representing interference in X, Y, and Z direction. 17
Figure 2.7 Value functions for expected component value based on its age for a typical solenoid [81]. 23
Figure 2.8 the number of documents on evolutionary computation in scheduling problems [85]. 25
Figure 2.9 General block diagram of genetic algorithm [107]. 28
Figure 2.10 Selective disassembly planning steps [112]. 31
Figure 2.11 A block diagram of a typical cognitive robotic structure [146]. 40
Figure 3.1. (a) BorgWarner turbocharger (b) Turbocharger CAD model (c) Turbocharger exploded view..... 63
Figure 3.2 Flow chart of the proposed model. 64
Figure 3.3 Hybrid graph model for turbocharger..... 65
Figure 3.4 a) Calculation time under different population b) Average fitness values under different population number. 68
Figure 3.5 a) Average fitness values under different generations b) Running time under different generation number..... 68
Figure 3.6 a) Average fitness values under different probability b) Running time under different probability. 69
Figure 3.7 Disassembled components of the turbocharge. 71
Figure 3.8 a) Water pump b) Disassembled components c) Exploded view. 72
Figure 3.9 Average fitness values under different generations. 74
Figure 4.1 Peg-Out-Hole disassembly operation steps. 79

Figure 4.2 Possible peg and hole contact states and their force and torque analysis: (a) line contact state; (b) one-point contact type one; (c) one-point contact type two; (d) two-point contact state. 80
Figure 4.3 θtp with respect to the peg's depth for D=31 and d=30 83
Figure 4.4 The robotic peg-out-hole disassembly system set up. 85
Figure 4.5 Data collection strategies; a) one-point contact state type one, b) one-point contact state type two, c) two-point contact state 86
Figure 4.6 One-point contact state type one maps: (a) experimentally generated map; (b) Redundancy Map. 91
Figure 4.7 One-point contact state type two maps: (a) experimentally generated map; (b) Redundancy Map. 92
Figure 4.8 Two-point contact state maps: (a) experimentally generated map; (b) Redundancy Map. 92
Figure 4.9 Error estimation for maps with different QFM. 95
Figure 4.10 All possible peg and hole contact states. 96
Figure 4.11 Block diagram of position and orientation estimation of peg and hole using F/T sensor information. 99
Figure 4.12 (a) Mean Pz estimated using proposed method compared to robot reading; (b) Mean Ry estimated using proposed method compared to robot reading. 100
Figure 5.1 Human-robot collaborative disassembly workcell 107
Figure 5.2 Different collaboration classes based on the autonomy parameter level 109
Figure 5.3 The flowchart for classifying and assignment of disassembly operations 112
Figure 5.4 Reproduction operator examples, a) Crossover, b) Mutation, c) Cut-Paste, d) Break-Joint 123
Figure 5.5 Experimental robotic platform for peg-ot-hole disassembly operation. 124
Figure 5.6 Measured a) Forces and b) Torques for peg-out-hole disassembly operation. 126
Figure 5.7 a) CAD model and b) exploded view of the fuel pump 127
Figure 5.8 Flowchart and structure of the proposed method 128
Figure 5.9 a) Total produced generation to convergence for each population, b) Total computation time of algorithm with different population sizes. 130
Figure 5.10 Computational calculation time for different reproduction operator probabilities 131
Figure 5.11 AND/OR graph-based disassembly process representation of the fuel pump 132
Figure 5.12 a) fitness values of the proposed method in comparison with the PSA method, b) Computational calculation running time of the proposed method and PSA method 133
Figure 5.13 The Gantt chart of human-robot collaboration for the first solution. .. 134

List of Tables

Table 3.1. Disassembly Handling categories and scores [165]. 51
Table 3.2. Disassembly operation categories and scores [165]. 54
Table 3.3 The properties and required disassembly tasks for all individual components 63
Table 3.4 Disassembly handling analysis and Disassembly operation analysis for turbocharger. 67
Table 3.5 Final optimum disassembly process sequence based on the proposed method in this work. 69
Table 3.6 Optimum disassembly process sequence generated by conventional time-based method. 70
Table 3.7 Disassembly operations and process times for turbocharger. 70
Table 3.8 The properties and required disassembly tasks for all individual components. 72
Table 3.9 Disassembly handling analysis and Disassembly operation analysis for turbocharger 73
Table 3.10 Final optimum disassembly process sequence based on the proposed method in this work. 74
Table 3.11 Optimum sequence generated by time-based method 75
Table 3.12 Disassembly operations and process times for water pump. 75
Table 4.1 Dimensions and materials of the peg and hole. 84
Table 4.2 Different actions for labelling datasets. 88
Table 4.3 Force and torque indices for different contact state classes. 98
Table 5.1 Disassembly operation difficulty and complexity categories and scores 111
Table 5.2 Physical details of the peg and hole. 123
Table 5.3 The disassembly operation classification parameters and corresponding scores. 125
Table 5.4 The individual components and properties of the fuel pump 127
Table 5.5 Genetic algorithm's optimal parameters 131
Table 5.6 Three near-optimal solutions of disassembly sequences of the case study 134

List of Abbreviations and Symbols

ACO: Ant colony optimization

AI: Artificial Intelligence

CAD: Computer aided design

CPU: Central processing unit

Cr: Relation matrix

d: Peg diameter

D: Hole diameter

Dc: Constraint matrix

DC: Disposal cost

DCI: Disassembly Cost Index

DDI: Disassembly Demand Index

DHI: Disassembly Handling Index

DOI: Disassembly Operation Index

DOF: Degree of freedom

DP: Disassembly planning

DPI: Disassembly process index

DPN: Simplified Petri net representation

EM: Expectation maximization

EOL: End-of-life

EUP: Energy-using Products

EV: Electric vehicle

EVL: End-of-life vehicles

F/T: Force and torque

GA: Genetic algorithm

GHz: Giga hertz

GMM: Gaussian mixtures method

h: Peg depth

i: Number of components

IoT: Internet of Things

ISO: International standard organisation

k: number of classes

KR: Knowledge representation

LD: Level of demand

LRM: Laboratory for Responsible Manufacturing

m: Selected operations

n: Total number of operations

ncr: Initial population

Op: Operation

OT: Operation time

P: Part

PLA: Poly (lactic acid)

PHI: Part handling index

PN: petri Net

Pos: Position

PPX: Precedence preservative crossover

PSA: Particle Swarm algorithm

R&D: Research and design

RM: Redundancy Map

RoHS: Restriction of Hazardous Substances

TC: Tool change

WEEE: Waste electrical and electronic equipment

Chapter 1- Introduction

1.1. Background

In recent years, the generated waste of material and products at the end-of-life (EOL) is rapidly increasing and in many countries has become a challenging problem. In addition, decreasing new resources for industrial materials has increased production costs of new products and added to environmental problems. Figure 1.1 shows global material resource extraction and its changes between 1980 and 2008. The trend shows a 133% increase in metals extraction which mostly are used in manufacturing. As our planet resources are limited this trend results in a catastrophic impact on our environment [1]. Without new strategies and methods, especially in production and manufacturing due to the sharp increase in global population, humankind requires 2.1 times of our planet's resource by 2030 and this will grow to 2.9 by 2050 [2].

Furthermore, new legislation and environmental rules have forced the manufacturers to deal with EOL products more responsibly. For instance, regulations such as EVL, RoHS, WEEE and EUP state that manufacturers must responsibly collect, recycle, remanufacture, and reuse the EOL products in order to consider the environmental issues [3]. The main motivations to put forward such legislation are material security, climate change and population and demand growth [4]. Figure 1.2 shows the traditional manufacturing process. From resource extraction to final disposal it has impact on the environment, and it is inefficient.

In contrast, there are different methods and strategies for each manufacturing steps to save material, reduce the emission and costs and improve efficiency of

production. Figure 1.3 shows a product life cycle and each method that could be used to reduce environment impact. EOL products could take many different paths by which we will be able to save materials, reduce emission and also reduce production costs.

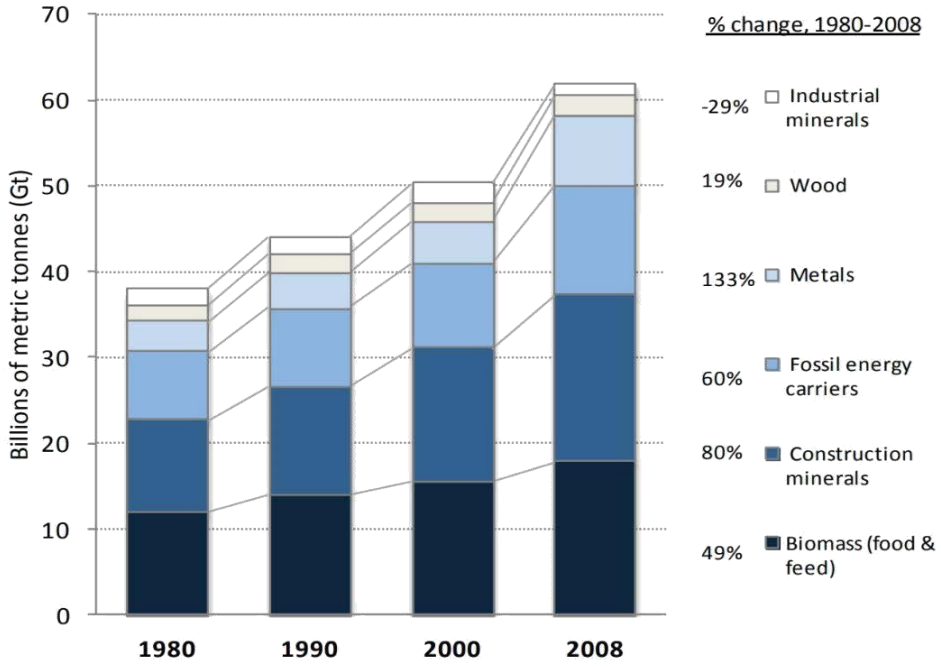


Figure 1.1 Global resources extraction and their changes between 1980 and 2008 [1].

Almost, all products and systems are made of different individual parts and components which made of different materials and have different properties. I order to be able to efficiently carry out any of the EOL methods in Figure 1.3, the product should be disassembled to a certain level. For instance, a product cannot be efficiently recycled or remanufactured unless it is disassembled to its individual components or sub-assemblies. Therefore, for the most EOL products processing, disassembly operation is the first and main process. Also, since 80's generally assembly and disassembly costs have contributed to almost one-third of the products costs [5]. Therefore, developing an efficient and effective plan for

disassembly process by which to meet the environmental regulations and reduce product costs is essential.

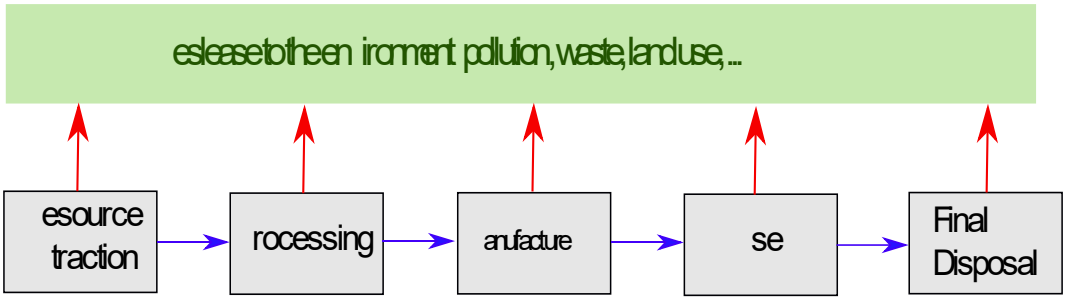


Figure 1.2 Traditional manufacturing process [1].

In addition, disassembly is the main resource of acquiring data and knowledge about EOL product. Most of the EOL product has no data accompanied with them and taking apart of the components is the only way of acquiring data such as components condition, material and properties and decide on the efficient method to deal with that product.

Market size of remanufacturing in UK and Ireland is $4.4 billion [6]. Average global growth rate of remanufacturing is almost 10% and increasing. By remanufacturing an EOL product, 50% costs, 60% energy, 70% material and 80% emission could be reduced compared to manufacturing a new product [7]. First step of remanufacturing is disassembling the EOL product that start dealing with the product. In addition, disassembly is the main source of adding uncertainty to the process. If the disassembly process is not efficient and reduce it uncertainty level, the remanufacturing of the EOL products cannot be efficient and economic. Figure 1.4 shows the relationship between disassembly time, disassembly cost and recovery

profit. Inefficient disassembly process results in reducing net benefit significantly and makes hole recovery process uneconomic.

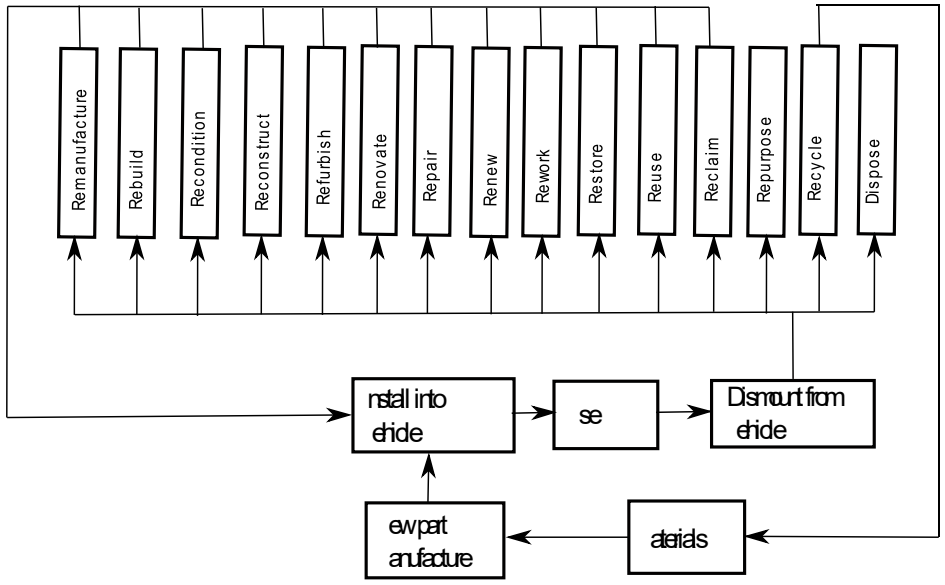


Figure 1.3 product life cycle and each method that could be used to reduce the environment impact [6]

Therefore, finding an efficient, economic, and state-of-the-art method for disassembly is an essential key-point for remanufacturing industry. The recognition of the importance of disassembly process has attracted several research institutions to conduct research in this field. Among these, several institutions such as Stanford University, Northeastern University, The Laboratory for Responsible Manufacturing (LRM) and Manufacturing Modelling Group have already made impressive development in disassembly process re-

search [8].

The earlier studies assumed that the disassembly process can be regarded as a reverse assembly process [9]. However, the nature of disassembly process which deals with both necessary and unnecessary parts in the process at the same time, demands novel ideas and new approaches to satisfy the disassembly aims. Another

main characteristic of the disassembly that distinguishes it from the other traditional manufacturing processes, is the high-level uncertainty in disassembly process. The EOL products due to their nature contain high level uncertainty. Same EOL product could have different condition. Product could arrive with different levels of damage, cleaning, or corrosion. Therefore, new methods and strategies should be developed for disassembly to address these challenges.

Robotic disassembly and automated disassembly operations proved to be an efficient solution to reduce process costs. Using robotic disassembly system, a significant recovery value can be achieved. However, the nature of the disassembly process and high-level uncertainty process automatization for disassembly is challenging. Intelligent planning approaches and new automation methods based on the artificial intelligence are promising.

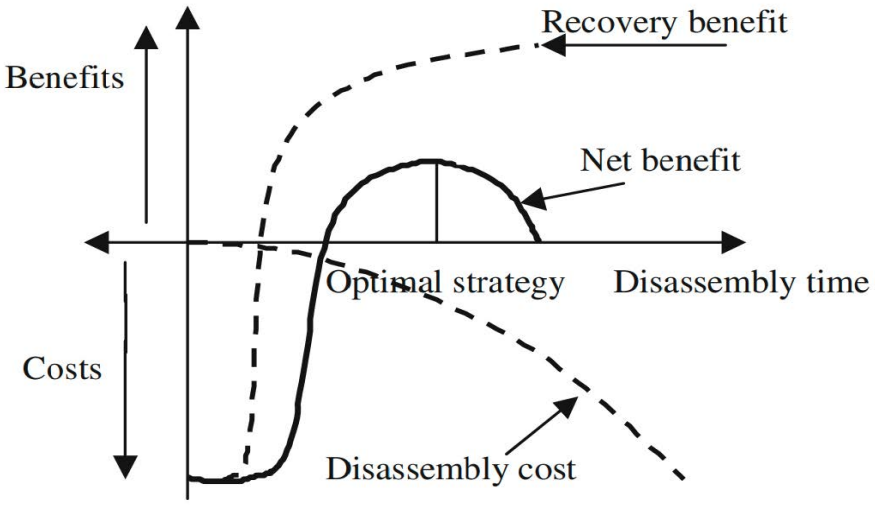


Figure 1.4 Relationship between disassembly time, disassembly cost and recovery prof-its [10]

1.2 Aim and objectives

The aim of this research was to develop and validate new methods and strategies for effective and optimised planning for disassembly of the automotive products. Automated and collaborative disassembly was the focus of this research to find a solution for an optimised disassembly plan.

The objectives of the research are as follows:

Objective 1 (Obj. 1): Investigate manual disassembly planning to reveal the effect of different parameters such as time, tool change, etc. on the disassembly process and propose new method parameters to improve the efficiency of the disassembly process.

Objective 2 (Obj. 2): Study a basic disassembly operation (namely peg-out-hole operation) to understand the mechanic and model of the operation and investigate its automated disassembly to propose a new method for a reliable disassembly operation automation.

Objective 3 (Obj. 3): Study the requirement of human-robot collaborative disassembly operation and propose and validate a new method for an efficient and reliable human-robot collaborative disassembly process.

The relationships between overall aim and objectives are shown in Figure 1.5 Objective 1 (manual disassembly) and objective 2 (automated disassembly) support objective 3 (collaborative human-robot disassembly) which is aimed at a reliable and efficient robotic disassembly.

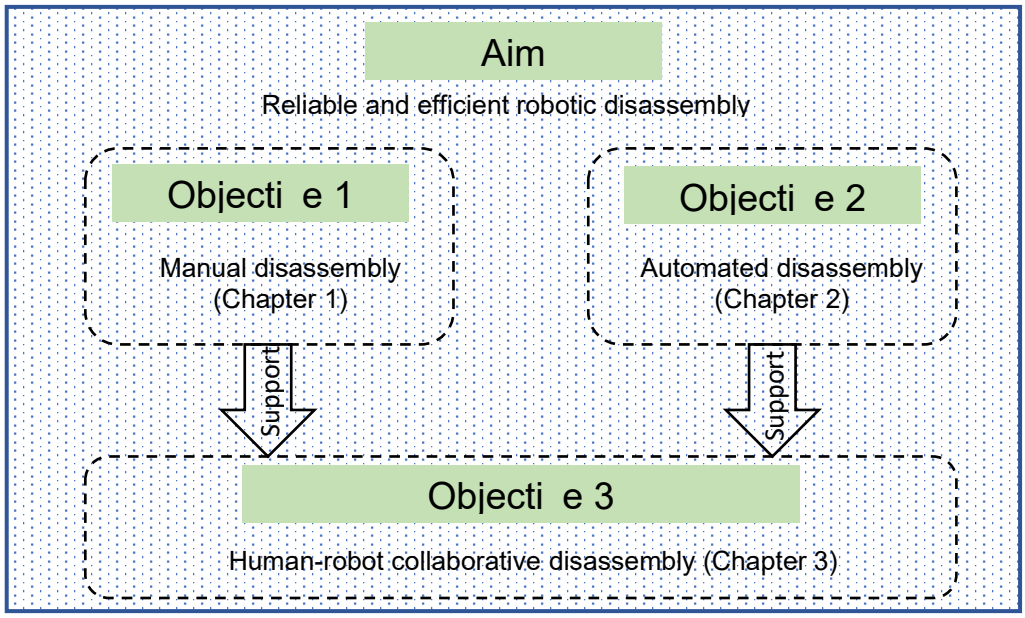


Figure 1.5 Relationships between overall aim and objective.

1.3 Thesis outline

Chabert 1 presents a general background on disassembly process and the motivation behind improving disassembly reliability and efficiency. It outlines the current trend in the field and the aim and objectives of the project are described.

Chapter 2 presents a broad and detailed literature review on disassembly planning. Different steps and requirements of disassembly planning appeared in the researches are discussed and different concept, approaches and methods critically reviewed.

Chapter 3 reports on investigating current manual disassembly planning parameters and proposes a novel method based on new disassembly planning parameters. Then, the proposed method is tested on real automotive case studies.

The results show the effectiveness of the proposed method and are used to achieve **objective 3**.

Chapter 4 presents the study on peg-out-hole disassembly operation, as a common disassembly task and presents a mathematical model for this operation. It is then, proposes a new method for automated peg-out-hole operation and validates it using experimental results. The results are used to support **objective 3**.

Chapter 5 gives the details of the investigation on human-robot collaborative disassembly planning. First, the main parameters and requirement of a human-robot collaborative workcell are outlined. Then, the results of **objective 1** and **objective 2** are employed to propose a reliable and efficient human-robot collaborative disassembly planning. The proposed method and hypothesis are validated using a real automotive case study and experimental results.

Chapter 6 concludes the research and summarises the project findings, contributions, and future works' directions.

Chapter 2- Literature review

2.1 Introduction

The product disassembly process has different types and methods which depend on the aim of the disassembly and process that follows the disassembly operations e.g. remanufacturing, recycling, etc. Figure 2.1 shows different types and methods of disassembly process. Based on the purpose of the disassembly a method or combination of them should be selected in order to achieve an efficient disassembly method. For instance, if the purpose of disassembling a product is to repair or remanufacture it, it is inefficient to use a complete disassembly process [11].

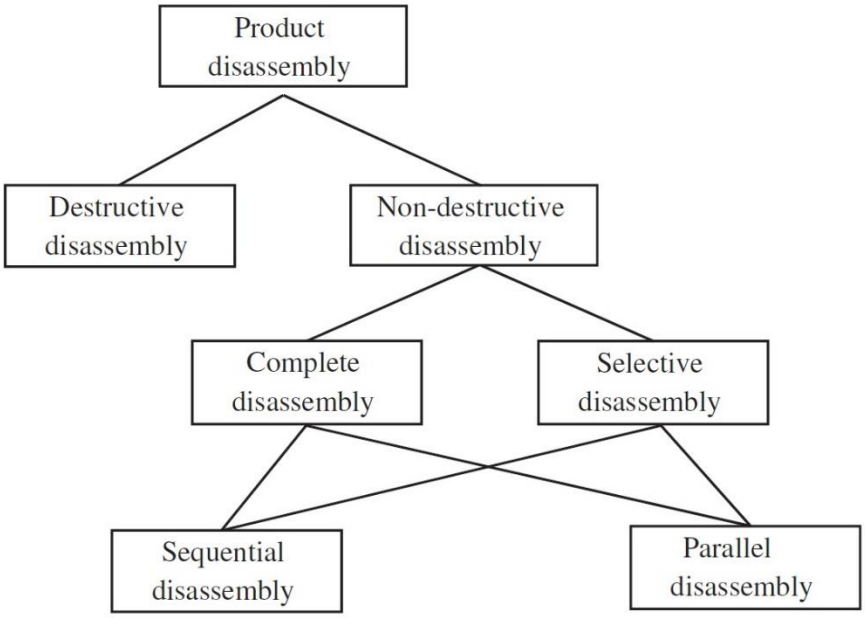


Figure 2.1 Disassembly process types and methods

A disassembly planning problem can be divided into two parts: First to represent product parts and sub-assemblies and all the disassembly process possibilities and sequences, i.e. solution domain [9]. Three different product representation methods have been introduced and widely is used, i.e. Graph-based representation, Petri Net and Matrix-based representation [9, 12, 13]. Also, a combination of these methods such as hybrid graph has been employed to reduce computational time.

The second part is to search the solution domain and find an optimum solution for disassembly process sequence based on the process criterion and disassembly aim and objectives. Many different methods and strategies have been exploited to find an optimal or near optimal solution for disassembly planning. Optimization of the disassembly planning especially where the number of parts rises is categorized as NP-hard problems. It means that the number of possible disassembly sequence solutions rises dramatically by increasing the number of product components. A promising approach for these kinds of problems is metaheuristic-based optimisation algorithms such as Genetic Algorithm (GA) [14], Bees Algorithm [15], Ant Colony optimization [16] and Particle Swarm optimization [17].

In particular, different steps of a general disassembly planning approach are shown in Figure 2.2. All these steps can be categorised in two parts that mentioned above. In fact, the two parts of the disassembly planning have close relations [18]. If the representation of the components and sub-assemblies is not effective, it is not possible to run the optimisation algorithm efficiently and find the required solution. In the followings, sate-of-the-art of disassembly planning methods and strategies is explored and latest findings, improvements, gaps, and challenges in this field are discussed.

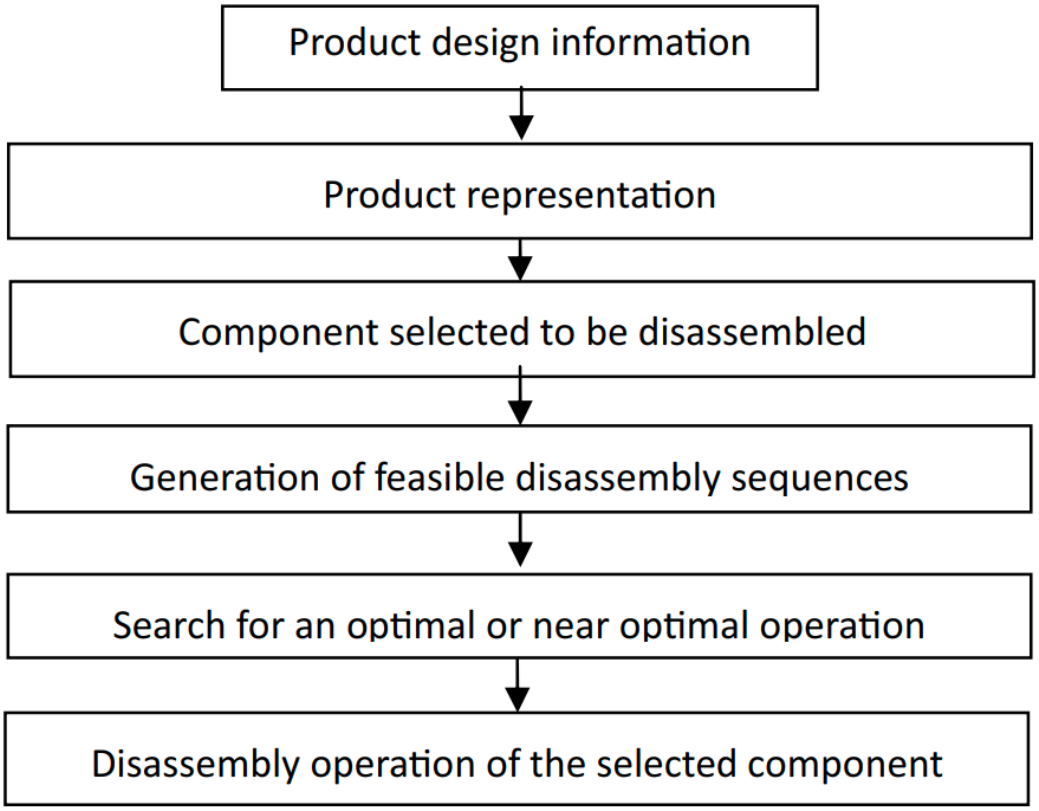
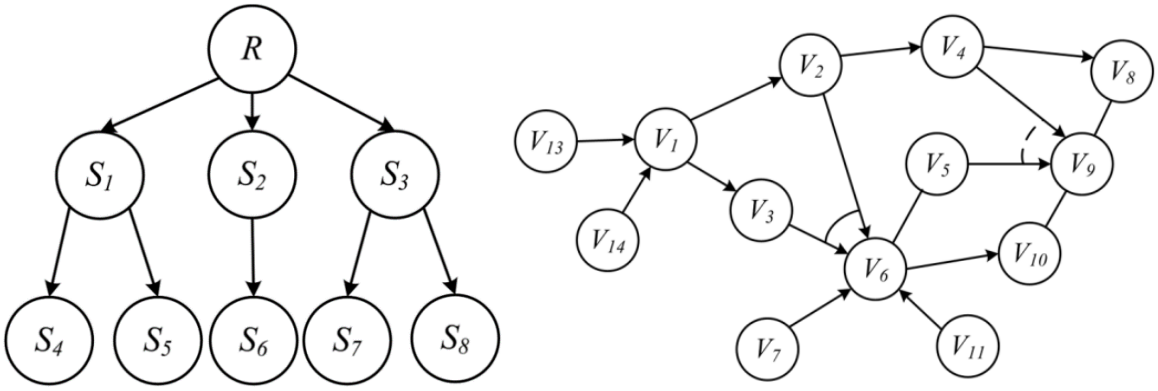


Figure 2.2 General steps of disassembly sequence planning [19]

2.2 Product disassembly representation

To generate a model that represents the disassembly precedence and interface relationships among the product components and sub-assemblies, different methods were employed. A representation method should be able to present the precedence and interface relationship mathematically so the optimization method could be employed. Also, it should be able to model the disassembly constraints among the components and subassemblies [20]. Based on this definition there are four different categories for product disassembly representation: Graph-based representation, Petri nets, Matrix-based representation, and a mixture of these models [21].



(a) (b)

Figure 2.3 Different graph representation types. 2.3a, shows a basic graph where R node denotes the main EOL product and Si denotes the components and sub-assemblies. 2.3b, represents a network graph that relationships and constraints are shown using arrows and arcs [21].

2.2.1 Graph-based representation

Bourjault proposed disassembly trees as a basic graph-based disassembly representation [22]. The representation which is a combination of nodes is started with a root node representing the EOL product and continuing with branches that represents the components and sub-assemblies [23]. This basic representation was just able to show the structural relationship among components and sub-assemblies as shown in Figure 2.3a.

Another graph-based representation which can model more information about the product structure and disassembly constraints is disassembly network graph as shown in Figure 2.3b. It can store more elements of the disassembly process. Different researches have used different numbers of elements in network graphs. A five-element network graph was proposed by Song et al. indication the direction of

disassembly, relationship between parts, constraints, interfaces, and structure of the product [24, 25].

One of the widely used graph-based product representation methodologies is AND/OR method [26]. An AND/OR method uses a combination of nodes and hyperarcs to demonstrate product sub-assemblies and parts and all possible disassembly routes [27]. In this method product sub-assemblies and parts are shown using nodes and hyperarcs are used to represent the disassembly operations. A branch is assigned to each node which can be either AND or OR. If a node is indicated with AND label its successors nodes will be parts or sub-assemblies that are disassembled from that node. An OR label indicates the possible disassembly sequence for that node [28]. All possible disassembly sequences and product sub-assemblies and parts can be shown using AND/OR graph. However, when the number of the product parts increases it will be very complicated and impractical and generation of the graph from product information is difficult [29, 30]. S. Min et al. employed a combination of AND/OR method and weights to model mechanical product disassembly process based on constraints elements [29]. Zhang et al. used a modified method of AND/OR graph to represent disassembly process of a dishwasher door [31].

For products with a higher number of parts, the AND/OR method can be computationally complicated, and it causes to increase the solution time dramatically [32, 33, 34].

Unlike the pre io us network graphs that didn't show the disassembly direction, directed disassembly network was developed to model the direction of disassembly

process [35]. This method starts with a root node for EOL product and ends with an end-node which denotes the disassembly of all components as shown in Figure 2.4 [36]. In this method the direction of the optimum disassembly sequences of operation can be shown (Bold direction in Figure 2.4). Each middle-node represents disassembled component and their associated sub-assembly. For instance, A/D/BC shows components A and D and sub-assembly BC.

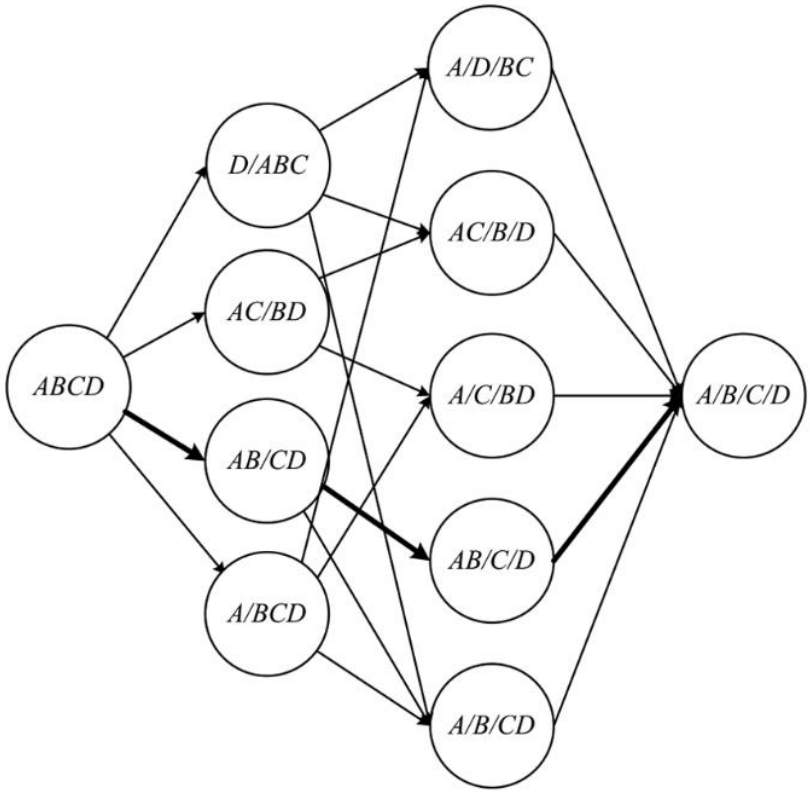


Figure 2.4 Graph-based directed disassembly network where the optimum solution can be seen in a bold direction.

2.2.2 Petri Net

Petri Net (PN) is also a graph-based method to represent the disassembly process and product parts and sub-assemblies. However, in this method sub-assemblies and components and conditions of disassembly operations are represented by places. Petri Net uses same hyperarcs relations as AND/OR method [37]. A simplified Petri net representation method uses five parameters to model the disembody product as defined in Equation 2.1.

$$DPN = (P, T, I_{n*m}, O_{m*n}, M) \qquad (2.1)$$

Where P and T are places and transitions which defines sub-assemblies and disassembly operations respectively. In addition, n and m are the places and transitions number respectively. I and O are definition matrices and M describes the state of the disassembly product. Figure 2.5 shows a typical Petri net representation [38]. The description of the product disassembly structure is richer than the previously discussed graph-based representations. In addition, it provides the reuse values and disassembly costs [39]. Based on the five-tuple Petri net, an extended higher-level method was proposed which included more parameters such as time of disassembly operations, quality conditions of the sub-assemblies and probability value function [40].

A bottleneck of the traditional Petri net methods is high computational costs. Specifically, by increasing the number of the products components, the computational time rises dramatically and makes it hard to generate the products graph. To address this problem, Dong et al. proposed a simplified PN method using synchronous nets [41]. To deal with uncertainty and to provide a robust method,

researchers proposed Fussy based and Bayesian learning based Petri net representation model [42, 43, 44].

Kuo and Wang employed Petri Net to study disassembly planning of the EOL electrical products [45]. It also has application in automated sequence planning, robotic disassembly sequence planning, assembly process optimization and product design for assembly planning. Same as the other graph-based representation method the Petri Net is hard to be generated automatically from initial information [46, 47, 48].

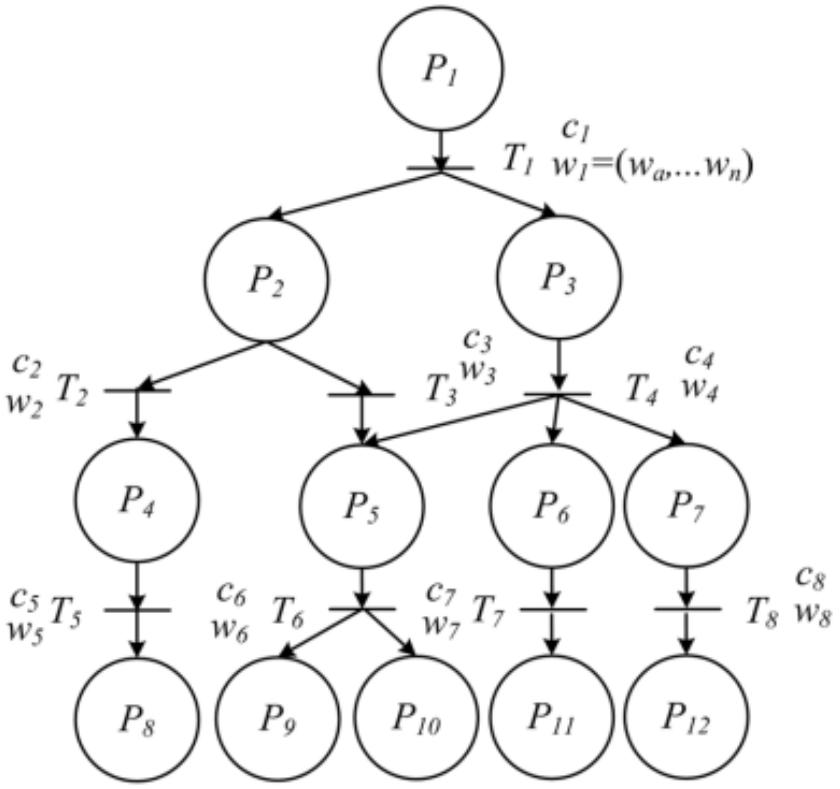
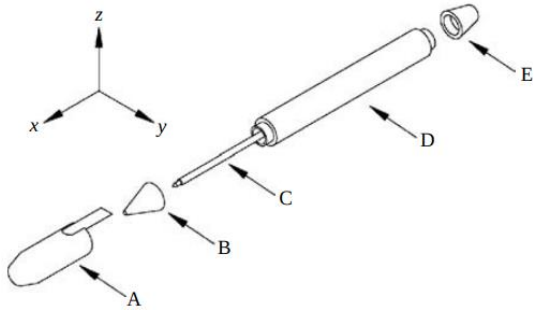


Figure 2.5 A typical Petri net disassembly model representation where c is the disassembly operation costs and w is a weight function.

2.2.3 Matrix-based representation

In this method, a series of matrices are used to encode the disassembly process information, product components and their precedence relationships. Different formats of matrices can be used to represent disassembly process mathematically such as constraints matrix, components matrix, fasteners matrix and element relationship matrix [49]. The number and type of the matrices can be varied for different applications and disassembly processes. These matrices can contain all data and information of disassembly process, product component and their relations, constraints, etc. which can be generated automatically and used for automatic optimization [50].

The most common matrix-based representation is the interference matrix method which can be seen in Figure 2.6 [51, 52]. Based on this method, the precedence relationships of the components are represented with matrix that its arrays are either 0 or 1. If part i is disassembled before j, then the array b_{ij} = 1, otherwise it is 0.



(a)

	A	B	C	D	E
A	000	110	110	110	000
B	111	000	110	110	000
C	111	111	000	110	110
D	111	111	110	000	110
E	001	001	111	111	000

(b)

Figure 2.6 Matrix representation. 2.6a, shows the basic component of a ball pen and 2.6b, represents a matrix-based method, where uses a three-element array representing interference in X, Y, and Z direction.

Matrix-based representation is much easier to be generated automatically and its efficiency in the computational application have attracted researcher toward employing this method in recent researches [53, 54, 55]. Smith et al. proposed four matrices to encode disassembly process information and represent product: Components matrix, fasteners matrix, fasteners constraint matrix and components constraints matrix [56]. Chung et al. used matrix-based representation to study product maintainability [57].

To represent the directions of the product's components using matrices, different methods were proposed [58, 59, 60]. These methods used a simple six direction of (X+, X-, Y+, Y-, Z+, Z-). However, this method can represent the directions of the components for simple products, if the directions are mixed or product is complicated it cannot be efficiently used. In addition, these methods are not able to represent spatial interference of the components.

Therefore, to address these problems, an extended interference matrix was developed [61]. To increase the diversity of the directions, a local and a global coordinate system were proposed. The local coordinate system represents the direction from the prospective of the individual components, while the global coordinate system was employed to represent the relationships from a common frame view.

To reduce the complexity of the model Smith et al. developed a model to encode the spatial relationships of connections and components [62, 63]. Using this method, they presented components, connections, and their motions with four matrices and recorded disassembly progress simultaneously.

As it can be seen the bottleneck of the previously mentioned method is that they are static. In other words, they cannot be altered with the progress of the disassembly process. To deal with this problem, dynamic matrix representation was proposed [64]. Based on this model the representing matrices were updated attractively. In addition, to add the effect of gravity on the components and disassembly process, the enhanced support matrix method was developed [65].

Although the matrix base method is easier to implement computationally and it is more efficient than the graph-based model, it needs further studies to reduce the size of matrices and improve the computational time.

2.2.4 Other methods

Generic constraint handling model was developed by Li et al. to handle different disassembly models using a universal model [66, 67]. In this model, each operation is categorised into either with or without constraints. The position of the operation with constraint is adjusted with the precedence relations and for others, it remains unchanged. After adjusting the position of all constraint operations, a feasible sequence of disassembly operations is achievable. Many information such as operation direction or disassembly tools is not considered by this method to be generic.

For disassembly model representation, the most common method is graph-based method with just under 60% of the publications followed by matrix-based by around 40% of the publications. The other methods have been used in less than 2% of the publications [21]. Graph-based models are more intuitive while the matrix-based models perform much better in computer-based computations. On the other hand,

Petri net method proves more in formation of geometry and topology of the components.

Graph-based disassembly representation is one of the first methods which was proposed and developed in this field. The main advantage of this method is its illustrative representation approach which makes it more suitable to interpret the product's tree and study its structure. On the other hand, as the number of the product's components increases, the number of the nodes and branches rises dramatically and makes it impossible to encode all possible sub-assemblies graphically. Petri Net representation method is also a graph-based representation method. However, in this method sub-assemblies and components and conditions of disassembly operations are represented by places. This method improves the representation of the sub-assemblies, however, increases the computational time significantly. The matrix-based method improves the computational time of the mathematical encoding; however, the representation quality is highly dependent on the number and types of the defined matrices. This method promises a more efficient and reliable mathematical representation tool if defined matrices such as relation matrix and constraint matrix are improved.

2.3 Search for optimum solution

After representing the model of the disassembly product and its components, an optimum solution should be determined among all feasible solutions by employing an effective disassembly planning method. Finding an optimum solution for a sequence of disassembly operations is considered as an NP-hard problem category [14]. These types of problems require to use heuristic-based algorithms. In the

following sections the disassembly planning methods and the optimisation algorithms are covered.

2.3.1 Disassembly planning

The aim of disassembly planning is to use product representation information as the solution domain and plan the disassembly process i.e. finding the optimum disassembly sequence [68]. Based on the product representation method different DP methodologies have been developed [49]. As the nature of the disassembly planning problems is NP-hard type these methods are based on the heuristic algorithms [69]. In this method to find a near optimal sequence different variables such as cost, time and disassembly efficiency have been studied as the objective of the planning i.e. optimisation [48]. To search and find a near optimal solution for assembly process Pedrazzoli et al. introduces a set of rules [70]. Zhang et al. used search rules to study operation plan of robot gripper [71]. Objectives of the disassembly planning e.g. higher profit, lower environmental impact, lower cost, feasibility, etc. are tended to define the aim of disassembly planning. Based on the different purposes of disassembly process, specific objectives are determined. A comprehensive list of studied objectives can be found in [21]. The main categories of disassembly objectives are environmental objectives, process cost, revenue, and other objectives. Each of these categories has many sub-categories that were studied by different researchers. For instance, many researchers investigated process time, cost of disassembly tools, operation, and part numbers as part of cost objective [72].

Basic disassembly operation time i.e. the required time to complete a disassembly operation, has been studied by many publications. The basic disassembly time is simple to use and provides solutions much quicker, however, it is not accurate and highly dependent on many parameters and varies from case to case. To deal with this problem, additional disassembly times were added, such as allowance for tool change and movement from one point to another point. Many uncertainties such as EOL product condition can affect the disassembly time [73, 74]. Labour costs, part numbers, maintenance degree, and disassembly distance were studied as part of cost objective [75, 76, 77, 78].

Disassembly revenue as the objective of the disassembly planning has appeared in many publications [79, 80]. Some researchers have considered the recovered value and recovered weight as an index for a component revenue [37]. This parameter in this research is considered as a constant parameter, however, different EOL products of the same model can have different conditions based on their time being used and therefore different recovery values. To address this problem different methods a value curve which was an exponential function of time and pro t probability were proposed [81]. Figure 2.7 shows component value as a function of component age for an EOL solenoid parts.

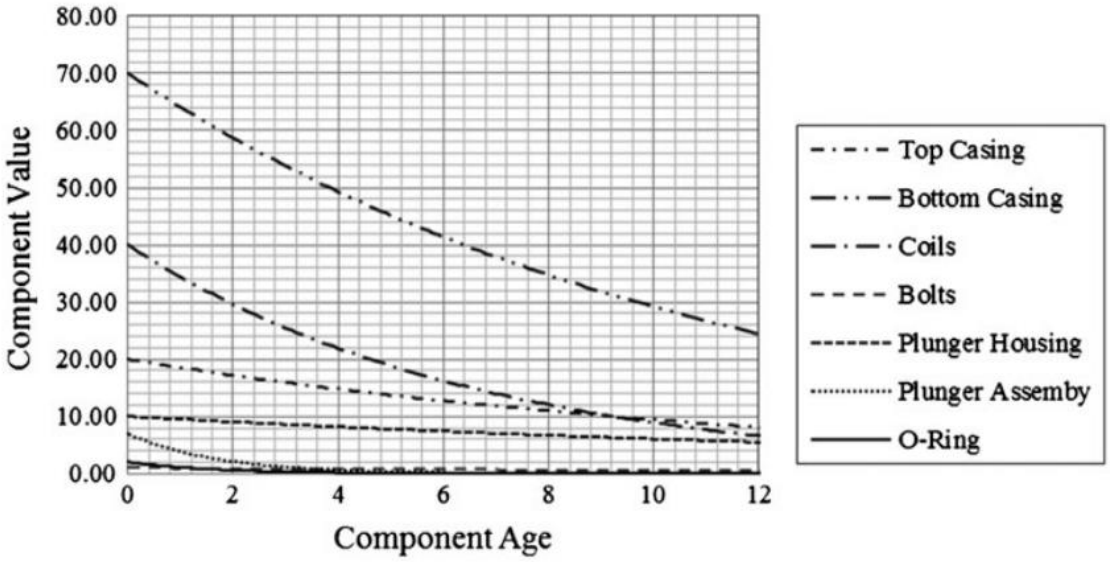


Figure 2.7 Value functions for expected component value based on its age for a typical solenoid [81].

However, there has been less focuses on environmental parameters as planning objective so far, it is getting more attention due to climate change and public demands. The main purpose of environmental objectives is to minimise the impact of production on the environment [35]. This objective tries to reduce potential harm of components after its been used by different approaches. For instance, by reducing hazardousness of the process. Li et al. developed a customisable decision-making method to deal with hazardous components of an WEEE EOL product [66]. Remanufacturing of EOL products is increasingly balancing the economic and environmental targets. Since 2003, instructions have been implemented in Europe to deal with EOL WEEE products. According to these instructions, the responsibility of the producer's ware e te nded to deal with OL products, rather than just selling or maintenance them. Same legislation is in place in other regions too. All this reason makes the environmental objectives more interesting in the planning field.

2.3.2 Optimisation algorithms

An optimisation algorithm is used to efficiently find a near optimal solution for a disassembly planning problem. As previously mentioned, a disassembly sequence planning is an NP-hard problem and requires a heuristic method to deal with. Stochastic simulation methods, rule-based techniques, linear programming optimisation and nature inspired optimisation algorithms are four approaches that researchers have employed to solve the disassembly planning problems. Figure 2.8 shows the number of documents on evolutionary computation in scheduling problems. In the followings these methods are discussed.

- **Stochastic simulation methods**

A stochastic method systematically integrates different methods such as sub-set generation, combination of solutions, diversification method and improvement of solution to achieve both diversity and quality among generated solutions [79]. To disassemble bigger and more complicated EOL products, Gue et al. employed the path relink combination operator method [39].

Stochastic simulation method can be an efficient approach in search of an optimum sequence of disassembly operations. Chen and Tian employed Monte Carlo simulation method to solve disassembly planning problem with stochastic operation time [73, 82]. The disadvantage of this approach is that it can be easily affected by sample size. Furthermore, its efficiency and accuracy are low compare to other methods. To tackle these problems, a two-phased method was employed to generate a function of disassembly probability density using frequency or time

domain instruction [83]. In addition, to solve disassembly planning problems with a stochastic cost function Neural Network method was employed [84].

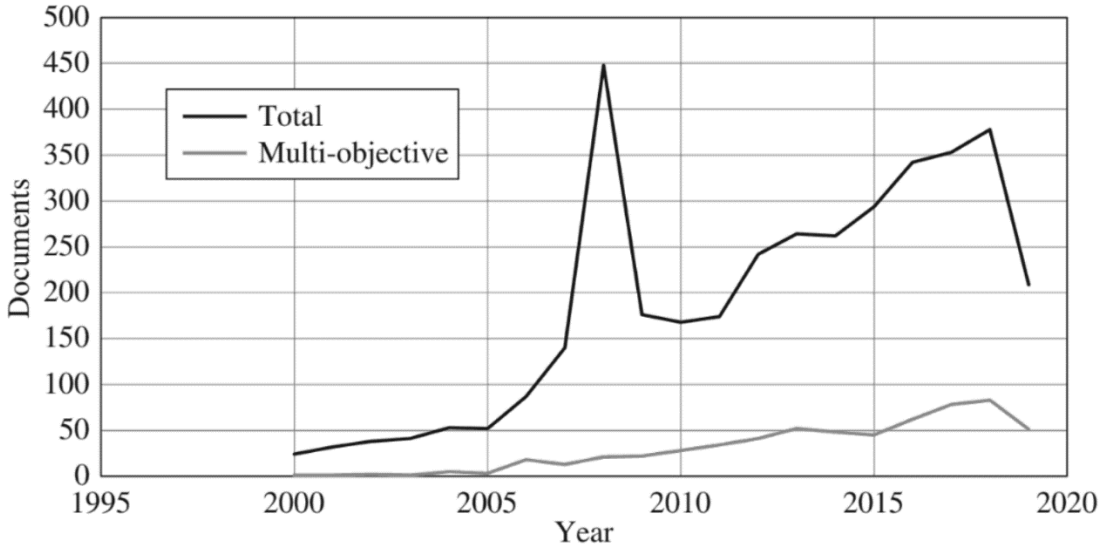


Figure 2.8 the number of documents on evolutionary computation in scheduling problems [85].

- **Linear programming optimisation**

The popular method of linear programming that is used in different areas for constrained extremum problems, was also modified to address disassembly planning problems. To reduce the complexity and improve the efficiency of the linear programming, a binary linear programming approach was proposed. Based on this method, the decision is a binary choice of either 0 or 1 [86]. However, this method more efficient, the implementation is more problematic [87].

Han et al. employed branch and band algorithm for selective disassembly planning with multiple target components and sequence-dependent steps to address linear programming weaknesses [69]. This method uses the lower and upper bounds and branching operations to find optimum solution of operation sequences. To reduce the number of possible solutions and therefore the solution domain, Gungure et al.

proposed two new variables to improve the efficiency of branch and hand method [88].

- **Nature inspired optimisation algorithms**

Naturally inspired optimisation algorithms were developed based on natural phenomena such as DNA evolution, (Genetic algorithm), bees hives (Bee algorithm) and ant foraging (ant colony algorithm). These methods are the most common approach for solving disassembly planning problem used in researches. Different nature inspired optimization algorithms have been employed to search possible disassembly process sequences and find a near optimal solution. Among these, Bees algorithm, Swarm Optimisation algorithm, Genetic Algorithm (GA) and Ant Colony Optimization Algorithm have been used more frequently.

The main algorithm that widely is used in disassembly planning researches is Genetic Algorithm that has been adapted based on the evolution theory in nature [8]. GA generates several solutions randomly in each generation and assigns a fitness level to each solution based on the disassembly process aim and objectives. Therefore, a fitness function should be de ned based on the disassembly process criterion. The fittest solutions in each generation survive and are used to form next generation. Figure 2.9 shows a typical block diagram for GA.

GA can find a near optimal disassembly sequence [89]. Studies show that the implementation of Genetic Algorithm in disassembly planning problems is simple, but the interpretation of its behaviour can be difficult [90, 91, 92]. Mohanta et al. combined Petri Net representation method with GA to study path planning strategies of mobile robots [93]. Also, Xie et al. proposed a combined method of Genetic

Algorithm and simulating annealing to search near optimal solution for DP problems [94].

The feasibility of the generated solution by GA is not guaranteed and sometimes the optimum sequence is not possible due to product's structure. Therefore, to sol e this problem feasibility of the possible solution was added to cost function of the algorithm [36]. Another problem of GA is that it can stock in local optimal. To improve the quality of the solution, adaptive mutation and crossover rate were proposed [95]. Furthermore, a combination of GA with other methods such as Tabu search, Chaotic, binary tree were explored [96, 97, 98].

Another nature inspired population based is bee's algorithm which was developed in 2005 [99]. This algorithm was developed based on the honeybee's behaviour in search and finding food [100]. Liu et al. used this algorithm for robotic disassembly sequence planning in remanufacturing [101]. Another optimization method that appears in some DP studies is Ant Colony optimization algorithm. This method is also inspired by nature and is based on the behaviour of the colony of the ants in search of an optimal path between their colony and another destination. Wang et al. used ant colony algorithm to find the optimal sequence of disassembly process for a simplified automotive engine and showed that this algorithm can be efficient to solve computational problems [102]. To avoid premature converging, the max-min method was developed based on the pheromone limitation [103]. In addition, a two-stage ant colony optimisation was studied to explore the efficiency of it [104].

Another common method in disassembly planning is particle swarm optimisation which is based on the beha iou r of the birds' flocking behaviour. Based on this method in each iteration the position and velocity of each particle is updated. To

avoid pre-mature converging adaptive mutation rate and inertia weight were used [105]. To improve the quality of the solution, Li et al. introduced a shift operator, a crossover operator, and an escaping mechanism [66]. Yah et al. proposed a simplified form of swarm optimization algorithm and studied procedures of the parameter control in disassembly process planning [106].

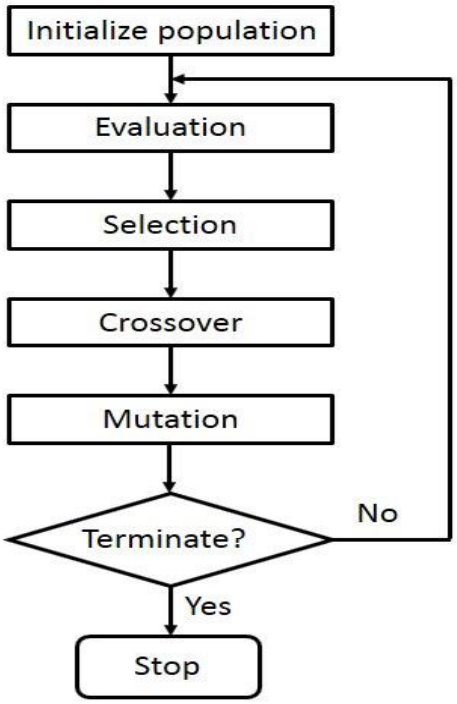


Figure 2.9 General block diagram of genetic algorithm [107].

- **Rule based methods and other techniques**

Rule based method was used to produce feasible solutions and filter out unrealistic answers for disassembly planning [49 108]. According to this method, different riles were checked iteratively for partial disassembly planning and continued until the targeted parts are disassembled with feasible sequences of operations. To reduce

the computation time by limiting the search domain, Smith et al. employed a combination of ruled based method and genetic algorithm [109]. Using a projection matri for product's part, they achieved a lower time for search among possible solutions.

Different disassembly parameters such as time, tool change, robot travel, disassembly revenue, etc. have been investigated as the criteria to find a near-optimal solution for the disassembly planning problems. All these efforts considered the time of the disassembly operation as the main parameter or tried to convert the other parameters in time unit. For instance, to consider tool change effect in the disassembly planning, they added a certain amount of time to the operation to reflect the effect of the tool change on the operation. Using time-based parameters has different weaknesses and can be considered as an inefficient approach. One problem is that operation time is not constant and can be different for same product with different conditions. For instance, two same oil pump models with different ages can have different times for each operation. The other weakness is that to calculate actual operation time for each operation, the entire product should be disassembled to measure the operation time which is inefficient and for most cases infeasible.

2.4 Selective disassembly planning

Current demand for more effective disassembly strategies makes full disassembly unproductive [110, 111, 112]. To find an optimal solution for planning problems, selective disassembly which aims to disassemble a product partly to retrieve demanded components is receiving more attraction in current studies. The purpose

of selective disassembly planning method is to search the solution domain to find a near optimal sequence of disassembly operations to disassemble targeted parts of the product. Disassembly process will be terminated when this condition is met.

The aim of selective disassembly can be repairing, recycling, remanufacturing, or reusing. Current disassembly planning studies have demonstrated that full disassembly process can be economically inefficient and increase the disassembly process costs significantly. As a promising alternative, selective disassembly planning by which product can be partially disassembled and meet the economic requests and other requirements has become a research trend in disassembly planning [113, 114, 115]. Figure 2.10 shows all steps of a typical selective disassembly planning. Based on Sanches and Haas [116], very few researches carried out in field of selective disassembly especially for reuse of buildings structures. In fact, a brief literature search shows that there is a lack of research and analyses in this field and an established methodology has not been developed. To address this gap, Sanches et al. proposed a multi-objective method for optimisation of selective disassembly planning using combining various de-construction approaches [117].

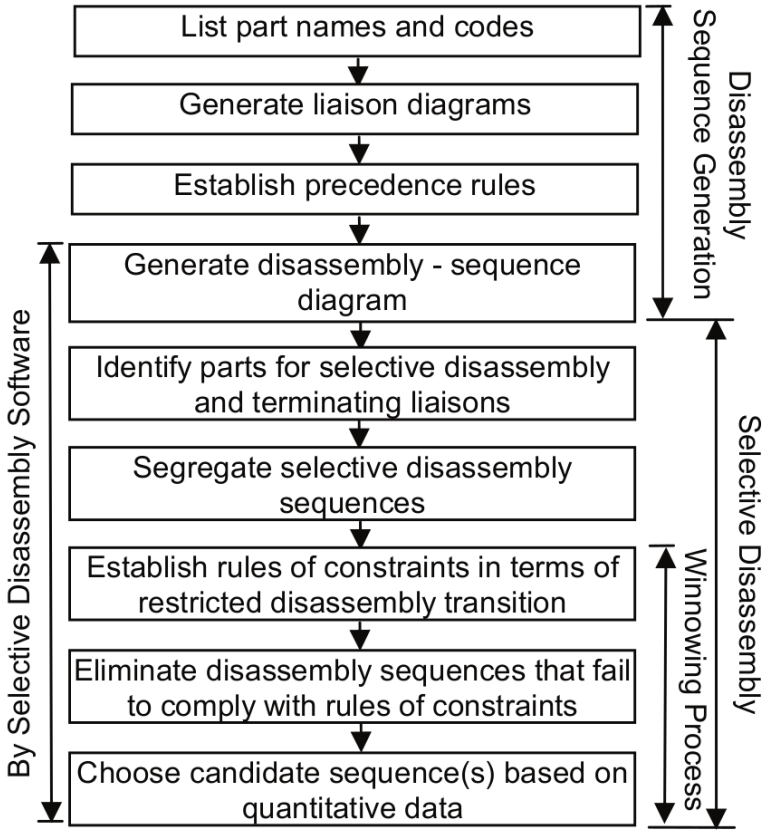


Figure 2.10 Selective disassembly planning steps [112].

Wang et al. studied selective disassembly planning for EOL products to establish a methodology for separating the targeted and usefully parts without disassembling unwanted components [118]. In their method, the distinctive operations were considered to maximise the efficiency of the selective disassembly sequence planning. They aimed to improve the recycling characteristics of EOL products. They tested their hypothesis on an industrial product - a robot arm - to validate the proposed method. Although this method seems to be efficient in a selective disassembly approach, it is destructive. Therefore, it is more considerable for recycling rather than remanufacturing or repair of EOL products.

Another method to improve the selective disassembly planning approaches was proposed by Guo et al. [119]. They employed Lexicographic multi-objective Scatter

search to propose a sequence dependant selective disassembly planning. To evaluate the selective disassembly efficiency, they adopted the energy consumption. The proposed method maximised the process pro t by minimising the disassembly process time and its energy consumption.

Random disassembly operation times were assumed by Kim et al. to remove one or more targeted parts in a parallel disassembly setting with a single disassembly operation in the same time [120]. They employed extended process graph representation to model the product mathematically. In addition, they used a stochastic integer programming model to minimise the costs of the disassembly optimisation objectives. The costs of the disassembly planning objectives included the penalty cost of exceeded disassembly operation time and costs related to sequences set up of operations. They concluded that the proposed method improves the both process time and solution quality. However, the practicality of their method remains in doubt as it relies just on one certain example as the case study. In addition, other uncertainty factors such as defective parts and disassembly operation failures were not considered.

AlSayed et al. investigated an intelligent automated disassembly cell which disassembled products online and selectively [121]. They modelled an online GA (Genetic Algorithm) for selective disassembly to optimize the disassembly sequences. A selective disassembly planning method for waste electrical and electronic equipment (WEEE) was proposed by Li et. al. They develop a selective disassembly planning method based on particle swarm optimisation with customisable decision making. They applied this model on WEEE to maximise the economical pro t and reduce environmental problems [66]. Ziqiang et al. employed

selective disassembly method to target the product components for reuse or remanufacturing [110]. They demonstrated that the revenue of the EOL products and efficiency of disassembly process can be increased by the combination of selective disassembly method and partial destructive disassembly method.

El-Sayed tried to reduce computational time by introducing a less complex representation matrices to obtain selected components one at a time [121]. However, this method can only search for single-target partial disassembly process planning. Smith and Hung classified the product parts into modules using modular design theory and proposed a selective parallel disassembly planning method [122]. They used this method to improve the green design and reduce disassembly steps and environmental issues. Smith et al. used disassembly criterions such as part direction, part order and the number of orientations to an optimum disassembly stop-point. They presented that in comparison with the traditional full disassembly planning, partial disassembly strategy can be more efficient and reduce environmental costs [123]. Also, other optimisation methods such as swarm optimization were used in selective disassembly planning.

Importance of the selective disassembly planning is highlighted especially in removing hazardous materials, retrieving valuable parts, and repairing EOL products. Investigating the literature that involves the selective disassembly planning shows that although the quantity of the works in this field is rather high, there is a lack of specific and comprehensive works on selective disassembly planning. In the other words, majority of the selective disassembly planning studies are part of the other proposed methods or developments such sequence

optimization or product representation. There is a gap for an effective and independent selective disassembly planning method in this field.

2.5 Automated disassembly planning

Manual disassembling of many EOL products is inefficient and economically infeasible at the moment, Therefore the remanufacturing industry pursuing the automation of the disassembly process. Robotic disassembly and automated disassembly operations proved to be an efficient solution to reduce process costs. Different approaches and methods have been proposed for automation of complex disassembly process of products such as automotive components, however, there is no industrial scale implementation of a fully automated disassembly process [124]. Growing use of industry 4.0 and emerging of its advantages, and latest improvement in collaborative robotics, disassembly process automation could be evolved into a state-of-the-art in the third decade of century.

Robotics in industry is growing sharply and its global market expanding significantly. Global sales of different robots have seen 30% increase in 2017 which was rising for five consecutive years. Improvement in collaborative robotics combined with decreasing the price of industrial robots lead to further use and popularity of the robots in future. In addition, as sensor prices falling rapidly, Internet of Things (IoT) and industry 4.0 are emerging in remanufacturing industry [125]. Forth industrial revolution i.e. intelligent automation, which integrate robotics and its accessories to infrastructures and factories cyber physical system makes disassembly automation inevitable in future. In addition, Artificial Intelligence (AI) improvements in

combination with adaptable end effectors provide more flexibility in disassembly automation.

Implementation of automation and robotics was described by The World Economic Forum as a positi e impro e ment for world's employment and jobs in the future. t argued that this development could lead to machine and human collaborative where they could complement each other. In order the companies working in EOL product treatment to remain competitive in the remanufacturing market a successful automation in the future is vital. Remanufacturing in general and disassembly process industry in particular, will not be able to survive in the future without an efficient automation strategy [124].

Several automated methods for EOL products disassembly have been investigated and proposed to increase recovery of valuable components and materials. Li et al. utilised a robotic disassembly system to increase recovery of important materials from electric vehicles [126]. They showed that using robotic disassembly system a significant recovery value can be achieved. Different disassembly methods were investigated by Duflou et al. [113] and importance of autonomous disassembly systems was highlighted. Knothm et al. [127] employed vision system to detect product components for disassembly and proposed an intelligent automated disassembly system. Vongbunyong et al. [128] studied automated disassembly process of TV screens and employed vision system to develop cognitive robotic systems. They showed that further configurability and more flexibility for robotic disassembly systems can be achieved.

The disassembly of the electric vehicle (EV) products has become a research trend in recent years especially since 2010. Robotic applications have been employed to

target most valuable EV components such as batteries. Although there is no evidence of robust and fully operated solution, the overview of the allocated funding and dedicated researches are promising. Furthermore, researchers such as Minca et al. [129] employed mobile robot systems in manufacturing application that could be possibly effective in product disassembly. A modular robotic system was introduced by Kasperzyk et al. [130] to rebuild the disassembled modules in the building sector. Apart from common robots with 6-DOF, Cartesian robots and Scara robots were used in some robotic disassembly concepts. The effectiveness of automated disassembly could be significantly improved with pre-product design considerations such as design for disassembly concepts.

Moreover, to develop a robust and applicable robotic disassembly system, specific tooling concept, state-of-the-art sensory system and effective system vision is inevitable. Among these peripheral systems, vision system has been applied and investigated in variety of cases [131, 132]. They were used to detect and identify products, parts, and components and for robotic disassembly trajectory planning. In addition, to achieve further accuracy, tactile sensors were used in combination with vision system. Although the lack of computational power was the bottleneck of developing an integrated and robust vision system in the past, it is not the case anymore. Specifically, on the concept of disassembly and assembly, Umeda et al. [133] developed a method for shape recognition as part of a basic research. Furthermore, the detection and identification of the product fasteners were developed using vision system.

Apart from basic part detection using vision system, colour sensor concepts were used in disassembly automation for automated sorting. Sometimes, sensory

systems were combined with specific tooling systems to improve the effectiveness of the disassembly systems. In-line with this trend, high versatility and in-hand manipulation were exploited to develop KIT Swiss Knife gripper for disassembly purpose [134].

An effective path planning method for autonomous disassembly robot cells needs to be in place to employ the robotic disassembly. An adaptive trajectory planning method to address process uncertainties was proposed by Zussman et al. based on Petri net. In addition, collision of the operating robot arms between each other's and the disassembly cell environments was investigated in several researches. Components mobility and surface contacts were considered to determine possible motion paths based on the CAD models. Also, general path planning algorithms were modified based on configurable parameters to improve mobility of the components and articulated parts [135].

In addition to trajectory planning and peripheral systems, in some situations grasping points of the disassembly components can affect the whole disassembly process significantly. To fill this gap investigations were carried out by Puente et al. in this area [136]. The aerospace sector's maintenance tasks were employed by Aguinaga et al. to target path planning especially regarding the disassembly grasping [137].

Overall, collaborative, and highly automated systems are the main current trends in disassembly atomisation research field. Computational power improvements mean that it is not limiting the Artificial Intelligence algorithm of path planning and disassembly planning. In addition, the use of industry 4.0 advantages, namely use of sensors especially vision sensors have been thoroughly established. Although, in

comparison to the other industries such as assembly the number of published researches is still limited. The main research gap can be seen in most level of data process structure control and information managements. This bottleneck could be addressed by digitalisation framework integration and use of concepts such as IoT. Also, in compare with other sectors, only a limited number of full-scale automated disassembly concepts have been developed and validated by successful applications.

Most of the knowledge on the automated disassembly is based on the assembly process. As the disassembly requirements are significantly different from assembly due to the products condition new studies with focus on disassembly are required. Particularly, mathematical, and experimental studies and the basic disassembly operations such as peg-out-hole, separation, unscrewing, etc. are missing in the current literature. In addition, efficient and reliable automated disassembly method that can deal with high-level uncertainty in EOL products is required to deal with disassembly planning problems.

2.6 Cognitive robotics and collaborative disassembly

According to Moreno, a cognitive autonomous system is a system that uses cognitive in a high level performance, which allows the system to revise, reason and adapt itself in an uncertain environment and respond to unpredictable changes robustly and abortively in order to accomplish the tasks [138]. A practical method based on reasoning and knowledge representation was proposed by Levesque et al. to solve problems in a dynamic environment and without complete knowledge using an autonomous robot system [139]. The research categories the cognitive

robotics studies into three fields; a) high level control, b) reasoning and decision and c) knowledge representation (KR).

A layout for a cognitive robotic system architecture was provided by Sardina et al. [140]. A structure of proposed cognitive robotic architecture overview is shown in Figure 2.11. The author defines the structure as a close relation between three main elements: 1) knowledge, 2) perception and c) action. First, the cognitive robot system employs different end effectors and sensors to interact with its environment and other objects. Also, high level control and programming are enabled to organise the system behaviours. Finally, sequences of different actions related to the desired conditions are generated using the high-level control and programming based on its logic. The desired conditions can include results of sensing, initial states, primitive actions etc.

One of the fundamental and common disassembly operations is pulling out a cylindrical part from a cylindrical hole or peg-out-hole operation [141]. Many disassembly operations such as pulling out shafts, pins or any other cylindrical object can be represented as a peg-out-hole operation. Although there are numerous studies on peg-in-hole assembly operation [142, 143], there is a lack of fundamental research on peg-out-hole disassembly.

Furthermore, research on automated peg-out-hole disassembly remains almost untouched. Zhang et al. [144] investigated disassembly of peg and hole using active compliance. They analysed the boundary condition of peg and hole two-point contact state and effects of different variables. Zhang et al. [145] focused on a two-phased scheme using a compliant dual arm robot to investigate peg and hole

assembly. They used Baxter robot and adjusted position and orientation of peg and hole using force torque (F/T) sensor and an active compliant.

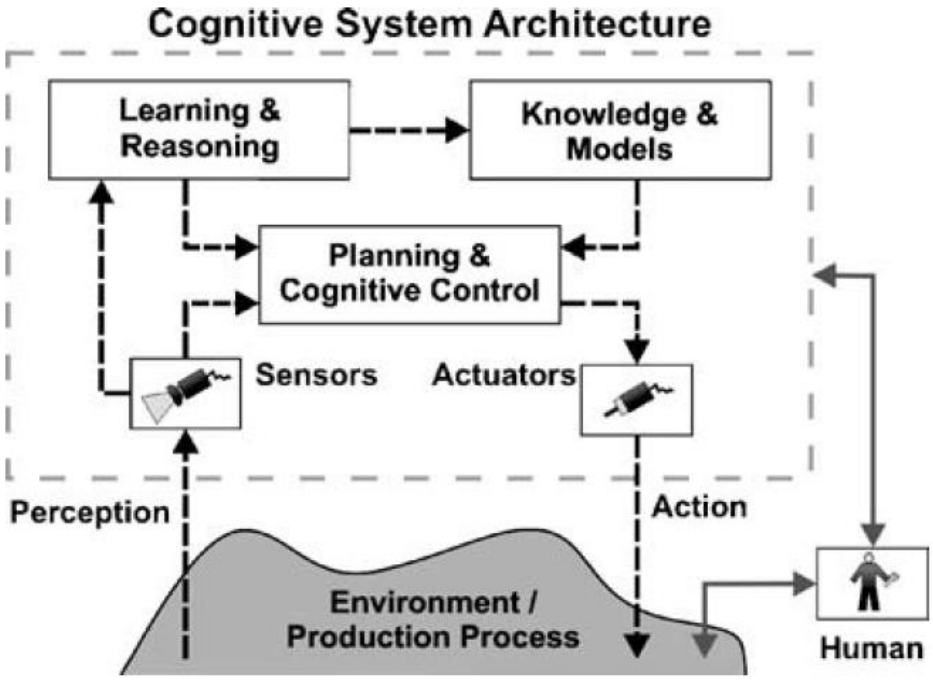


Figure 2.11 A block diagram of a typical cognitive robotic structure [146].

Many studies have employed F/T sensor to investigate different areas of assembly operations especially peg in hole assembly, however, using F/T sensor for peg out hole disassembly has not been studied fundamentally [147, 148]. Wang et al. [149] employed F/T sensors to analyse long peg and hole assembly and predict contact torque and forces. They proposed a model for robot position adjustment for large length-diameter ratio. Tang et al. [150] developed an autonomous system using force/torque sensor measurement for peg and hole robotic assembly. They used a three-point contact model between peg and hole to estimate position misalignment by measuring force data and analysing peg and hole geometry. Rigid dual peg-in-hole assembly was studied by Kuangen et al. using force/torque sensor and fuzzy

force control strategy was developed. Then they analysed contact forces and peg and hole contact states [151]. Utilising F/T sensor to develop new strategies for automated peg and hole assembly systems proven to be effective.

Automated disassembly Process of EOL products mostly contains high level of uncertainty. This uncertainty is largely due to the condition of the products. One area for disassembly research that F/T sensors can be effective is to deal with uncertainty and estimation of contact states. Generating force and torque maps from F/T sensor signal and using them to estimate position and orientation errors to tackle uncertainty seems to be applicable [152]. Force-torque maps can be de ned as contact state model of disassembly operation. During disassembly operation if peg is in contact with hole and a contact state is established, the position and orientation parameters can be obtained based on measured contact force and torques [153]. A drawback for this model is that online force-torque map generation requires collecting many data points for each contact states and it is considerably time consuming. Dietrich et al. [154] investigated force-torque maps and proposed a strategy reduce effect of friction and enhance force and position control based on force-torque maps.

Torque-force maps contain useful information; however, they need to be combined with other models and methods to be efficient. Employing classification models such as Neural Network and Gaussian mixtures model to improve generated maps can increase efficiency of automation [155]. Jasim et al. employed expectation maximisation based Gausian mixture model (EM-GMM) to address contact state monitoring problem for robotic assembly of peg and hole. They showed that

combined classification method can be effective for automated assembly based on force and torque information [156].

Full autonomous and robotic systems are not reliable enough to deal with complex disassembly tasks [157]. In practical disassembly shop floor, more likely both human and robot are required to work together in parallel and synchronously which called collaborative disassembly [158]. To improve disassembly efficiency of complex and high-volume products, collaborative disassembly is inevitable [159]. Harmony, collaboration and cooperation between different workers (human or robots) in a collaborative disassembly cell has been the subject of many studies recently [160]. For instance, optimisation of task classification, task planning and task allocation for robots and human collaboration results in improvement of disassembly efficiency [161].

For a long time, the manufacturing model was to separate the manual and robotic production and human-robot collaboration had remained an extensive R&D activity [162]. Introducing collaborative robots (cobots) along with intelligent algorithm and multi-model sensors, changed this trend and opened a new window in manufacturing shop floor, especially for disassembly operations. These systems employ the accuracy and repeatability of the robots along with the flexibility and ability to deal with complex tasks of human, to improve the reliability and efficiency of the disassembly process.

However, collaborative robots have been widely the subject of various research for assembly and employed in manufacturing assembly lines, their application for disassembly remains open for improvement [163]. It is considered that this area is in user experience stage that further theoretical and intelligence knowledge need to

be developed [164]. Main difficulties in this field are perceiving product location and motion, robot motion and human intention. In addition, the decision making for robot and human collaborations remains another major challenge. The decision-making algorithms should consider both experience-based knowledge of the collaborative cell elements along with the real-time dynamic of the process. Rapid and promising development of both computing power and artificial intelligence methods make the collaborative systems more feasible.

Human-robot collaborative disassembly method is a new approach to deal with EOL products. These methods employ the ability of dealing with complex tasks of human combined with accuracy and repeatability of the robots to propose a reliable and efficient method. The main gap in this field is that the characteristics of human-robot collaborative workcell are not established yet. Main aspects are yet to be defined and different literatures use different terminologies. In addition, task allocation to either human or robot remains a large gap. It is essential to have a method that assigns the disassembly tasks to the human or robot efficiently. Moreover, despite there are various disassembly sequence planning methods for manual and robotic disassembly process, there is a lack in literature for an efficient sequence planning method for human-robot collaboration.

2.7 Summary

The graph-based representation method interprets the product's model in a more illustrative approach. It represents the components and operations in nodes and arcs, to encode the product mathematically. However, as the number of the product's components increases, the number of the nodes and branches rises

dramatically and makes it impossible to encode all possible sub-assemblies graphically. Petri Net representation method is also a graph-based representation method. However, in this method sub-assemblies and components and conditions of disassembly operations are represented by places. This method improves the representation of the sub-assemblies, however, increases the computational time significantly. The matrix-based method improves the computational time of the mathematical encoding; however, the representation quality is highly dependent on the number and types of the defined matrices. In this research, a combination of graph and matrix-based representation methods is proposed to increase the efficiency of product representation. This approach ensures the use of illustrative advantages of the graph-based method and computationally efficiency of the matrix-based methods.

Researchers for disassembly sequence planning have considered the operation time as the main planning criteria. In addition, different parameters such as tool change have been converted in time unit. Using time-based parameters has different weaknesses and can be considered as an inefficient approach. One problem is that operation time is not constant and can be different for the same product with the different conditions. For instance, two same oil pump models with different ages can have different times for each operation. The other weakness is that to calculate actual operation time for each operation, the entire product should be disassembled to measure the operation time which is inefficient and for most cases infeasible. Therefore, in this work, the geometry of the product's component and difficulty of the disassembly operations are analysed and considered as the main disassembly sequence planning criteria. These parameters are based on the

disassemblability characteristics of the components and operations. Using disassemblability characteristics instead of time-based parameters is a new approach which is investigated in this work.

In addition, based on the surveying on the current literature, it is noticed that there is a lack of specific and comprehensive works on selective disassembly planning. In the other words, majority of the selective disassembly planning studies are part of the other proposed methods or developments such sequence optimization or product representation. There is a gap for an effective and independent selective disassembly planning method in this field. Therefore, in this thesis, Cleanability, Repairability and Economy are defined as the new remanufacturability parameters to target and select the product's components. The proposed method uses these parameters to prioritise the disassembly order of the components to increase the efficiency of the process.

Furthermore, it was noticed that most of the knowledge on the automated disassembly are based on the assembly process. Especially, mathematical, and experimental studies and the basic disassembly operations such as peg-out-hole, separation, unscrewing, etc. are missing in the current literature. Thus, a thorough theoretical study is carried out on the peg-out-hole as a basic disassembly operation to establish mathematical foundations. In addition, a new method is proposed and validated experimentally to tackle high-level uncertainty in automated disassembly processes.

Finally, it can be seen that the human-robot collaborative disassembly method is a new approach to deal with EOL products. The main gap in this field is that the characteristics of human-robot collaborative workcell are not established yet. Main

aspects are yet to be defined and different literature use different terminologies. In addition, task allocation to either human or robot remains a large gap. It is essential to have a method that assigns the disassembly tasks to the human or robot efficiently. Moreover, despite there are various disassembly sequence planning methods for manual and robotic disassembly process, there is a lack of literature for an efficient sequence planning method for human-robot collaboration. Therefore, in this research, a disassembly planning method based on human-robot collaboration is proposed. Also, human-robot collaboration characteristics are defined, and an algorithm is proposed to classify the disassembly task and allocate them to either human or robot.

Chapter 3- Disassembly Planning Based on Disassemblability Characteristics of Product Components

3.1 Introduction

Many studies have used different optimisation methods to find near-optimal solution by optimising the disassembly operations sequence. These studies have used disassembly operation time as the main optimisation parameter, and other parameters such as direction change, or tool change are converted to time scale. To determine accurate operation time, a product needs to be completely disassembled, noting that same EOL products can be in a different condition and result in a different operation time. Furthermore, same operation in different sequence order can have a different disassembly time. In addition, in real industrial cases, a product does not usually disassemble completely; the disassembly process continues until the targeted components are disassembled. The aim of this chapter is to investigate the current manual disassembly planning parameters and establish a new planning method based on disassemblability of the components. In this chapter, new optimisation parameters based on the disassemblability and components demand are defined. These include Disassembly Handling Index (DHI), Disassembly Operation Index (DOI) and Disassembly Demand Index (DDI). To consider the operation time and other costs, Disassembly Cost Index (DCI) is further defined. A modified Genetic Algorithm optimisation method was employed to optimise the process sequence. Here, the most demanded components with the

easiest disassembly operations are disassembled first without requiring disassembling the unwanted components and avoid complicated operations. Two case studies were analysed to determine the effectiveness and compatibility of this method. The results and developed method in this chapter is used to support objective 3 and achieve the project overall aim.

3.2 Methodology

3.2.1 Introducing new parameters for intelligent selective disassembly planning

A full disassembly plan allows a product to be fully disassembled. However, in realistic industry problems a product does not require to be fully disassembled and it can be inefficient. Full disassembly plan disassembles all the individual parts of the product regardless of the disassembly process requirement. Selective disassembly planning considers the disassembly aims and objectives and makes it efficient and practical. The total number of required operations in full disassembly plan is n and the number of required operations in selective disassembly is m where $n \geq m$. In selective disassembly some parts are indicated as target parts to be disassembled and disassembly process will be continued until the target parts are disassembled.

Since the early 1990s to solve the disassembly sequence problems, researchers have started to use intelligent heuristic methods and majority of studies are going in this direction. The mainly accepted methodology among the professional is “graph model + solving method”. Howe e r, some differences among these methods are noticed, the main idea is same. Based on the “graph model + sol i ng method”

disassembly planning problems can be divided into three sub-problems: a) product disassembly modelling b) sequence generating c) disassembly sequence optimization. Most of the researches on disassembly sequence optimization have focused on cost and time of the disassembly operations as the main parameters of disassembly optimization. Using times and costs of disassembly operations as the main optimization parameter lead to inaccurate and unrealistic results. First, majority of the studies estimate the time of a disassembly operation as measuring actual times of operations requires to disassemble product completely. Also, same EOL products have different condition which leads to different time for same operation. Secondly, same disassembly operation in different sequence of operations has different disassembly time and measuring or estimating all this time can be problematic.

Therefore, in this section Disassembly Handling Index (DHI) and Disassembly Operation Index (DOI) are introduced to consider the difficulty and feasibility of the disassembly operations as the main optimization parameters instead of the time and cost. Main advantage of this method is that the disassembly operations can be evaluated easily and quickly without need to disassemble the EOL product. Also, this evaluation can be done for same EOL product with different condition individually. Furthermore, Disassembly Demand Index (DDI) is defined to prioritise the demand for each component. This parameter indicates the level of demand for each component in the product. In addition to these parameters, Disassembly Cost Index (DCI) is defined to include costs and times of disassembly operations. In a sequence of disassembly process the operation for component i is shown as Op(i) and the position of the Op(i) in the sequence is shown as Pos(Op(i)).

3.2.2 Disassembly Handling Index

First parameter for new approach to the intelligent disassembly planning is the Disassembly Handling Index (DHI). Disassembly Handling Index is found by analysing the part's shape, size, weight, orientation, part handling difficulty, and where it fits into the product. To analyse each part's disassembly handling a table that categorises the product parts is defined, which is shown in Table 3.1. This categorisation is based on the part's geometric characteristics and also the handling of the parts during a disassembly operation. DHI analyses each part of the product using three parameters; A. size of part, B. weight of part, and C. shape of the part. As it can be seen from Table 3.1, each characteristics of a part allocated with a score. Higher score means that the part is more difficult to be handled during a disassembly operation. First, Part Handling Index (PHI) for each part P(i) is defined as below:

PHI(P(i))=A+B+C (3.1)

Where A, B, and C can be found using Table 3.1. For example for P(1), a difficult to be grasped part (A=4), light (B=2) and symmetric (C=0.8), PHI(P(1))=6.8.

Then DHI for a set of operations during disassembly process is calculated as below:

$$DHI = \sum_{i=1}^{n} PHI(P(i))/Pos(P(i)) \qquad (3.2)$$

Where Pos(P(i)) is the position of the part in the disassembly process sequence. For example if P(1) with PHI(P(1)) is disassembled with the third operation it need to be divided by 3. A smaller DHI indicate that the parts that are easier to be handled are disassembled first and ensures that the unnecessary parts with high PHI will not be disassembled. Dividing PHI(P(i)) by Pos(P(i)) allows to the algorithm to arrange

the disassembly process in a way that the parts with smaller PHI be disassembled earlier. For example, consider component {P1, P2, P3} with PHI {2, 4, 6} respectively. Now Assume two possible disassembly sequences as seq1={P2, P1, P3} and seq2={P3, P2, P1}. For seq1, DHI=(4/1+2/2+6/3)=7 and for seq2, DHI=(6/1+4/2+2/3)=8.67. It can be seen that, DHI1 is smaller than DHI2 therefore component with higher PHI i.e. P3 is at the end of the sequence, while for seq2 with higher DHI, P3 is at the beginning of the sequence.

Table 3.1. Disassembly Handling categories and scores [165].

A. Component Size ***One*** **of the following:**		**C. Component shape** ***One*** **of the following:**	
Easily grasped	2	Light and symmetric	0.8
Moderately difficult to grasp	3.5	Light and semi-symmetric	1.2
Difficult to grasp	4	Light and asymmetric	1.4
B. Component weight ***One*** **of the following:**		Moderately heavy, symmetric	2
		Moderately heavy, semi-symmetric	2.2
		Moderately heavy, asymmetric	2.4
Light (<7.5 lb)	2	Heavy and symmetric	4.4
Moderately heavy (<17.5 lb)	2.5	Heavy and semi-symmetric	4.6
Very heavy (<27.5 lb)	3	Heavy and asymmetric	5

3.2.3 Disassembly operation Index

Disassembly Operation Index (DOI) analyses the difficulty of each operation in disassembly process. In order to calculate the DOI, main disassembly operations were categorised into four categories; A. Disassembly force, B. Requirement of tools for disassembly, C. Accessibility of joints/grooves, and D. Positioning. Each category has several sub-categories to which a score is given which can be seen in Table 3.2. Higher score indicates that an operation is more difficult to be carried out in disassembly process. Disassembly Operation Index (DOI) for each operation Op(i) is computed as below:

DOI(Op(i))=A+B+C+D (3.3)

Where A, B, C, and D can be found using Table 3.2. For instance Op(1), a pull operations with hand with moderate effort (A=1), with common tool requirement (B=2), on a plane surface (C=1) and symmetry with high accuracy requirement (D=5) has DOI(Op(1))=9.

Disassembly Process Index (DPI) all operation in a selective disassembly process is computed as below:

$$DPI = \sum_{i=1}^{n} DOI(OP(i))/Pos(Op(i)) \quad (3.4)$$

Where Pos(Op(i)) is the position of the operation in the disassembly process sequence. For example if Op(1) with DOI(Op(1)) is the third operation in the sequence it need to be divided by 3. A smaller DPI is beneficial by which the operations with lower DOI is carried out first and ensures that the unnecessary and difficult operations will not be carried out. Dividing DOI(Op(i)) by Pos(Op(i)) allows to the algorithm that arrange the disassembly process in a way that the operations with smaller DOI be started earlier.

3.2.4 Disassembly Demand Index

In selective disassembly planning the goal is to first disassemble specific targeted components without disassembling the product completely. In this research, Disassembly Demand Index (DDI) is defined to optimise the disassembly process

in a way that the most demanded components disassembled first without disassembling unwanted components. Therefore, the level of demand of each component is categorised in four level, i.e. low, medium, high and very high which can be represented quantitatively by (5, 3, 1, 0) for (low, medium, high and very high) respectively. DDI can be calculated using the following equation:

$$DDI = \sum_{i=1}^{n} LD(i)/Pos(i) \qquad (3.5)$$

Where LD(i) is the level of demand of the component i and Pos(i) is the position of the component i in the disassembly sequence. For example, for sequence of operations of (3, 1, 4, 2) and LD of (5, 3, 0, 2) respectively, DDI=5/3+3/1+0/4+2/2=5.67.

3.2.5 Disassembly Cost Index

Disassembly Cost nde DC is defined to analyse each operation's cost to disassemble a specific part of the product in a disassembly process in term of time. It can be used to determine the cost of each operation to allow the operations with lower cost be carried out earlier. DCI can include different operation costs which all converted in time unit. In this research DCI parameters are as below:

Operation Time:

The basic time require to disassemble part P(i) using operation Op(i) is shown as OT(Op(i)). As the CDI need to have the same effect as the other parameters in optimisation algorithm the operation times are normalised as below:

$$OT_N(Op(i)) = \frac{OT(Op(i)) - OT_{min}}{OT_{max} - OT_{min}} \qquad (3.6)$$

Where $OT_n(Op(i))$ is the normalised time for each operation and OT_{max} and OT_{min} represent the maximum and minimum operation times of all possible disassembly operations respectively.

Table 3.2. Disassembly operation categories and scores [165].

A. Disassembly force One of the following			**C. Accessibility One of the following**		
Push/pull operations with hand, Straight line motion without exertion of pressure	Little effort required	0.5	Dimensions	Shallow and broad fastener recesses	1
	Moderate effort required	1		Deep and narrow fastener recesses	1.6
	Large amount of effort required	3		Very deep and very narrow fastener recesses	2
Twisting and push/pull operations with hand, Straight line and twisting motion without pressure	Little effort required	1	Location	On plane surface	1
	Moderate effort required	2		On angular surface	1.6
	Large amount of effort required	4		In a slot	2
Inter-surface friction and/or wedging, Straight line motion with exertion of pressure	Little effort required	2.5	**D. Positioning One of the following**		
	Moderate effort required	3	Level of accuracy required to position the tool-Symmetry	No accuracy required	1.2
	Large amount of effort required	5		Some accuracy required	2
Inter-surface friction and/or wedging, Straight line and twisting motions with exertion of pressure	Little effort required	3		High accuracy required	5
	Moderate effort required	3.5	Level of accuracy required to position the tool-Asymmetry	No accuracy required	1.6
	Large amount of effort required	5.5		Some accuracy required	2.5
Material stiffness, Twisting motions with pressure exertion	Little effort required	3		High accuracy required	5.5
	Moderate effort required	4.5			
	Large amount of effort required	6.5			
B. Requirement of tools for disassembly One of the following					
Exertion of force	No tools required	1	Exertion of torque	No tools required	1
	Common tools required	2		Common tools required	2
	Specialized tools required	3		Specialized tools required	3

Tool Change:

The other parameter of DCI is Tool Change. In this work tool changing for an operation is penalized in time unit.

$$TC(Op(i)) = \begin{cases} 0\ (s) \text{ if tool changed} \\ 1\ (s) \text{ if tool not changed} \end{cases} \quad (3.7)$$

Where (s) represents time unit in second.

Disposal Cost:

Finally, the last factor is the disposal cost of a part after it is disassembled. If after a disassembly process a part of the product is not reusable and it costs to be disposed of, the operation will be penalized in time unit:

$$DC(Op(i)) = \begin{cases} 0\ (s) \text{ if part is reusable} \\ 1\ (s) \text{ if part is not reusable} \end{cases} \quad (3.8)$$

Now total DCI for disassembly process can be calculated:

$$DCI = \sum_{i=1}^{n} OT_N\big(Op(i)\big)/Pos\big(Op(i)\big) + \sum_{i=1}^{n} TC(Op(i))/Pos\big(Op(i)\big) + \sum_{i=1}^{n} \mathrm{DC(Op(i))}/Pos\big(Op(i)\big) \quad (3.9)$$

3.3 Improved genetic algorithm optimisation

3.3.1 Disassembly representation using Hybrid graph model

Graph based methods such as AND/OR which introduced by Lambert and Homem is widely used to represent disassembly sequences and precedencies space, however the number of nodes rises dramatically by rising the number of the components. For example, there will be 16383 nodes in the AND/OR graph if the product consists of 14 components. In this work a hybrid graph method is used to represent disassembly sequences and precedencies space. The hybrid graph method describes the topological structure of the product in form of a graph. It defines the relationships of the constrains between the components of the product using a four-tuple, G = {V; Ef; Efc; Ec}. In this four-tuple nodes set V={v1, v2, v3, .., vn} defines a minimum disassembly component unit (part or sub-assembly) where n is the number of units. Ef={ef_1, .. ef_i} represents the contact constraints between two components and is shown using an undirected solid line. Efc={efc_1, .., efc_j} is disassembly contacted constraints and precedence between two components and is shown using a directed solid line. Direct of the line defines the disassembly precedence between the components. Finally Ec={ec_1, …, ec_k} which is represented by a directed dashed line defines the disassembly precedence constraints for two non-connected components.

3.3.2 Disassembly Feasibility and constraint matrices

Relation between product components and disassembly constraints are represented mathematically by two matrices:

1- Components relation matrix detonated by C_r which represents relationship between product components:

$$C_r = \{cr_{ij}\}_{n\times n} = \begin{bmatrix} cr_{11} & cr_{12} & \cdots & cr_{1n} \\ cr_{21} & cr_{22} & \cdots & cr_{2n} \\ \vdots & \vdots & \ddots & \vdots \\ cr_{n1} & cr_{n2} & \cdots & cr_{nn} \end{bmatrix} \quad (3.10)$$

Where, i,j=1, 2, 3, …, n and

$$cr_{ij} = \begin{cases} 1 & if\ (v_i, v_j) \in E_f \\ 2 & if\ (v_i, v_j)\ or\ (v_j, v_i) \in E_{fc} \\ 0 & else \end{cases} \quad (3.11)$$

2- Disassembly constraints matrix, D_c, represents the disassembly constraints mathematically

$$D_c = \{dc_{ij}\}_{n\times n} = \begin{bmatrix} dc_{11} & dc_{12} & \cdots & dc_{1n} \\ dc_{21} & dc_{22} & \cdots & dc_{2n} \\ \vdots & \vdots & \ddots & \vdots \\ dc_{n1} & dc_{n2} & \cdots & dc_{nn} \end{bmatrix} \quad (3.12)$$

Where i,j=1, 2, 3, …, n and

$$dc_{ij} = \begin{cases} 1 & if\ (v_i,v_j) \in E_c \\ 2 & if\ (v_i,v_j)\ or\ (v_j,v_i) \in E_{fc} \\ 0 & else \end{cases} \quad (3.13)$$

This matrix provides geometrical constraints and disassembly precedencies to determine whether a part can be disassembled without restriction. Unit v_j can be disassembled if:

$$\sum_{i=1}^{n} dc_{ij} = 0\ and\ \sum_{i=1}^{n} cr_{ij} > 0 \quad (3.14)$$

3.3.3 GA Parameters and operators

Several studies have investigated different optimization methods in order to find optimum disassembly sequences such as ant colony optimization (ACO), simulated annealing and genetic algorithm (GA). Genetic algorithm is a nature inspired method based on the Darwin's natural selection of evolution. It has been used for optimising constrained and unconstrained problem. GA repeatedly modify and generate new population of possible solutions as a new generation. In order to produce new generation, better solutions of current population combined together and mutate to produce offspring. The aim is that the characteristics of the better solutions pass to the next generation and population evolve toward an optimum solution. To initiate the algorithm a set of the possible solutions which called population, is selected in which any member can be encoded as chromosome. A chromosome is identified using a combination of several different characters. Different characteristics of product and disassembly can be encoded in each chromosome. Then chromosomes are given scores. These scores are based on a fitness function. The fitness function depends on the disassembly parameters which in this work are DHI, DOI, DDI and DCI. To identify a chromosome with optimum score, new population need to be generated iteratively in each step in which mutation can happen. Also, the crossover may happen in which two different chromosomes can mate and a child is produced. Depend on the disassembly aim and objectives the disassembly parameters in objective function can be customised by using different weights. In the following these parameters are defined:

- **Chromosome representation**

To represent the disassembly solutions and parameters the disassembly sequences are encoded in chromosomes. A chromosome is a sting of genes that occupy specific locations in a chromosome. Parameters of the disassembly operations are encoded in each chromosome as genes. Each chromosome indicates disassembly sequence and its operations characteristics. A combination of numbers and other characters are used to encode solutions and parameters. For example, if disassembly process has five variables, they will be codified in a chromosome form composed of five equal section in which each parameters of operations are represented respectively. In this research each chromosome consists of five string; Sequence, Disassembly Handling Index (DHI), Disassembly Operation Index (DOI), Disassembly Demand Index (DDI) and Disassembly Cost Index (DCI).

- **Objective function**

An objective function was defined to evaluate the chromosomes and find their fitness level. This function depends on the disassembly process parameters. In this work, these parameters are Disassembly Handling Index (DHI), Disassembly Operation Index (DOI), Disassembly Demand Index (DDI) and Disassembly Cost Index (DCI) which previously were defined. Therefore, the objective function is calculated as follows:

$$f(ch, gn) = \alpha DHI + \beta DOI + \gamma DDI + \varepsilon DCI \qquad (3.15)$$

Where $f(ch, gn)$, is the fitness value of the chth chromosome in the gnth generation and $\alpha, \beta, \gamma \; and \; \varepsilon$ are user defined weights for disassembly process parameters

which are dependent on the aims and objectives of the disassembly. In this research the objective of the GA is to minimise the fitness function by minimising DHI, DOI, DDI and DCI of each chromosome.

- **Initial population**

To initiate the optimisation algorithm a series of randomly selected chromosomes are considered as initial population. The number of chromosomes in initial population (ncr) is defined depends on the disassembly process characteristics. Higher ncr can result higher numerical calculation time while smaller ncr can result wrong solutions. All constraints and other relationships based on structure graph (feasible solutions) must be satisfied among these chromosomes. In this work ncr was examined and the optimum ncr subject to optimum numerical calculation time and better solution was selected.

-Chromosome selection

Roulette wheel technique was employed to select chromosomes of each generation as parents to generate new population. In roulette wheel technique each chromosome is assigned a probability of selection based on its fitness level. Probability of a chromosome to be selected is calculated by Equation (3.16).

$$P_i = \frac{1}{f_i \sum_{j=1}^{n} \frac{1}{f_j}} \qquad (3.16)$$

Where f_i is the fitness value of individual chromosome in the population. This technique is used to assure that the chromosomes with the lower fitness level is selected. However, some chromosomes with higher fitness value can be selected as parents of new generation.

- **crossover**

To generate new population, crossover operator must be applied on the most efficient chromosomes of the previous generation. In this study, the precedence preservative crossover (PPX) was employed to generate new populations. In this methodology, two chromosomes are selected as parents and considered as parent 1 and parent 2. The algorithm starts with generating randomly selected masks which contain 1 and 2 and have the same length of the first section of the chromosomes. These masks impose the order of each child in a new generation. Then an empty offspring is initialized, and crossover operation based on the relative mask is applied and the offspring chromosome is filled with new genes. The mask specifies that which parent should be considered to select the gene and after the selected gene will be removed from both parents. This algorithm is repeated until both parents are emptied and a new child is generated. As an example, consider the first two chromosomes of the initial population as parent 1 and parent 2 respectively. Two randomly selected masks which contain 1 and 2 to generate child 1 and child 2 are:

Mask 1: 1 2 1 2 2 2 1

Mask 2: 2 1 1 2 2 1 2

Using (PPX) method to generate new population, the chromosomes of child 1 and child 2 are as follows:

Child 1: 1 7 5 3 6 2 4

Child 2: 7 1 5 3 6 4 2

- **mutation**

After a new population is generated using crossover operation the chromosomes are subjected to mutation. Mutation is not a dominate operator in genetic algorithm

method and just a small number of the chromosomes are subjected to mutation. Several chromosomes are selected randomly, and some genes are exchanged. The mutation happens with a defined mutation probability Pm and in such a way that all relations and constraints are preserved. The mutation operation preserves the diversity of the chromosomes and makes sure that the new solution candidates are explored. In this study, swap technique was used as the mutation operator and different probabilities were investigated. If a chromosome is selected its genes will be subjected to mutation otherwise its properties will be preserved, and it remains unchanged.

- **termination conditions**

Two conditions are set to terminate GA calculations. If one of these conditions is met GA will be terminated. First condition is that if the number of produced generations exceeds a maximum value GA will be terminated (In this work 40). Second condition is that if the difference between the average fitness of the new generation and the fitness of the previous generation is smaller than a pre-defined number, i.e., the solutions is remaining constant.

3.4 Case study and performance analysis

3.4.1 Case study 1: Turbocharger

As the first case study, a turbocharger supplied by Reco Turbo Ltd. is selected to verify the proposed method. It is made by BorgWarner and is used in different cars such as Renault, Nissan and Dacia. Figures 3.1(a), 3.1(b) and 3.1(c) show the turbocharger, CAD model and exploded drawing. As it can be seen the turbocharger made of 12 individual components which can be categorised into 7

different types; A, B, C, D, E, F and G. Components such as A and C can be disassembled further, but in this work, they assumed as individual components that do not require further disassembly. The properties and required disassembly tasks for all individual components are shown in Table 3.3. The main disassembly operations to disassemble the product completely are unscrewing and removing.

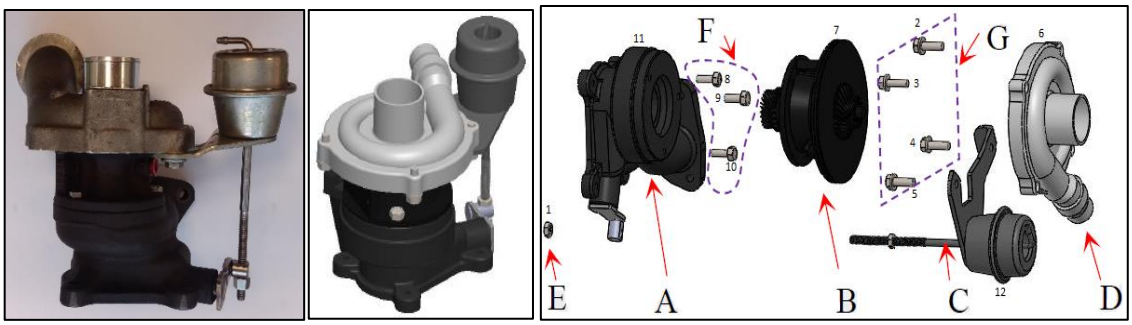


Figure 3.1. (a) BorgWarner turbocharger (b) Turbocharger CAD model (c) Turbocharger exploded view

It is assumed that whole disassembly process is carried out manually. The penalty time for tool change is calculated by Equation (3.6). In order to disassemble this product completely one spanner and one hammer are required. Also, disposal cost penalty is described by Equation (3.7). Figure 3.2 shows a general flow chart of the proposed model.

Table 3.3 The properties and required disassembly tasks for all individual components

Number	Component	Disassembly task	Disassembly tool	Reusable	Disassembly point (x,y,z)(mm)	Mass (g)	Demand
1	Nut	Unscrewing	Spanner	No	(175, 75, 0)	4	Low
2	Bolt 1	Unscrewing	Spanner	No	(50, 100, 100)	7.5	Low
3	Bolt 2	Unscrewing	Spanner	No	(50, 30, 100)	7.5	Low
4	Bolt 3	Unscrewing	Spanner	No	(100, 30, 100)	7.5	Low
5	Bolt 4	Unscrewing	Spanner	No	(100, 100, 100)	7.5	Low
6	Turbine housing	Removing	Hammer	Yes	(80, 80, 105)	1770	Very High
7	Cartridge	Removing	Hammer	Yes	(80, 80, 70)	1174	High
8	Bolt 5	Unscrewing	Spanner	No	(60, 60, 50)	5	Low
9	Bolt 6	Unscrewing	Spanner	No	(65, 70, 50)	5	Low
10	Bolt 7	Unscrewing	Spanner	No	(70, 65, 50)	5	Low
11	Compressor Housing	Removing	No tool	Yes	(80, 80, 50)	480	Very High
12	Electronic Actuator	Removing	No tool	Yes	(140, 50, 105)	260	Medium

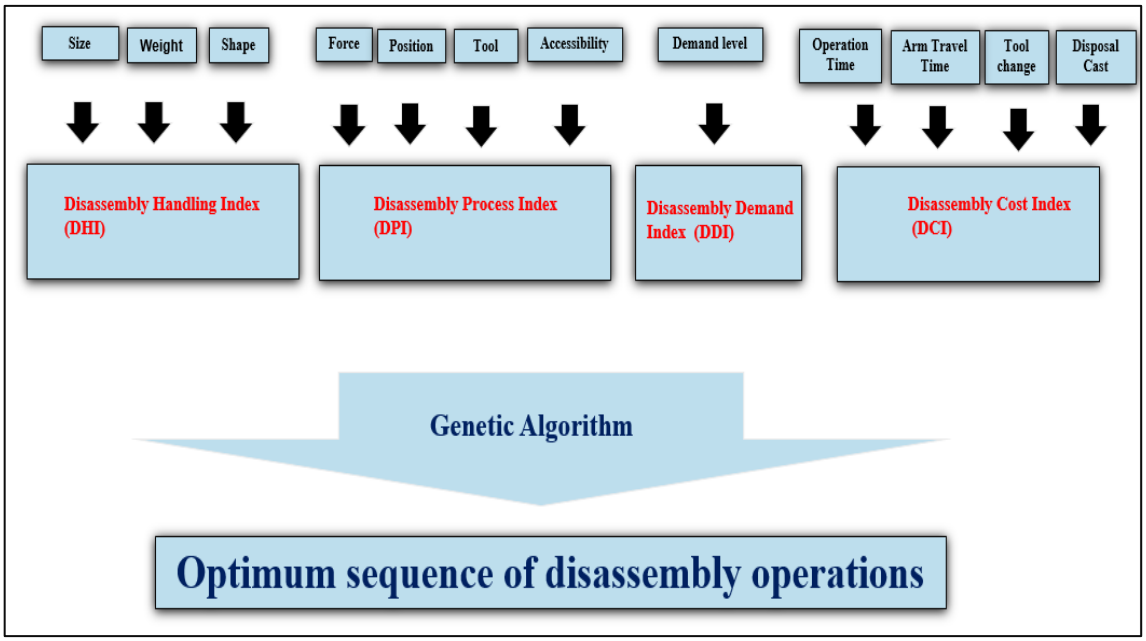


Figure 3.2 Flow chart of the proposed model.

Proposed Genetic Algorithm method was programmed on MATLAB© (version: 8.5.0 (R2015a)). Then it was run on a computer with ntel® Core™ i5 6500 C @ 3.2 GHz and 8.00 GB RAM. In this section, first convergence capability of the proposed method is discussed and performance of this method for different iteration and generation is investigated. Then, optimum sequence of the operations based on this method is obtained and discussed. Finally, in order to validate this method, the turbocharger is disassembled based on the sequences proposed by this method, conventional time-based genetic algorithm and total disassembly time compared.

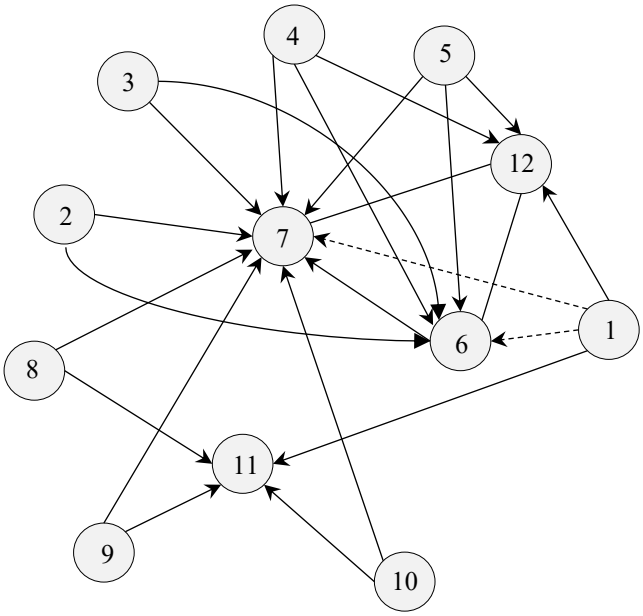


Figure 3.3 Hybrid graph model for turbocharger

To represent the product disassembly proceedings and constraints mathematically, hybrid graph method is used. Figure 3.3 shows the hybrid graph model for turbocharger. It is constructed according the rules described in section 3.2. Based this model relation matrix Cr and constraint matrix Dc are as followings:

$$Cr = \begin{bmatrix} 0 & 0 & 0 & 0 & 0 & 0 & 0 & 0 & 0 & 0 & 2 & 2 \\ 0 & 0 & 0 & 0 & 0 & 2 & 2 & 0 & 0 & 0 & 0 & 0 \\ 0 & 0 & 0 & 0 & 0 & 2 & 2 & 0 & 0 & 0 & 0 & 0 \\ 0 & 0 & 0 & 0 & 0 & 2 & 2 & 0 & 0 & 0 & 0 & 2 \\ 0 & 0 & 0 & 0 & 0 & 2 & 2 & 0 & 0 & 0 & 0 & 2 \\ 0 & 2 & 2 & 2 & 2 & 0 & 2 & 0 & 0 & 0 & 0 & 1 \\ 0 & 2 & 2 & 2 & 2 & 2 & 0 & 2 & 2 & 2 & 0 & 1 \\ 0 & 0 & 0 & 0 & 0 & 0 & 2 & 0 & 0 & 0 & 2 & 0 \\ 0 & 0 & 0 & 0 & 0 & 0 & 2 & 0 & 0 & 0 & 2 & 0 \\ 0 & 0 & 0 & 0 & 0 & 0 & 2 & 0 & 0 & 0 & 2 & 0 \\ 2 & 0 & 0 & 0 & 0 & 0 & 0 & 2 & 2 & 2 & 0 & 0 \\ 2 & 0 & 0 & 2 & 2 & 1 & 1 & 0 & 0 & 0 & 0 & 0 \end{bmatrix}$$

$$Dc = \begin{bmatrix} 0 & 0 & 0 & 0 & 0 & 1 & 1 & 0 & 0 & 0 & 2 & 2 \\ 0 & 0 & 0 & 0 & 0 & 2 & 2 & 0 & 0 & 0 & 0 & 0 \\ 0 & 0 & 0 & 0 & 0 & 2 & 2 & 0 & 0 & 0 & 0 & 0 \\ 0 & 0 & 0 & 0 & 0 & 2 & 2 & 0 & 0 & 0 & 0 & 2 \\ 0 & 0 & 0 & 0 & 0 & 2 & 2 & 0 & 0 & 0 & 0 & 2 \\ 0 & 0 & 0 & 0 & 0 & 0 & 2 & 0 & 0 & 0 & 0 & 0 \\ 0 & 0 & 0 & 0 & 0 & 0 & 0 & 0 & 0 & 0 & 0 & 0 \\ 0 & 0 & 0 & 0 & 0 & 0 & 2 & 0 & 0 & 0 & 2 & 0 \\ 0 & 0 & 0 & 0 & 0 & 0 & 2 & 0 & 0 & 0 & 2 & 0 \\ 0 & 0 & 0 & 0 & 0 & 0 & 0 & 0 & 0 & 0 & 2 & 0 \\ 0 & 0 & 0 & 0 & 0 & 0 & 0 & 0 & 0 & 0 & 0 & 0 \\ 0 & 0 & 0 & 0 & 0 & 0 & 0 & 0 & 0 & 0 & 0 & 0 \end{bmatrix}$$

Table 3.4 shows the Disassembly Handling analysis, Disassembly operation analysis and demand for the product which calculated using Tables 3.1, 3.2 and 3.3. For each component, size, weight, and shape were considered to find PHI using Equation (3.1) and Table 3.4. Then DHI was calculated using Equation (3.2). To analyse the Disassembly Operation for each component, force, requirement of tool, accessibility and positioning were considered. The values for these properties are shown in Table 3.4 which were used in Equation (3.3) to calculate DOI. Then, DPI was calculated using Equation 3.4. Finally, based on the demand level in Table 3.3, demand for each component was determined.

Table 3.4 Disassembly handling analysis and Disassembly operation analysis for turbocharger.

Number	Component	Disassembly Handling analysis			Disassembly Operation analysis				Demand
		Size	weight	shape	force	Tools requirement	Accessibility	Positioning	
1	Nut	2	2	0.8	4	2	1	2	5
2	Bolt 1	2	2	0.8	4	2	1	2	5
3	Bolt 2	2	2	0.8	4	2	1	2	5
4	Bolt 3	2	2	0.8	4	2	1	2	5
5	Bolt 4	2	2	0.8	4	2	1	2	5
6	Turbine housing	4	2	1.4	1	3	1	1.2	0
7	Cartridge	3.5	2	1.2	3	3	1.6	1.2	1
8	Bolt 5	2	2	0.8	4	2	2	5	5
9	Bolt 6	2	2	0.8	4	2	2	5	5
10	Bolt 7	2	2	0.8	4	2	2	5	5
11	Compressor Housing	3.5	2	1.2	1	3	1	1.2	0
12	Electronic Actuator	2	2	1.2	1	3	1	1.2	3

In this work it is assumed that the basic operation time to disassemble a component is constant and does not depend on the position of the operation in the sequence. Different initial population numbers (ncr) were examined to determine the optimum convergence time and more realistic solutions. Figures 3.4(a) and 3.4(b) show the calculating time and average fitness values under different population number respectively. It can be seen that higher ncr results in higher calculating time, however, it leads to lower average fitness values. It can be seen after ncr=30 the average fitness value remains constant; however, the calculating time rises with increasing the ncr. Therefore, ncr=30 was selected as the optimum population number for this study. Figure 3.5(a) and 3.5(b) show the average fitness values and calculating time under different number of generations.

The effects of different mutation probabilities on the proposed method characteristics were studies. Average fitness values trends and calculation times for different probabilities are shown in Figures 3.6(a) and 3.6(b) respectively. It can be seen that mutation probability has a significant effect on both fitness value and

calculating time. Selecting a very small or very high mutation probability leads to higher calculating time and higher average fitness function. Therefore, choosing an optimum mutation probability to achieve an optimum solution is essential. Analysing these results show that the mutation probability from 0.1 to 0.15 gives best results, which minimise both calculating time and fitness value.

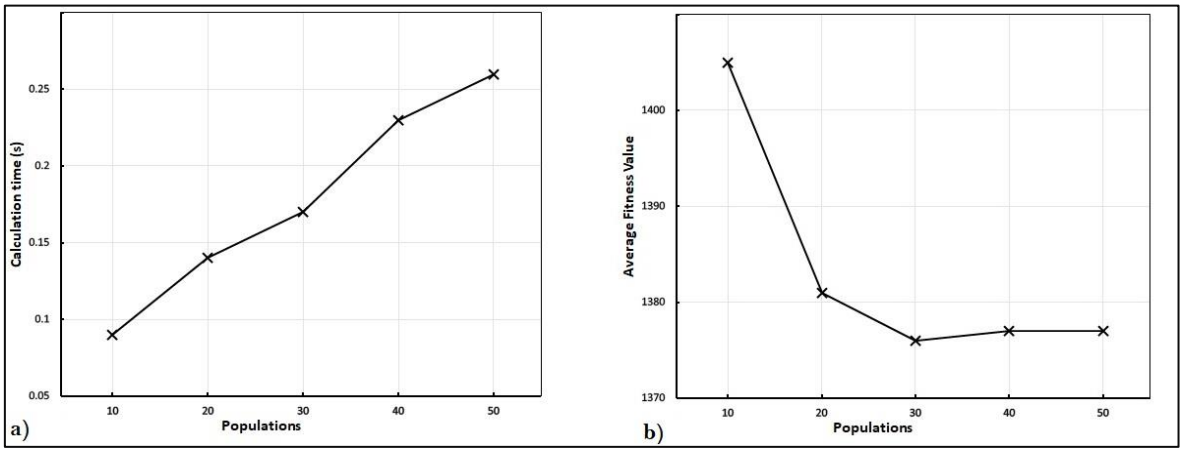


Figure 3.4 a) Calculation time under different population b) Average fitness values under different population number.

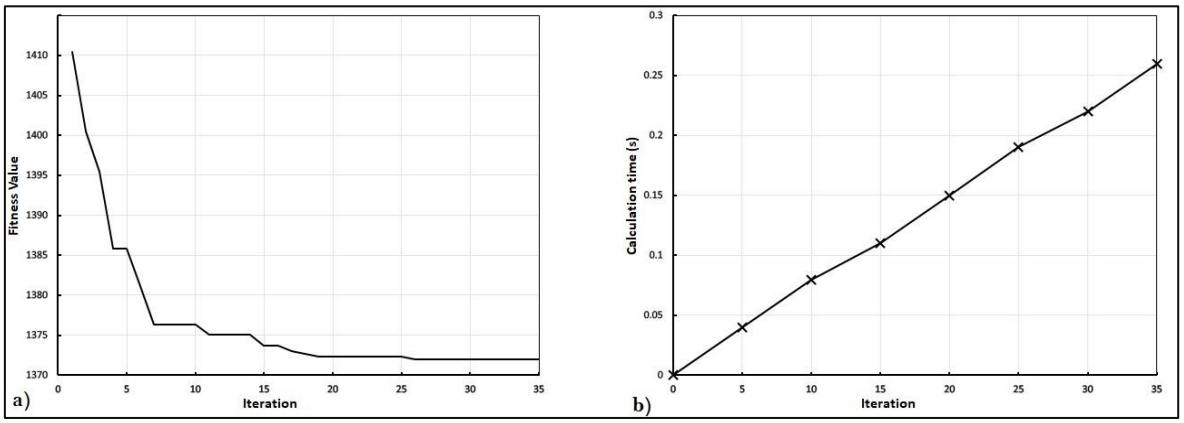


Figure 3.5 a) Average fitness values under different generations b) Running time under different generation number.

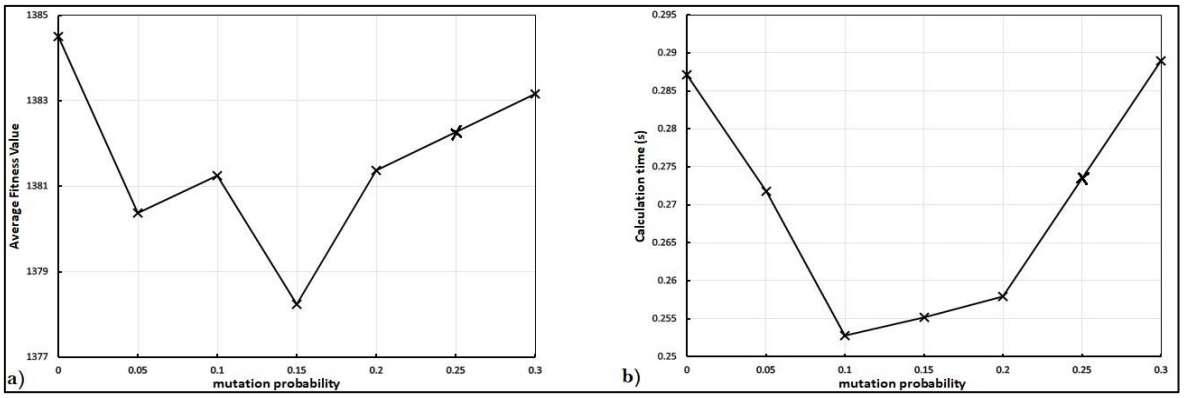


Figure 3.6 a) Average fitness values under different probability b) Running time under different probability.

The optimum disassembly process sequence based on the proposed model and its fitness value is shown in Table 3.5. This optimised solution was achieved in 0.25 second using proposed method.

Table 3.5 Final optimum disassembly process sequence based on the proposed method in this work.

Optimum solution	*F(ch,gn)*
1→ 4 → 5 →12 → 2 → 3 → 6 → 8 → 9 → 10 → 7→ 11	1362.0333

In order to compare the proposed method with conventional methods, the turbocharger was disassembled manually based on the sequences generated by this research and conventional GA method and operations times and the total disassembly process time were measured. To generate a sequence based on the conventional GA, the method proposed by Parsa and Saadat [20] was employed. Based on their method, the main parameter for GA objective function to find an optimum solution is basic operations times which should be estimated to initiate the algorithm. Also, as in this research the method for disassembly is manual, the algorithm used at [20] was modified to remove the automation parameter i.e. time

travel of the robot arm. The sequence generated using this method cam be seen in Table 3.6.

Table 3.6 Optimum disassembly process sequence generated by conventional time-based method.

Optimum solution	*F(ch,gn)*
8 → 9 → 10 → 4 → 3 → 5 → 2 → 1 → 6 → 12 → 11 → 7	1372.0333

Then, the turbocharger was disassembled 5 times to minimize the error and mean times for operations and total disassembly process calculated. The disassembled turbocharger can be seen in Figure 3.7. Also, the turbocharger was disassembled 5 times based on the sequence generated by conventional GA method and mean times calculated. The measured and calculated times are shown in Table 3.7.

Table 3.7 Disassembly operations and process times for turbocharger.

Disassembly operations and process times based on proposed method							**Disassembly operations and process times based on conventional method**						
Disassembled part	**Trial 1 (s)**	**Trial 2 (s)**	**Trial 3 (s)**	**Trial 4 (s)**	**Trial 5 (s)**	**Mean Time(s)**	**Disassembled part**	**Trial 1 (s)**	**Trial 2 (s)**	**Trial 3 (s)**	**Trial 4 (s)**	**Trial 5 (s)**	**Mean Time(s)**
1-Nut	8	8	7	9	7	**7.8**	8-Bolt 5	26	25	30	24	26	**26.2**
4-Bolt 3	20	17	18	21	22	**19.6**	9-Bolt 6	24	22	26	26	23	**24.2**
5-Bolt 4	22	27	25	24	20	**23.6**	10-Bolt 7	26	22	21	30	28	**25.4**
12-Electric Actu.	7	5	5	8	8	**6.6**	4-Bolt 3	24	30	29	20	21	**24.8**
2-Bolt 1	20	26	23	22	23	**22.8**	3-Bolt 2	22	23	25	20	25	**23**
3-Bolt 2	24	20	22	23	19	**21.6**	5-Bolt 4	28	28	35	35	25	**30.2**
6-Turbine hous.	10	9	8	11	8	**9.2**	2-Bolt 1	23	20	23	26	24	**23.2**
8-Bolt 5	20	21	23	25	20	**21.8**	1-Nut	8	8	7	7	9	**7.8**
9-Bolt 6	22	18	22	25	20	**21.4**	6-Turbine hous.	10	11	11	10	9	**10.2**
10-Bolt 7	23	19	24	26	27	**23.8**	12-Electric Actu.	7	5	9	7	8	**7.2**
7-Cartridge	5	6	7	6	8	**6.4**	11-Comp. Hous.	9	10	9	10	11	**9.8**
11-Comp. Hous.	9	7	8	9	8	**8.2**	7-Cartridge	7	8	8	5	6	**6.8**
Total process time (s)	**190**	**183**	**192**	**209**	**190**	**192.8**	**Total process time (s)**	**214**	**212**	**233**	**220**	**215**	**218.8**

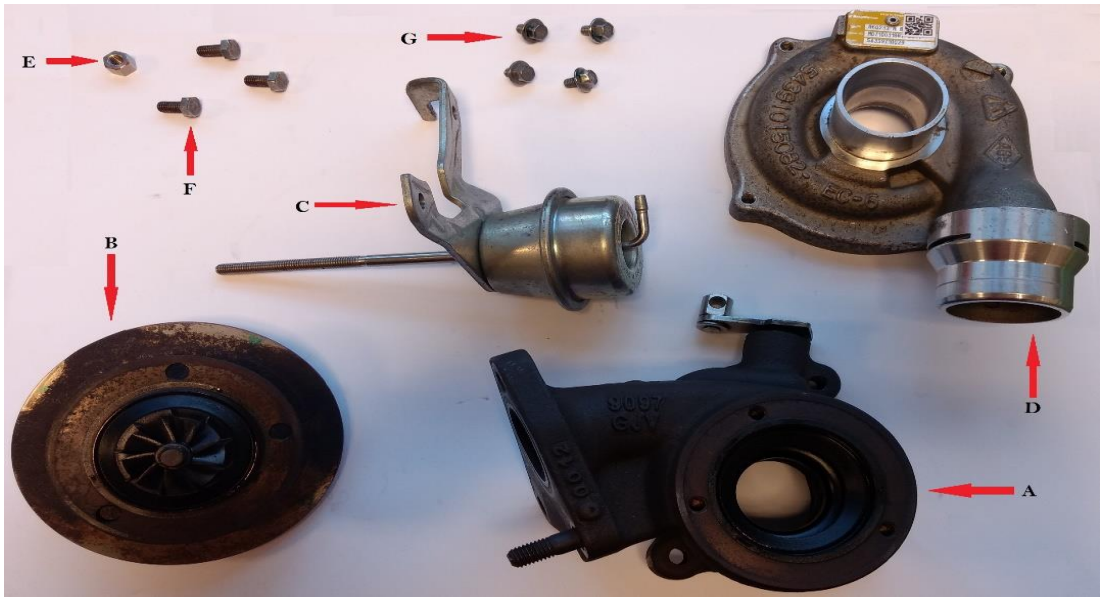


Figure 3.7 Disassembled components of the turbocharge.

Although, the main advantage of the proposed method in this research is to avoid initial time estimation and generate more realistic sequences of disassembly operations based on the disassemblability of the products, it can be seen the overall disassembly time was improved by 13%. This improvement can be due to more realistic objective parameters and avoiding estimating operations time which reduce the errors. It should be noticed that the main objective of the conventional time-based method is to minimize the overall disassembly time, however, the proposed method in this research consider other objectives such as demand and disassembly times alongside main objective which is disassemblability.

3.4.2 Case study 2: Water pump

Second case study is a water pump model GMP187. Figure 3.8(a), 3.8(b) and 3.8(c) show the water pump, exploded drawing and disassembled components of the water pump respectively. The water pump made of 7 sub-assemblies. Table 3.8 shows the properties and required disassembly tasks for all individual components.

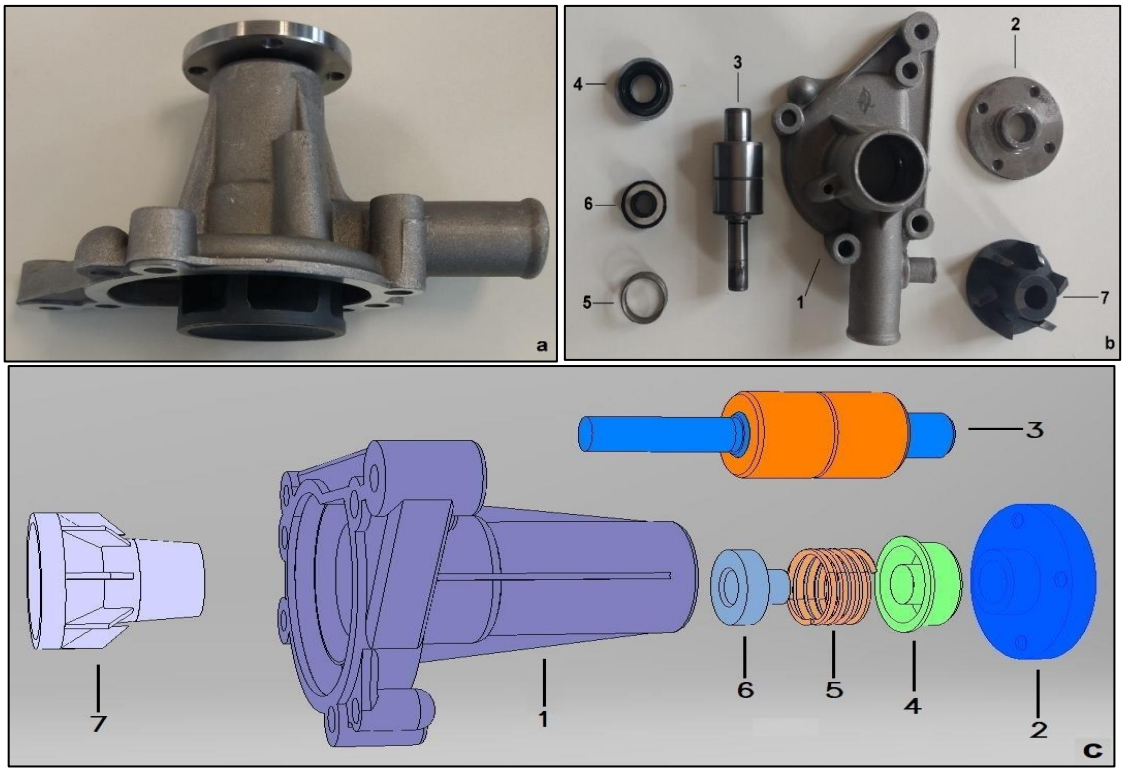


Figure 3.8 a) Water pump b) Disassembled components c) Exploded view.

As it can be seen the disassembly operations are carried out manually and just on tool is required. Furthermore, demand for each component, disassembly tasks and required tool are detailed in Table 3.8. Same method as the case study 1, is employed to represent the product disassembly proceedings and constraint, therefore, presenting the graph and matrices are not repeated for this case study.

Table 3.8 The properties and required disassembly tasks for all individual components.

Number	Component	Disassembly task	Disassembly tool	Reusable	Disassembly point (x,y,z)(mm)	Mass (g)	Demand
1	Crankcase cover	Removing	Manual	Yes	(40, 40, 45)	1021	Very High
2	Crankcase	Removing	Manual press	Yes	(23, 23, 5)	129	Medium
3	Bearings and shaft	Pulling out	Manual press	Yes	(30, 30, 45)	152	High
4	Spring chamber	Removing	Manual press	No	(35, 35, 900)	16	Medium
5	Spring	Removing	Manual	No	(30, 30, 90)	9	Low
6	Ring	Pulling out	Manual	No	(35, 35, 95)	35	Medium
7	Rotor	Pulling out	Manual press	Yes	(50, 50, 100)	250	Very High

The disassembly handling analysis, disassembly operation analysis and demand for product were calculated using Tables 3.1, 3.2, and 3.8 which presented in Table 3.9. It can be seen that component 1 and 7 have the highest demand. It is assumed that the basic operation time to disassemble a component is constant and does not depend on the position of the operation in the sequence.

Table 3.9 Disassembly handling analysis and Disassembly operation analysis for turbocharger

Number	Component	Disassembly Handling analysis			Disassembly Operation analysis				Demand
		Size	weight	shape	force	Tools requirement	Accessibility	Positioning	
1	Crankcase cover	2	2	0.8	0.5	1	1	1.2	0
2	Crankcase	2	2	1.2	3	3	1	1.2	3
3	Bearings and shaft	2	2	0.8	3	3	2	2	1
4	Spring chamber	2	2	0.8	3	1	2	1.2	3
5	Spring	3.5	2	1.2	1	1	2	2	3
6	Ring	2	2	0.8	0.5	1	2	1.2	3
7	Rotor	2	2	0.8	3	3	1	2	0

GA parameters and operators were set up to find an optimum operation sequence based on the DHI, DOI, DDI and DCI. For the case study, ncr=20, as the component number is lower than the first case study. This help to reduce computational cost. Analysing the results of the first case study showed that mutation probability from 0.1 to 0.15 archived the best results, therefore, mutation probability for this case study was set on 0.15.

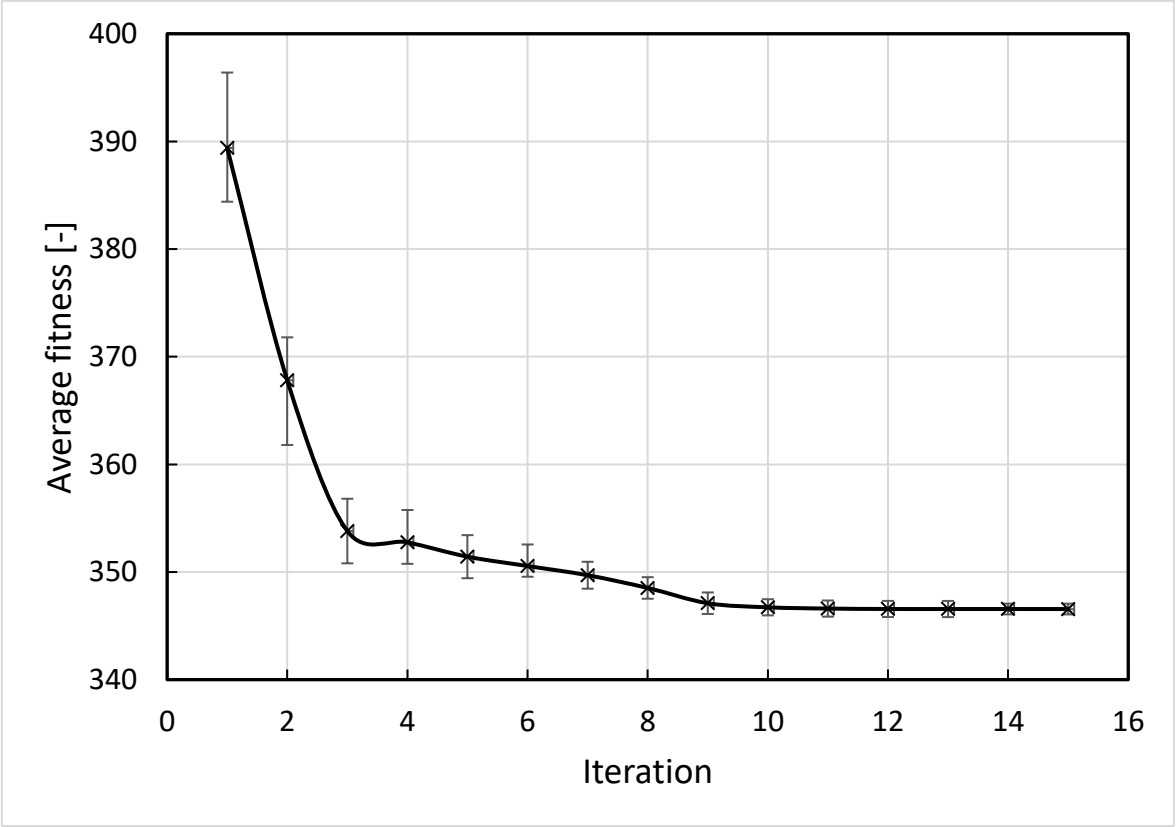


Figure 3.9 Average fitness values under different generations.

Figure 3.9 shows average fitness values under different number of generations. It shows that at generation 10 the algorithm reaches its minimum fitness value and running it further does not improve the results. The optimum disassembly process sequence based on the proposed model and its fitness value is shown in Table 3.10. This optimised solution was achieved in 0.16 second using proposed method.

Table 3.10 Final optimum disassembly process sequence based on the proposed method in this work.

Optimum solution	*F(ch,gn)*
2 → 1 → 7 → 6 → 3 → 5 → 4	34.65

Same method as the first case study was employed to generate a time-based disassembly sequence which is shown in Table 3.11. Then the water pump was

disassembled manually based on the two different disassembly sequence. To minimise the error, the water pump was disassembled 5 times based on each sequence and average times were calculated which can be seen in Table 3.12. It can be seen the overall disassembly time was improved by 10% which is slightly less than the first case study. This can be due to lower components for this case study than the first one.

Table 3.11 Optimum sequence generated by time-based method.

Optimum solution	*F(ch,gn)*
2 → 1 → 7 → 3 → 6 → 4 → 5	42.22

Table 3.12 Disassembly operations and process times for water pump.

Disassembly operations and process times based on proposed method							**Disassembly operations and process times based on conventional method**						
Disassembled part	**Trial 1 (s)**	**Trial 2 (s)**	**Trial 3 (s)**	**Trial 4 (s)**	**Trial 5 (s)**	**Mean Time(s)**	**Disassembled part**	**Trial 1 (s)**	**Trial 2 (s)**	**Trial 3 (s)**	**Trial 4 (s)**	**Trial 5 (s)**	**Mean Time(s)**
2-Crankcase	18	19	20	17	17	**18.2**	2-Crankcase	18	18	16	20	17	**17.8**
1-Crankcase cover	5	5	6	6	4	**5.2**	1-Crankcase cover	4	5	6	5	6	**5.2**
7-Rotor	15	14	16	17	14	**15.2**	7-Rotor	12	15	17	16	15	**15**
6- Ring	5	4	4	5	7	**5**	3-Bearings and shaft	14	14	13	15	14	**14**
3-Bearings and shaft	11	13	12	11	9	**11.2**	6- Ring	8	8	10	7	7	**8**
5-Spring	8	8	7	8	7	**7.6**	5-Spring	8	9	10	7	10	**8.8**
4-Spring chamber	10	12	12	10	9	**10.6**	4-Spring chamber	12	12	11	11	14	**12**
Total process time (s)	**72**	**75**	**77**	**74**	**67**	**73**	**Total process time (s)**	**76**	**81**	**83**	**81**	**83**	**80.8**

3.5 Conclusion

In this section, a new method was introduced to solve disassembly sequence planning problems. Most studies have focused on time as the main parameter to find an optimum solution and other parameters such as tool change requirement and disposal casts are converted in time unit. These studies estimate the time

require to disassemble a component of a product as it is difficult to determine the time accurately. This is due to this fact that the product should be disassembled completely to measure the time. Also, same EOL products can have different conditions, which cause different disassembly times. Furthermore, the same disassembly operation in a different sequence order can have a different disassembly time. In this work, DHI, DOI and DDI were introduced as optimisation parameters to analyse handling, disassembly difficulty and demand of a product. Additionally, DCI was introduced to consider disassembly time and other disassembly costs. The hybrid graph method was used to represent the mathematical model of the product and disassembly constraints. Genetic Algorithm was then employed to search the possible sequences and find a near-optimum solution. Finally, a turbocharger as an industrial product was selected to test and verify the proposed method. The results showed the effectiveness and compatibility of the method. One of the solutions with the minimum fitness value was presented as the optimum sequence for this case study. In this sequence, all disassembly constraints are met. To compare the effectiveness of this method with conventional time-based GA methods, the turbocharger was manually disassembled based on the sequences generated by the proposed method and conventional method. Disassembly operations and process times were measured and compared. The results showed 13% and 10% improvement in disassembly time for case study 1 and 2 respectively. The knowledge and methods developed in this chapter will be core foundation for chapter 3. In the next chapter, automated disassembly will be investigated.

Chapter 4- Automated Peg-Out-Hole Disassembly planning Using Force/Torque Sensor

4.1 Introduction

In the previous chapter, to solve disassembly sequence planning in manual process, a new method was proposed based on disassemblability of the components of a EOL product. To solve this problem, most studies have focused on time-based parameters as the main criteria. In this study, the geometry of the components and difficulty of the operation were considered. In the next chapter, disassembly sequence planning for automated process will be investigated. Mathematical model for peg-out-hole operation will be presented and autonomous peg-out-hole operation will be studied.

To achieve a reliable and efficient automated disassembly system, developing new strategies and methods are required. Conventional control methods such as force or position control are not efficient nor reliable due to high level uncertainty embedded in disassembly operations nature. Unlike assembly, disassembly operations have not been investigated thoroughly and there is a research gap in fundamental understanding of automated disassembly operations.

In this chapter peg-out-hole disassembly operation is selected as a common disassembly task to investigate and develop a reliable and efficient automated disassembly method. This chapter presents a mathematical and experimental model for peg-out-hole disassembly operation and propose a novel approach for estimating contact states of peg and hole using Force/Torque (F/T) sensor information.

First, different contact states of peg and hole are modelled mathematically. Experimental peg-out-hole operations and data collection strategies are proposed and F/T maps for each contact state were generated and analysed. Then, analysed, and improved F/T maps are used to classify the peg and hole contact states. A novel method is proposed to estimate position and orientation of the peg with respect to the hole using generated F/T maps and online measured F/T information inputs. Then, experiments are carried out using TM robot arm which results show a reliable accuracy of peg and hole contact states estimation for automated disassembly. The results and proposed method of this chapter are used to support objective 3.

4.2 Methodology

4.2.1 Peg-out-hole mathematical model

In this section, peg-out-hole operation was selected as a basic disassembly operation. Both position and orientation errors can lead to failure of the automated operation. Furthermore, different condition of same product causes more uncertainty in disassembly operation, which is the main difference between assembly and disassembly operation.

Three main steps can be identified for automated peg-out-hole disassembly operation as shown in Figure 4.1. First, robot approaches to the top of the peg (Fig. 4.1.a). Then, robot grasps the peg (Fig. 4.1.b) and finally, extraction of the peg out of the hole is carried out (Fig 4.1.c). In each step different parameters such as orientation and position error of peg or hole, grasping error and uncertain environment can add to errors and therefore high level of uncertainty. These errors

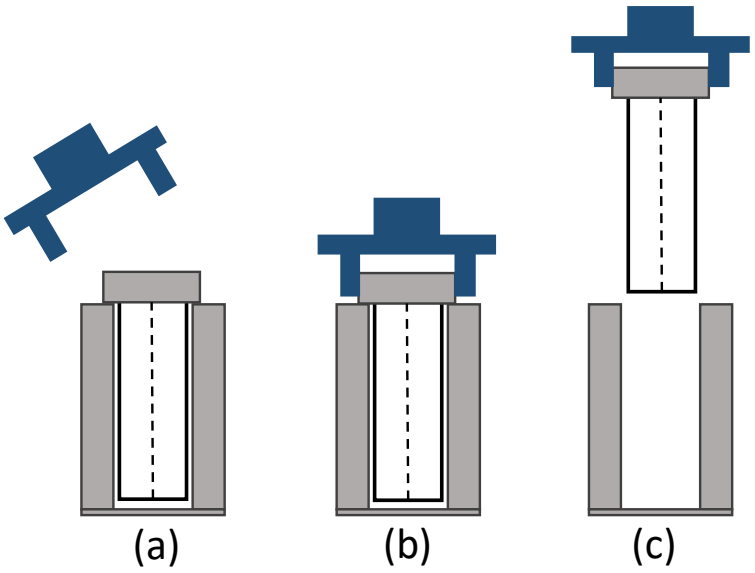


Figure 4.1 Peg-Out-Hole disassembly operation steps.

When the peg is being pulled out of the hole four possible contact states can happen which can be theoretically categorized into three different categories: line, one-point and two-point contact. These different contact states are shown in Figure 4.2 in which (a) is line contact, (b) and (c) are one-point contact type one and two respectively and (d) is two-point contact.

In line contact case, the axes of the peg and hole are parallel and there is no oriental errors and the only error is position of peg and hole. Therefore, line contact condition can be considered as one-point contact state where angle between peg and hole is zero. In this case, analysis, and equations for these two conditions can be considered as equal. One-point contact state occurs when there are both position

and orientation errors. The only difference between (b) and (c) is that in type one, the contact point always is on the edge of the hole, while in type two, the contact point can be any point of the hole along the Z direction. Two-point contact state is the worst case that can occur as the degree of freedom is restricted and jamming can be happen. Forces and torques analysis for different conditions are shown in Figure 4.2

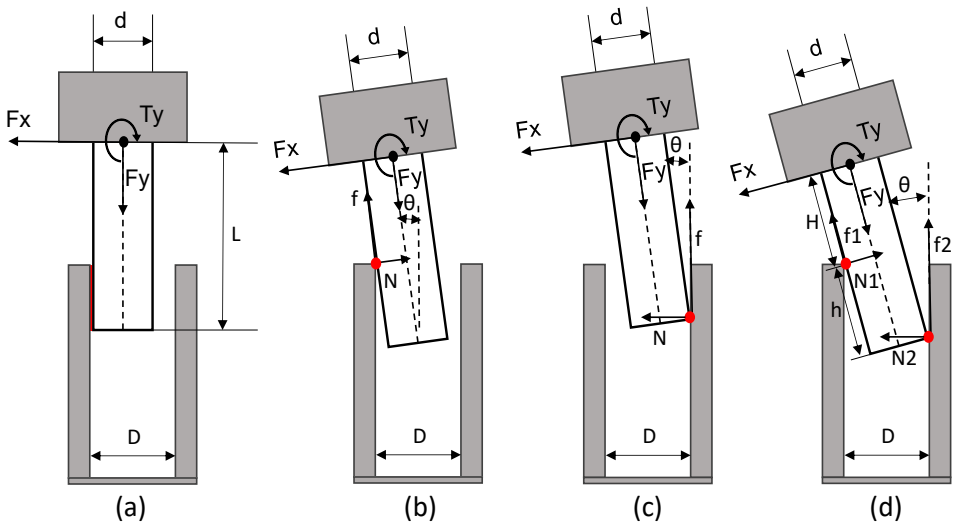


Figure 4.2 Possible peg and hole contact states and their force and torque analysis: (a) line contact state; (b) one-point contact type one; (c) one-point contact type two; (d) two-point contact state.

In a static equilibrium for one-point contact state where contact point is at the top of hole, (b), force and torque are calculated by Equation (4.1):

$$\begin{cases} F_x = -N \\ F_z = -f \\ T_y = -N.H + f.d/2 \end{cases} \quad (4.1)$$

Where d is peg diameter and f is friction and is defined as following:

$$f = \mu N \qquad (4.2)$$

Where μ is friction coefficient and N is normal force. Calculations for one-point type two condition where contact point is not at the top of the hole are shown in Equation (4.3).

$$\begin{cases} F_x = N\cos\theta - f\sin\theta \\ F_z = -N\sin\theta - f\cos\theta \\ T_y = N\cos\theta\,.\,l - f\sin\theta\,.\,l + N\sin\theta\,.\,d/2 - f\cos\theta.\,d/2 \end{cases} \qquad (4.3)$$

Where l is peg's length.

Two-point contact state happens when orientation error i.e. θ, reaches its ma i mum value. According to Figure 4.2, the angle θ for two-point contact as a function of peg's depth, *h*, peg's diameter, *d*, and hole diameter, *D*, can be expressed as following:

$$h\sin\theta = D - d\cos\theta \qquad (4.4)$$

if $\cos\theta = \sqrt{1 - sin^2\,\theta}$ (4.5)

hence,

$$h\sin\theta = D - d\sqrt{1 - sin^2\,\theta} \qquad (4.6)$$

Sol i ng this equation for θ gi es :

$$\theta_{tp} = \sin^{-1}\left(\frac{Dh}{h^2+d^2} - \sqrt{\left(\frac{Dh}{h^2+d^2}\right)^2 - \frac{D^2-d^2}{h^2+d^2}}\right) \qquad (4.7)$$

Where θ_{tp} is the angle of two-point contact state.

Also based on the geometry of the peg and hole, the minimum h for two-point contact state where tip of the peg contacts the edge of the hole can be calculated by Equation (4.8).

$$h_{min} = \sqrt{D^2 - d^2} \qquad (4.8)$$

Therefore, h_{min}=7.81 mm.

As peg and hole in this study is considered as rigid body, θ at a certain depth is fi e d when two-point contact happens. Therefore, θ can be found from Equation (4.7) where peg is in two-point contact condition with hole in a certain depth. f θ<θtp, then contact situation is one-point state and for θ=0 line contact happens. Figure 4.3 shows θtp with respect to the peg's depth for D=31 mm and d=30 mm which was studied in this work.

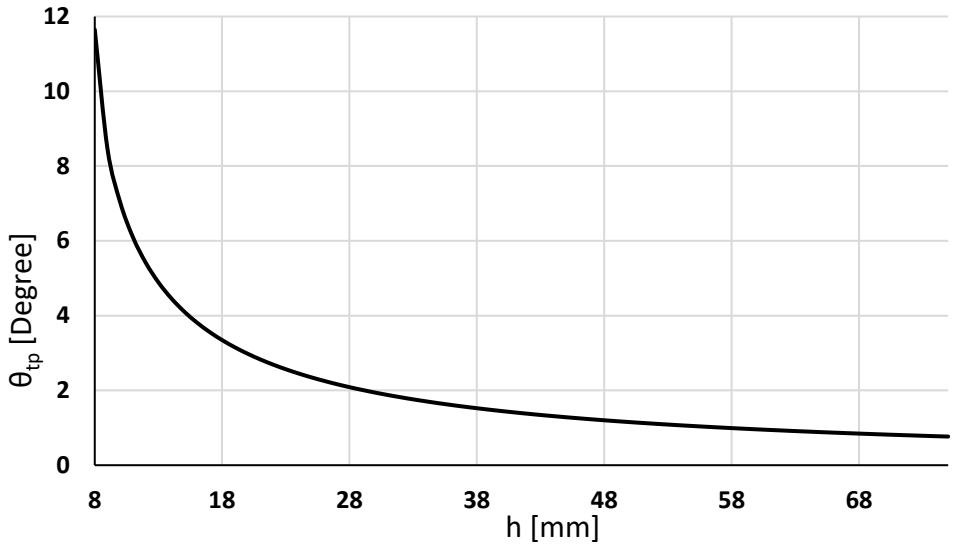


Figure 4.3 θtp with respect to the peg's depth for D=31 and d=30.

For two-point contact state, force and momentum analysis are shown in Equation (4.9):

$$\begin{cases} F_x = N_2 \cos\theta - N_1 - f_2 \sin\theta \\ F_z = -N_2 \sin\theta - f_1 - f_2 \cos\theta \\ T_y = -N_1.H + N_2 \cos\theta \,.\, l - f_2 \sin\theta \,.\, l + N_2 \sin\theta \,.\, d/2 - f_2 \cos\theta . \frac{d}{2} + f_1 . d/2 \end{cases} \quad (4.9)$$

Where $f_1 = \mu N_1$ and $f_2 = \mu N_2$.

4.2.2 Disassembly configuration

- **Experiment set up**

The experiment platform to perform peg-out-hole disassembly operation and measure force and torque data is shown in Figure 4.4. It consists of a 6-DOF collaborative robot arm, a 6-axis force and torque sensor and a 2-finger gripper. The

robot used in this research is TECHMAN TM14 with maximum load of 14 kg and repeatability of ±0.1 mm. F/T sensor model is ATI Axia80 which provides ±500 N for force and ±20 Nm for torque with resolution of ±0.1 N for force and ±0.005 Nm for torque. The 2-finger gripper model is ROBOTIQ 2F with electric actuator. The sensor is installed between the robot arm and gripper to measure force and torque that apply on end-effector as it contacts the object. In this research, peg is assumed to be gripped perfectly to eliminate the gripper's error. Characteristics of peg and hole are shown in Table 4.1.

Table 4.1 Dimensions and materials of the peg and hole.

	Diameter (mm)	*Length (mm)*	*Material*
Peg	30	75	PLA
Hole	31	80	PLA

The robot is controlled by TMflow controller and a computer with Intel Core i7-8550U and 8 GB ram which runs on Ubuntu 16.04 operation system. Protocol TCP/IP was used for communication between the computer and TMflow controller and EtherCAT was used for receiving data from the sensor.

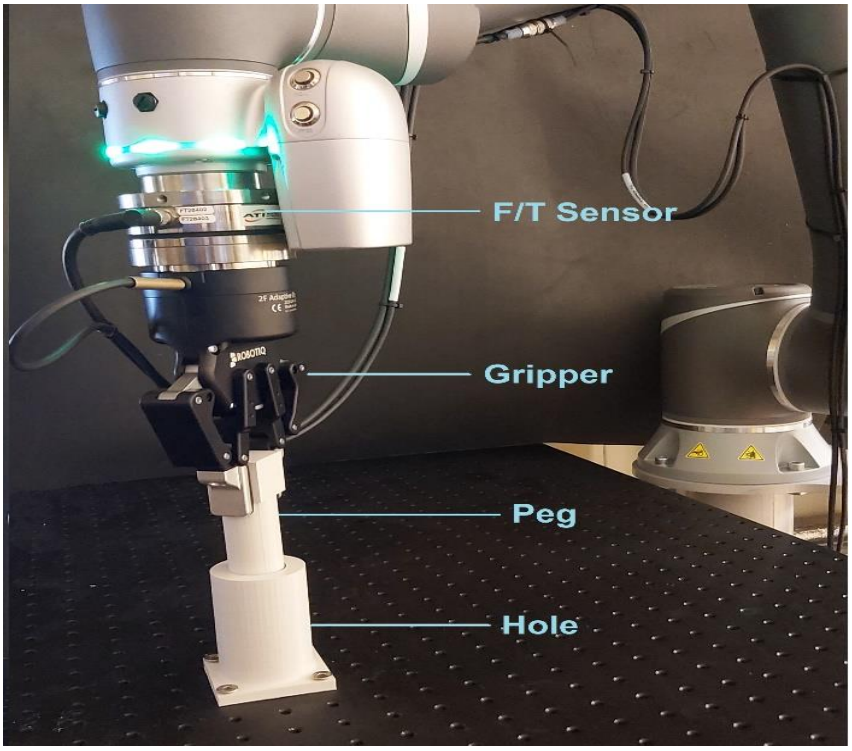


Figure 4.4 The robotic peg-out-hole disassembly system set up.

- **Data obtaining method**

Recent improvements in artificial intelligence and machine learning methods allows robot programming to be more flexible and reliable. These new methods enable industrial robots to handle new tasks without explicit programming or teaching. Obtaining, labelling, and analysing received dataset is a crucial step as it is the main ingredient for any machine learning based robotic task. In this research, dataset consists of three-dimension force and three-dimension torque received from F/T sensor, and peg's position and orientation with respect to the hole. First, recei ed F/T and robot position data need to be collected and recorded. Then, this recorded dataset should be labelled accordingly and pre-analysed to check it for possible collection or labelling errors.

In this work, the peg will remain in contact with hole during disassembly operation to investigate contact states. Each contact states require different strategies to collect useful data and investigate them. Three different strategies for three contact state were defined as shown in Figure 4.5.

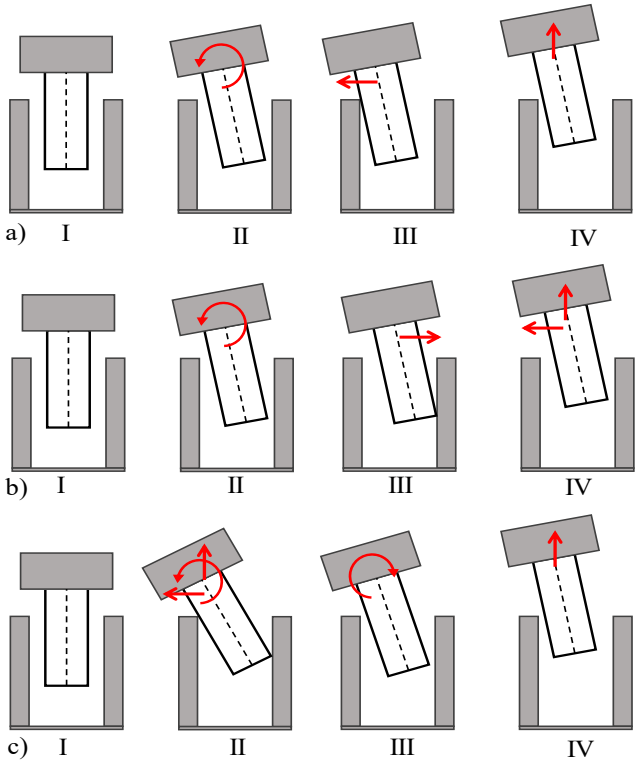


Figure 4.5 Data collection strategies; a) one-point contact state type one, b) one-point contact state type two, c) two-point contact state

The disassembly sequence operation for one-point contact state type one consists of five steps; I) position peg in hole with their known related positions, II) rotate peg around y a is with θ<θtp, mo e peg in -x direction until it contacts the hole and apply predefined force, IV) move peg in +z direction with predefined offset V) repeat (II), (III) and (IV) until peg is out of the hole.

The sequence for disassembly operation to collect data for one-point contact state type two is as following: I) position peg in hole with their known related positions, II) rotate peg around y-a i s with θ<θtp, mo e peg in + direction until it contacts the hole then apply predefined force, IV) move the peg in -x direction and the +z direction with predefined offset, V) repeat (II), (III) and (IV) until peg is out of the hole.

To simulate two-point contact state, disassembly operation sequence should be defined in a way that avoid jamming the peg in the hole. If jamming happens, the disassembly operation will be failed. The following sequence is proposed to demonstrate two-point contact state and collect disassembly operation data; I) position peg in hole with their known related positions, II) rotate peg around y-axis with θ=θtp until it contacts the hole and then apply predefined force in both z and direction , III) rotate peg around y axis until it disconnect the hole, IV) move peg in +z direction with predefined offset, V) repeat (II), (III) and (IV) until peg is out of the hole.

In this sequences peg is considered in contact with the hole if resultant force or torque is larger than a predefined threshold i.e. $F_{threshold}$ and $T_{threshold}$. Resultant force, Fr, and resultant torque, Tr, are calculated by Equation (4.10).

$$\begin{cases} F_r = \sqrt{F_x^2 + F_y^2 + F_z^2} \\ T_r = 1/3\sqrt{T_x^2 + T_y^2 + T_z^2} \end{cases} \quad (4.10)$$

Each data entry for different action steps that previously defined is labelled. Due to various uncertainty, position and orientation of peg and hole have errors. However, the actions of robot which are changing position and orientation of the peg are assumed accurate. Therefore, each input of force and torque measurement is labelled with its corresponding position and orientation changes i.e. actions. Table 4.2 shows different actions for labelling dataset. α and e are rotation angle and peg movement respecti e ly and αp and e_p are defined based on the clearance and dimensions of the peg and hole. A vector of {Fx, Fy, Fz, Tx, Ty, Tz, Px, Py, Pz, Rx, Ry, Rz, n} is defined to store sensor and robot reading for each data point where Fx, Fy, Fz, Tx, Ty, Tz are force and torque, Px, Py, Pz, Rx, Ry, Rz are position and orientation of the end-effector and n is data point counter. Furthermore, an action vector is defined as $\{DP_x, DP_y, DP_z, DR_x, DR_y, DR_z\}$ based on the robot actions.

Table 4.2 Different actions for labelling datasets.

Action	*Description*	*Action limits*	*Error vector*
Action 1	Rotate peg around ±y axis	$0< \alpha \leq \alpha_p$	0, 0, 0, 0, DR_y, 0, 0
Action 2	Move peg in ±x direction	$0< e \leq e_p$	DP_x, 0, 0, 0, 0, 0, 0
Action 3	Move peg in +z direction	$0< e \leq e_p$	0, 0, 0, DP_z, 0, 0, 0

4.2.3 Force-Torque maps

- Basics of force and torque maps

A force-torque map is defined as a function that maps position and orientation domain of the robot end effector to the domain of force and torque measured by the sensor when peg and hole are in contact with each other. It can be considered as $R^n \rightarrow R^m$ where n is the degree of freedom of the end effector and m is the degree

of freedom of the F/T sensor. In other words, it can be assumed that a force-torque map matches measured forces and torques by the sensor to the end effector position and orientation. Therefore, it is possible to find the estimated error of the position and orientation of the peg and hole by searching the force-torque map and match corresponding states. It means if force-torque map is a bijective function, then estimation of the position and orientation errors using measured force and torque is feasible. However, in realistic cases, force-torque map contain redundant measurement and it is not always possible to estimate errors. In other words, this function is non-injective and needs extra analysing to use its inverse to estimate contact state errors. In addition, presence of friction makes using force-torque map more challenging. Therefore, improving and analysing generated force-torque maps are necessary to use them for position and orientation error estimation and automated disassembly.

- **Generating force-torque maps**

To generate F/T maps experimentally for different contact states, it is necessary that peg be in contact with hole. Also, it is advantageous to select contact points of the interest area randomly and non-uniformly [154]. In this way, the experimental trials can be minimized, and maps accuracy can be improved. However, for the areas with high gradients, the samples density should be increased. Procedures for obtaining F/T maps for three contact states are as followings:

One-point contact state:

Random sample points with ariable peg's depth, h, and peg's orientation, θ, are selected to collect sensor and robot's data. Sample points are selected non-uniformly with bias toward high gradient areas. For one-point contact state, force or torque can be mapped to depth and orientation of the peg. In this research, torque map is generated for one-point contact state as it contains more information with les redundancy [154].

Two-point contact state:

In two-point contact state case, peg's orientation is dependent on the peg's depth. It means, one of them can be calculated if the other one is known. In addition, two-point contact state can contain more redundancy and results are more affected by friction. Therefore, both force and torque signals are used to generate its map. an dom sample points are selected based on the different peg's depth and F/T maps are generated.

4.3 Results and discussions

Experiments on peg and hole were conducted and F/T maps were generated for different conditions to test this hypothesis that orientation and position error can be estimated using interpreting force and torque maps. To minimize the effect of friction and dynamic on data collecting process, the robot speed and peg's approach to the hole was set on minimum possible speed of the robot. In Addition, to suppress noise, approximately 500 F/T signals over one second were sampled and averaged for each contact point. Although this slow data obtaining process is in contrast with aims to achieve high performance automated disassembly, it can be useful to extract

position and orientation estimation based on F/T information and develop artificial intelligent based method for high uncertainty environments.

To generate F/T map for one-point contact state type one, the robot was programmed and controlled to generate appro im ately 600 contact point o e r θ-h plane for 0≤θ<11.61 degree and 7.81≤h≤70 mm. Then, force and torque signals were recorded for contact points. Figure 4.6a shows measured Ty for θ-h plane. Same procedure was carried out to generate force and torque map for one-point contact state type two. Force and torque signals were recorded o e r θ-h plane for 0≤θ<11.61 degree and 7.81≤h≤70 mm which are shown in Figure 4.7a.

Experimental measurement for two-point contact state was carried out using robot set up. For 7.81 ≤h≤70 mm appro im ately 600 contact point were generated, and force and torque signals were collected. It is notable that in two-point contact state, θ and h are dependant. Therefore, force and torque for θ-h were presented to produce its F/T maps. Figure 4.8a shows measured Ty and F m ap for 7.81 ≤h≤70 mm.

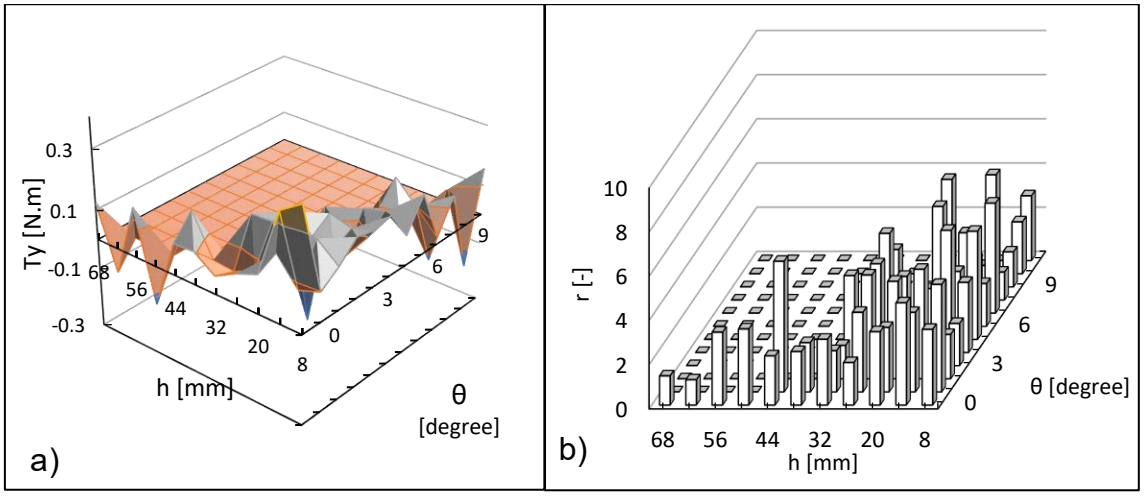


Figure 4.6 One-point contact state type one maps: (a) experimentally generated map; (b) Redundancy Map.

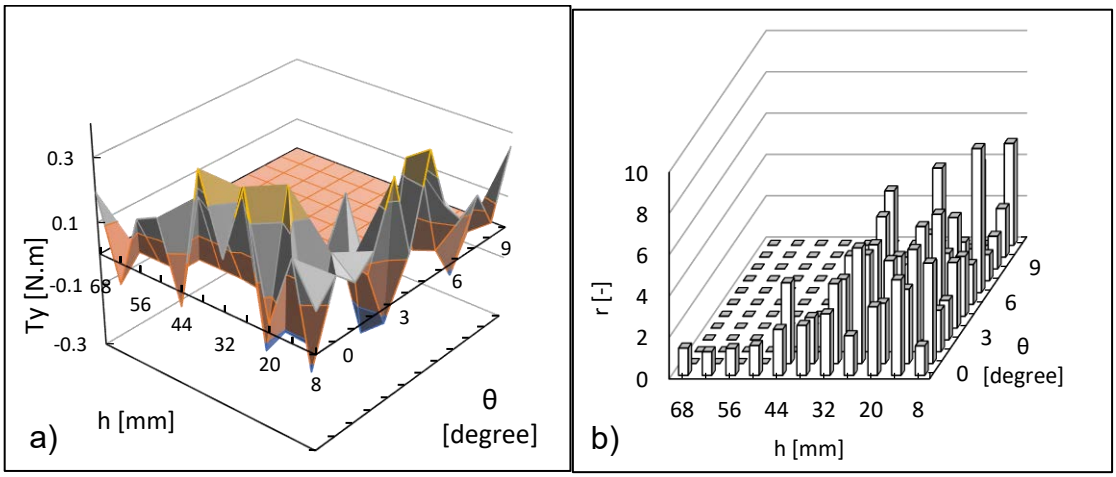


Figure 4.7 One-point contact state type two maps: (a) experimentally generated map; (b) Redundancy Map.

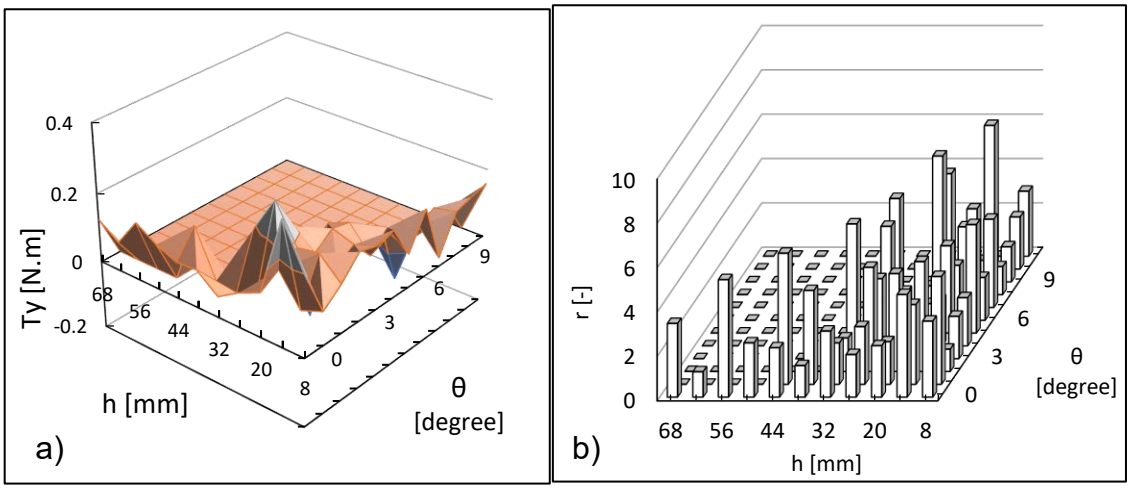


Figure 4.8 Two-point contact state maps: (a) experimentally generated map; (b) Redundancy Map.

4.3.1 Force and torque maps analysing

Although it may be possible to reverse mathematically computed F/T maps and estimate displacement, it is not feasible to directly inverse experimentally generated maps and estimate displacement. Presence of noise, friction, and experimental set up errors and uncertainties, make map functions highly irreversible which contain

redundant and similar measurements. Experimentally generated F/T maps contain useful information that after analysing and refinement can be used to improve automated operation in environments with high level uncertainty. In this study, Redundancy Map (RM) method is used to analysis and improve generated maps.

Redundancy Map was employed to analyse the quality of the F/T maps. A Redundancy Map projects measured force and torque signals to redundancy valve r, where r is the number of force and torque vector in an F/T map that has similar value for a specific position. In other words, the value of the function is calculated by the number of the positions that has the same F/T value as following:

$$r(x_i) = \sum_{j=1}^{n} \begin{cases} 1 & \left|FT(x_i) - FT(x_j)\right| < \epsilon \\ 0 & else \end{cases} \qquad (4.11)$$

Where ϵ is a small value which is selected based on the order of the sensor noise, x is the positions and n is the number of all F/T measurements. For this experiment based on the sensor accuracy ϵ=0.1 N for force and ϵ=0.005 Nm for torque. Then, for each two torque and force vector if the difference of both force and torque values are smaller than the thresholds, are considered as similar. Therefore, for each position if contain high level of similar data, the region is considered as high redundancy region in which estimating position based on the F/T map is problematic.

Figures 4.6b, 4.7b and 4.8b show redundancy maps for one-point type one, one-point type two and two-point contact states respectively.

RM can be used to avoid high value redundancy regions and overcome failure of operation in these areas. For each area, F/T maps are evaluated based on the RM

and with respect to r values. If force and torque value lie in high redundant reposition, a correction manoeuvre is carried out and a new force torque vector is generated to exit high redundancy area and enter in a position with lower redundancy. The aim is to reduce the number of trials to complete the operation by avoiding high redundancy regions. Quality of F/T maps based on their RM and r values can be evaluated as following:

$$\mathrm{QFM} = \frac{1}{n}\sum_{i=1}^{n} r_i \qquad (4.12)$$

Where n is total number of measurements for a map. If for an F/T map QFM is large, it contains high level of redundancy which can increase the probability of position and orientation estimation error and operation failure. To investigate the effect of QFM on the accuracy of the estimation, 10 different maps were generated and their QFM were calculated and the position and orientation were estimated based on the proposed method in section 4.3.3. Figure 4.9 shows mean errors with respect to the QFM of each map. As it can be seen that higher QFM results in higher overall estimation error for a map.

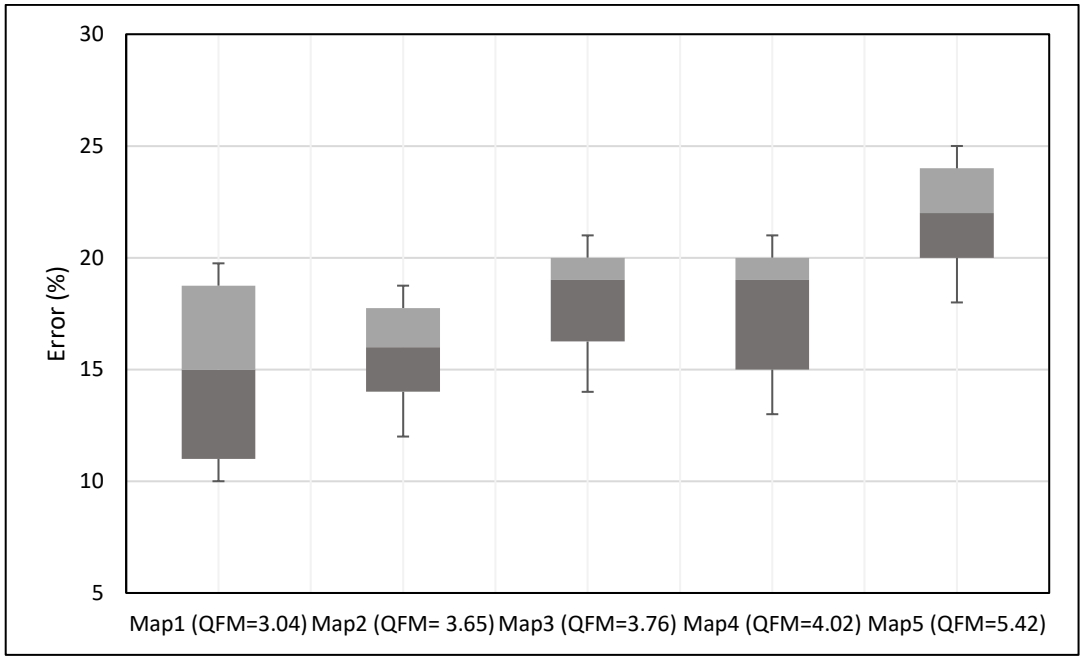


Figure 4.9 Error estimation for maps with different QFM.

4.3.2 contact state classification using EM-GMM

Figure 4.10 shows all possible contact states that can happen during peg-out-hole disassembly operation. There are eight different contact states which were categorized in three categories i.e. line, one-point and two-point contact state. As peg and hole case is symmetry on x-z and y-z plane, we classified the contact states on x-z plane. It is assumed that for each situation some of the measured force and torque elements are more significant than the others. Base on this assumption, for example for contact state (1) shown in Figure 4.10, +Fx and +Ty are more significant than the other force and torque measurements. The force and torque measured elements that are more significant for each contact state are categorised in Table 4.3.

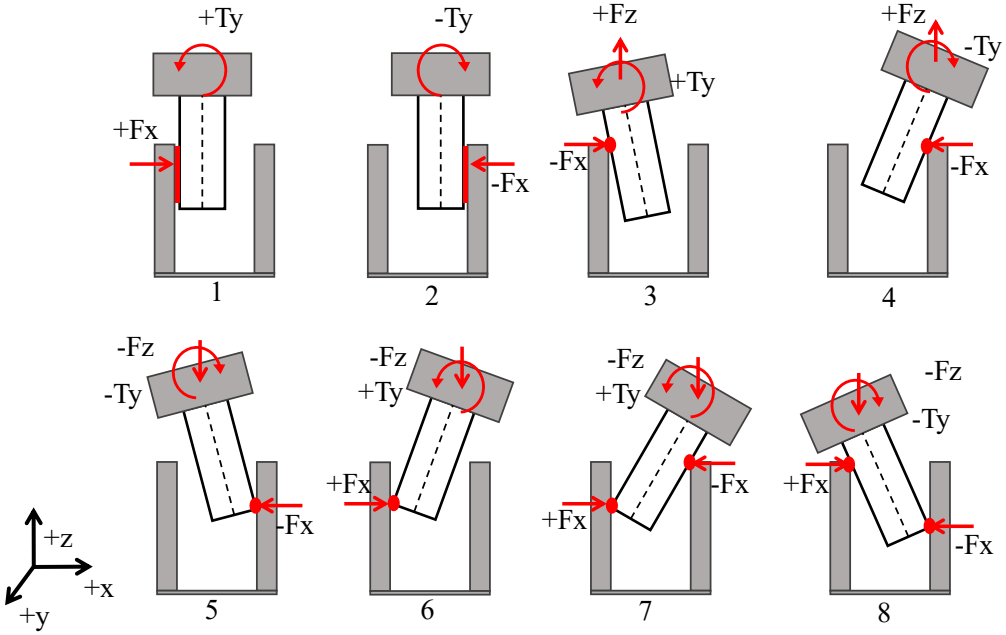


Figure 4.10 All possible peg and hole contact states.

In this work, to classify force and torque signals and determine contact state situation, expectation maximization-based Gaussian mixtures method (EM-GMM) is used. Different clusters or classes defined as several Gaussians that each described as $k \in \{1,2,\dots,k\}$, where k is the number of the classes and in this case contact states. In general, a Gaussian distribution can be defined as the followings:

$$N(x_k|\mu,\Sigma) = \frac{1}{|2\pi|^{D/2}|\Sigma|^{1/2}} \exp\left(-\frac{1}{2}(x_k-\mu)^T\Sigma^{-1}(x_k-\mu)\right) \quad (4.13)$$

Where D is the dimension of each data point, x is all data points, Σ is covariance and μ is the mean of the data.

Therefore, Gaussian Mixture Model (GMM) is defined as below:

$$P(x_k|z_i;\theta) = \sum_{j=1}^{n} \phi_j N_j(x_k, \mu_j, \Sigma_j) \qquad (4.14)$$

Where ϕ is the weight of jth Gaussian element and $\theta = \left[\theta_1, \theta_2, \dots, \theta_j\right]^T$ where $\theta_j = (\Sigma_j, \phi_j, \mu_j)$.

To optimise the classification process, optimised parameters for θ should be fined from measured data.

Expectation Maximisation (EM) which is considered as one of the simplest and most efficient algorithms is employed to find the parameters of θ. This algorithm is an iterative method that was proved to be computationally effective in finding Gaussian Mixture parameters. Each EM iteration composed of two steps; E-step and M-step. First, likelihood of the current parameters of θ is estimated in -step. Then, in M-step the parameters are updated to maximise the result.

The likelihood of the data x_k with parameters θ is presented as followings:

$$\log L(x_k;\theta) = \sum_{k=1}^{K} \ln\left(P(x_k;\theta)\right) \qquad (4.15)$$

Where K is total number of datasets, and optimised θ that ma im ises this equation is calculated as below:

$$\theta(t) = \arg max_{\theta} L(x_k;\theta(t)) \qquad (4.16)$$

General steps of the EM algorithm can be summarised as follows:

EM algorithm steps

Step 1: Parameters of θ is initialised randomly

Step 2: Convergence parameters, ϵ and Ɛ is initialised

Step 3: Compute responsibilities for current θ (E-Step)

Step 4: θ is re-estimated using current responsibilities

Step 5: Calculate the likelihood

Step 6: Check convergence using ϵ and Ɛ. Stop if converged otherwise go to step 2

Table 4.3 Force and torque indices for different contact state classes.

F/T Data / Contact state	+Ty	-Ty	+Fx	-Fx	+Fz	-Fz
1	1	0	1	0	0	0
2	0	1	0	1	0	0
3	1	0	1	0	1	0
4	0	1	0	1	1	0
5	0	1	0	1	0	1
6	1	0	1	0	0	1
7	1	0	1	1	0	1
8	0	1	1	1	0	1

4.3.3 Position estimation using F/T maps

A conventional method to estimate the position and orientation of the peg respective to the hole, i.e. position and orientation errors, is to inverse the generated F/T maps. As we discussed, due to redundancy and noise, inverse of the maps is not practical in some area. However, for high quality data areas the position and orientation of the peg with respect to the hole can be estimated based on map inversion to move away from jamming situations. In this work, a novel method is proposed to estimate position and orientation and avoid peg-out-hole disassembly operation failure as it

can be seen in Figure 4.11. First, the measured F/T data is passed to the classifier and the contact state of the peg and hole is determined using the classifier, and its map is selected from database. Then measured F/T data is compared with the map to see if it is within the high-quality data area. If the answer is yes, the position and orientation of the peg respect to the hole is estimated based on the map inversion using Neural Network method. If answer is no, i.e. direct inversion of the map is not possible, an action (defined in Table 4.2) based on the current contact state is

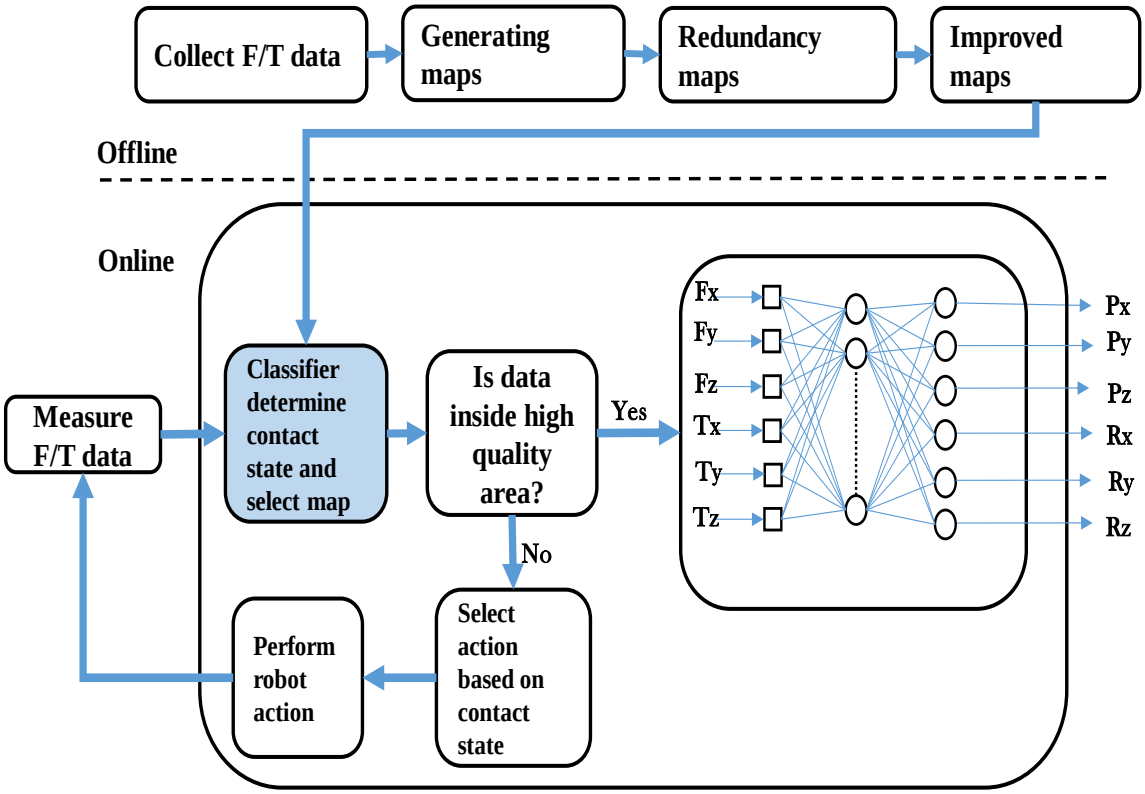


Figure 4.11 Block diagram of position and orientation estimation of peg and hole using F/T sensor information.

Figure 4.12 shows estimated position and orientation of the peg compared with the actual robot arm measurements for different contact states. The estimation using this model has good agreement with actual robot reading which shows the practicality and efficiency of the proposed method. The results show that the average error is less than 6%. It can be seen that the estimation of the position is more accurate than the orientation, however, it is still in an acceptable range to predict contact states and move away from jamming situation. It is notable that orientation error has more effect on accruing high contact forces or jamming, therefore future studies can be done to improve orientation estimation.

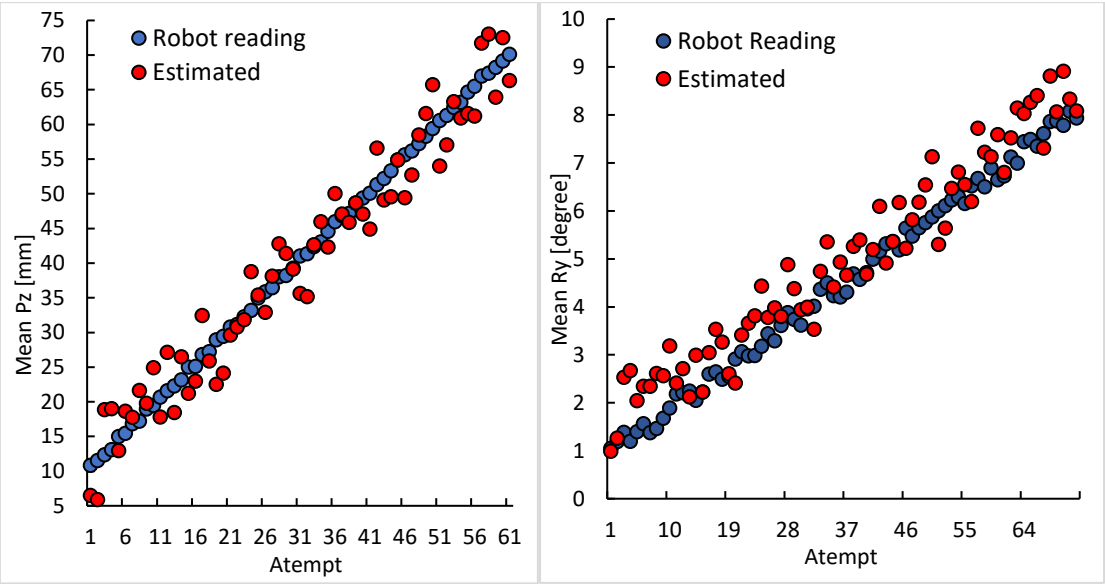


Figure 4.12 (a) Mean Pz estimated using proposed method compared to robot reading; (b) Mean Ry estimated using proposed method compared to robot reading.

4.4 Conclusion

Although there are various researches and literature on peg-in-hole assembly operation, it cannot be extended to the peg-out-hole disassembly operation due to

the fundamental differences. Therefore, whole new mathematical models and experimental strategies are required. Furthermore, high level uncertainty in disassembly operations, makes the conventional automated control strategies inefficient and unreliable. In this section, automated peg-out-hole disassembly operation was investigated mathematically and experimentally as a basic disassembly operation. Peg-out-hole disassembly operation was mathematically modelled, and different peg and hole contact states were distinguished and analysed. An estimation strategy for position and orientation of the peg and hole based on the Force/Torque sensor information was proposed. To estimate peg and hole contact states using F/T inputs efficiently and reliably, data collection strategies were introduced. Force and torque maps for different contact states were generated and analysed using Redundancy Map method. Also, peg and hole contact states were classified using EM-GMM classification method and eight different classes based on the F/T information were defined. Finally, a novel method proposed to estimate the position and orientation of the peg and hole based on the F/T sensor measured online data and generated F/T maps. TM robot arm equipped with ATI Axia80 sensor were employed to carry out the experiments and test the hypothesis. Then, robot reading for position and orientation were recorded and compared with estimations. Results show an efficient and reliable accuracy for estimating position and orientation of the peg and hole to be used for automated disassembly. The results of this chapter will contribute to meet objective 3 which will be investigated in the next chapter.

Chapter 5- Human-robot collaborative disassembly planning for a reliable and efficient disassembly process

5.1 Introduction

In the chapters 3 and 4, disassembly planning problem for manual and automated process were investigated and results were presented. New methods were developed to improve sequence planning for manual and automated disassembly process. In this chapter, human-robot collaborative disassembly process will be investigated. The results from the previous chapters – manual and automated disassembly – will be exploited in this chapter to develop an efficient and reliable human-robot collaborative disassembly planning.

The disassembly process is the main step of dealing with End-Of-Life (EOL) products. This process is carried out mostly manually so far. Manual disassembly is not efficient economically and the robotic systems are not reliable in dealing with complex disassembly operations as they have high-level uncertainty. In this chapter, a disassembly planning method based on human-robot collaboration is proposed. This method employs the flexibility and ability to deal with complex tasks of humans, alongside the repeatability and accuracy of the robot. Besides, to increase the efficiency of the process the components are targeted based on the remanufacturability parameters. First, human-robot collaboration tasks are classified and using a novel method the tasks are allocated to the human or robot. Then, the disassembly process is represented using AND/OR representation and

the mathematical model of the process is defined. New optimization parameters for human-robot collaboration are defined and the genetic algorithm was modified to find a near-optimal solution based on the defined parameters. To validate the task classification and allocation, a 6-DOF TECHMAN robot arm is used to test the peg-out-hole disassembly operation as a common disassembly task. The experiments confirm the task classification and allocation method. Finally, an automotive component was selected as a case study to validate the efficiency of the proposed method. The results in comparison with the Particle Swarm algorithm prove the efficiency and reliability of the method. This method produces a higher quality solution for the human-robot collaborative disassembly process.

5.2 Methodology

5.2.1 Selective and targeted disassembly

The full disassembly process is not an efficient nor an economic approach for disassembly planning problems. The inefficiency of full disassembly especially is highlighted where human and robot are in collaboration to do the process in a workcell. In addition, when the main purpose of disassembly is remanufacturing or repair of the product, full disassembly increases the cost of remanufacturing or repair, and make them uneconomic. Therefore, a reliable targeted disassembly planning strategy is required for an efficient human-robot collaboration approach.

In this work, to select and target the components based on the remanufacturing requirements, the proposed method in [166] and the PROMETHEE II method were modified to evaluate disassembly priority. Three different remanufacturability factors were introduced and their indices were quantified. Then the level of influence for each factor based on their indices determined to rank the disassembly priorities. To

systematically evaluate disassembly priorities and target the most valuable components based on the remanufacturing requirements and criteria, PROMETHEE II is employed.

Many different factors for targeting and selecting components can be defined and introduced. Howe e r, if the number of factors is high or the factor's influence in not high enough the efficiency and reliability of targeted disassembly are reduced. Therefore, in this work three main factors were introduced and quantified which are cleanability, repairability, and economy. In the following, each factor is defined.

1- Cleanability Four level of cleaning difficulty of the components were selected and defined to assess the cleanability of the components for remanufacturing purposes which are; a) cannot be cleaned economically, b) difficult to clean or special treatment required, c) moderate cleaning and d) easy cleaning. For each factor the corresponding value is C = {c1, c2, c3, c4} respectively. The level of cleanability is assessed manually based on the remanufacturing requirement using expert opinion. Then assessment for each component is calculated as Ec = {Ec1, Ec2, Ec3, Ec4} where e_i indicates the degree of the evaluation of the i^{th} difficulty level. Then, to calculate the quantitative cleanability value, expert opinion value is combined with the difficulty value as per Equation 5.1.

$$Cl = \begin{cases} C \times Ec^T \ \ if\ Cl \geq c1 \\ 0 \ \ if\ l < c1 \end{cases} \qquad (5.1)$$

2- Repairability This factor is basically defined to determine the damage level of a component and whether it is worth it to be disassembled. Four levels of damage for a component in the product are described as; a) not damaged, b) minor damage, c) moderate damage, and d) sever damage. Each level is assigned a corresponding value of R = {R1, R2, R3, R4} respectively. To assess repairability, manual expert

opinion is used and for each component, the expert decision is allocated as Er = {Er1, Er2, Er3, Er4} for each repairability level respectively. Then, the Repairability of each component is calculated using Equation 5.2.

$$Re = R \times Er^T \qquad (5.2)$$

Based on the calculated repairability, any component can be categorized into one of the following categories; easily repaired, can be repaired, repaired with difficulty, and cannot be repaired.

3- Economy Third factor to select and target the component for the disassembly process is economy which assesses the economic benefit of disassembling a component. It is to ensure that the cost of remanufacturing a part can be justified comparing to the cost of purchasing a new component. It is assumed if the cost of remanufacturing a part is up to 50% of buying a new one, it is considered as economically valuable for remanufacturing. Therefore, the economic benefit of the remanufacturing of a part is calculated using Equation 5.3.

$$E = \begin{cases} 1 \quad if \ \frac{C_r}{C_p} < 0.5 \\ 2 \times \left(1 - \frac{C_r}{C_p}\right) \quad if \quad 0.5 \leq \frac{C_r}{C_p} < 1 \\ 0 \quad if \quad \frac{C_r}{C_p} \geq 1 \end{cases} \qquad (5.3)$$

Where Cr is the total remanufacturing cost of a component and Cp is the purchasing cost of the same new component.

Finally, the PROMETEE II method is employed to objectively prioritize the disassembly of the components based on the remanufacturing requirements and factors. PROMETHEE II is a powerful decision-making tool that allows the selection of targeted disassembly components for the disassembly process. The main steps to select the targeted components using this method is as follows:

Step 1: For each criterion and each possible decision, reference degree value is computed. For two decision of x and y, the difference value of criterion i is calculated as:

$$d_i(x,y) = g_i(x) - g_i(y) \qquad (5.4)$$

Where $g_i(x)$ is the value of i[th] criterion of decision x. Then preference function $P_i(x,y)$ is defined as Equation 5.5 to calculate the preference degree of i[th] criterion for x and y.

$$P_i(x,y) = F(d_i(x,y)) \quad with\ \forall x \in]-\infty,\infty[\ ,\ 0 \le F(x) \le 1 \qquad (5.5)$$

Step 2: In this step, a global preference index is calculated for each possible decision pair. Then, for a possible pair of decisions of x and y, the global reference index is calculated as:

$$\pi(x.y) = \sum_{i \in C} w_i \times P_i(x,y) \qquad (5.6)$$

Where C is the set of all criterion and w_i is the weight of the ith criterion.

Step 3: in this step for a possible decision x, the positive and negative outranking flow is calculated as Equation 5.7 and 5.8 and respectively.

$$\emptyset^+(x) = \frac{1}{n-1}\sum_{t \in A} \pi(x,t) \qquad (5.7)$$

$$\emptyset^-(x) = \frac{1}{n-1}\sum_{t \in A} \pi(t,x) \qquad (5.8)$$

Where n is the total number of all possible decisions and A is the set of them.

Step 4: The final ranking for all possible decisions are carried out in this step by employing the outranking flows. Therefore, the net flow of possible decisions for each component is determined and the net flows are sorted. For a possible decision x, the net outranking flow is calculated as Equation 5.9.

$$\emptyset(x) = \emptyset^+(x) - \emptyset^-(x) \qquad (5.9)$$

The higher value of $\emptyset(x)$ for a decision i.e. priority of disassembly of component, the decision for that component for remanufacturing is better.

The calculated priority decision ranking from these steps is used to target and select the possible component for disassembly based on the remanufacturing requirements and criterion.

5.2.2 Collaborative human-robot disassembly

Figure 5.1 shows a typical human-robot collaborative workcell. The workcell consists of three main zones: 1) human-only zone, 2) robot-only zone, and 3) shared zone. A human-robot collaboration approach combined the repeatability and accuracy of the robot and flexibility and capability of handling complex tasks of the human worker.

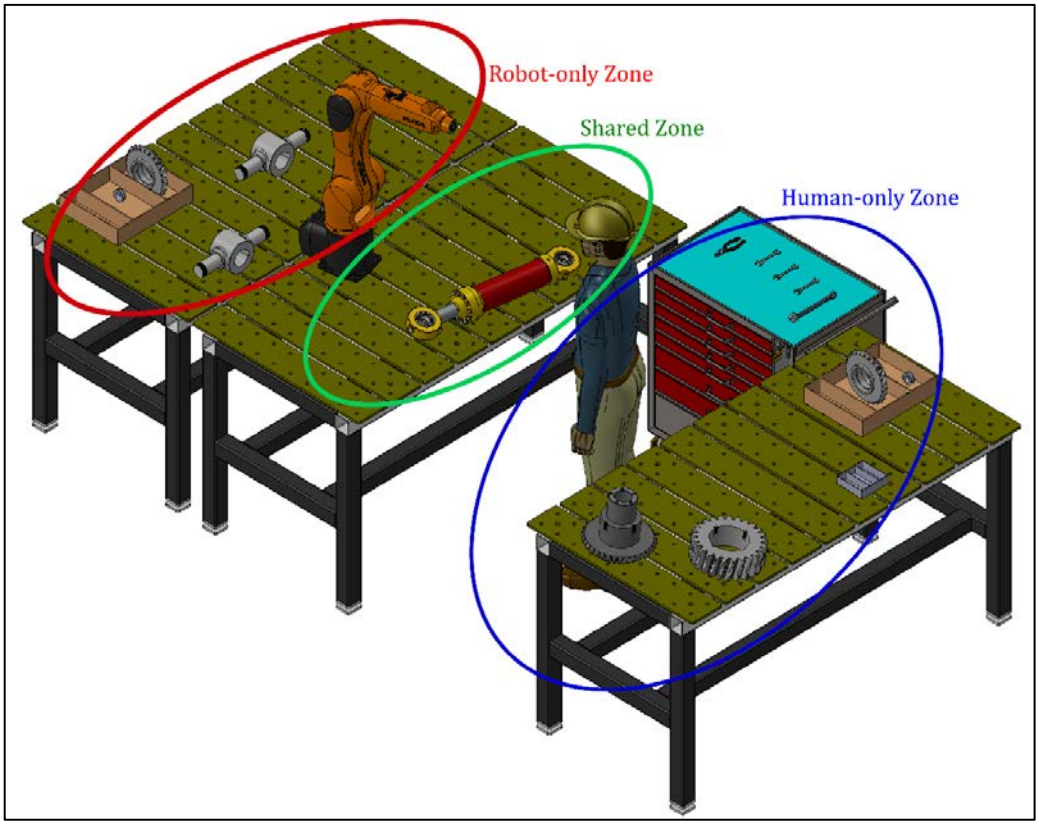


Figure 5.1 Human-robot collaborative disassembly workcell

A. Human-robot collaboration definition and characteristics

According to ISO 10218-1, safety requirement for industrial robots, and in context of production, human-robot collaboration is a “state in which a purposely designed robot system and an operator work on simultaneous tasks within a collaborative workspace’, i.e., where the robot system and a human can perform tasks concurrently or e e n jointly” [167]. Based on this definition, no spatial or temporary separations such as fences exist between human and the robot in the cell.

Different parameters are increasingly motivating the production industry to use human-robot collaboration systems. These factors include adaptability and flexibility, increased resilience and a higher degree of robustness, and more attractive and ergonomic work conditions. The combination of all these intelligence and skills of both robot and human has attracted the research and production industry toward using human-robot collaboration systems.

While in the assembly or disassembly lines a group of co-workers forms a team and works on the tasks, at a present human-robot collaboration typically a single or multiple humans collaborate with robot as co-worker or operator. The main factors that determine a human-robot collaboration characteristic not only in disassembly cells but across all production applications are autonomy and multiplicity. Based on the multiplicity factor, different classes and categories can be identified. Both robot and worker can work in single, multiple, or form a team. The difference between the multiple and team formation is that in multiple setting the agents can compete for resources or tasks, but in team setting, they are coordinated to act together.

The autonomy factor is to identify how much of human or robot's action is autonomous or determined by each other. In other words, the autonomy factor

expresses the leader-follower relationships between the human and the robot in a collaboration cell. Four different scenarios are assumed based on the autonomy level of either human or robot; a) Leading, b) supportive (which act as a follower to perform on the demand action, etc.), c) inactive (which is in standby), and d) intuitive and adaptable human and robot (which are capable of changing role). Based on the autonomy level different collaboration classes are possible which can be seen in Figure 5.2.

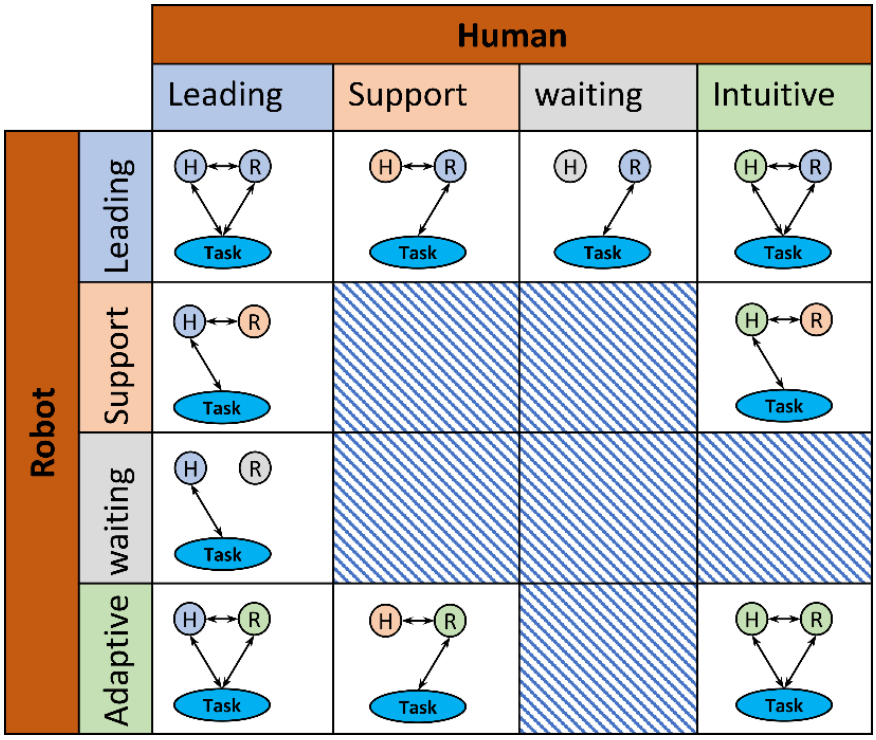


Figure 5.2 Different collaboration classes based on the autonomy parameter level

At a human-robot collaboration disassembly system, objects of the system, i.e. worker, robot, products, etc, are arranged in the space based on the activities and time, in order to disassemble a product based on optimized scheduling. In such a system the space is limited and occupied densely by EOL products and parts, workers, robots, and other technological components such as sensors, monitoring

systems, etc. Therefore, the main objects, i.e. The robot and human, are required to execute and handle a task in the shortest possible time within the scheduled sequences.

In addition to the above factors, task assignment is a main characteristic of the human-robot collaboration systems. To use the resources optimally and enhance the collaboration efficiency the task assignment should be carried out in an optimal and intelligent way. In the disassembly environment, due to the suitability of a task for human and robot or availability of them, a task may be re-allocated during the process.

B. Collaborative disassembly task classification and assignment

The primary aim of the human and robot task classification and allocation is to minimize the time and cost of collaboration. In a manual disassembly workcell it is assumed that all human workers have the same experience level, therefore, the task allocation is just about dividing the workload. However, in a human-robot collaborative workcell, robot and human have a different level of ability and skills. In addition, they are able to handle different levels of workload.

Disassemblability parameters introduced in [21] are exploited to classify and allocate the different disassembly operations. Eight parameters are defined that based on them any disassembly operation is categorized as: a) human only, b) robot only and c) human-robot collaboration. Table 5.1 shows different parameters for the classification of the disassembly tasks.

The defined parameters are used to indicate the disassembly task and therefore, they can be seen as decision variables for allocation of the collaboration classes.

The parameters are, component size (Cs), component weight (Cw), requirement of tools (T), accessibility (A), Component shape (Csh), operation complexity (Oc), positioning (P) and operation force (Of). Each parameter has a different level of difficulty or complexity to which a score allocated. Different level of scores indicates the difficulty or complexity of that parameter for disassembly operation. For instance, if Cs=2, indicates that the component is easy to grasp with respect to its size.

Table 5.1 Disassembly operation difficulty and complexity categories and scores

Component size (Cs)	Easily grasped	2	**Component shape (Csh)**	Symmetric	0.8
	Moderately difficult to grasp	3.5		Semi-symmetric	1.2
	Difficult to grasp	4		Asymmetric	1.4
Component weight (Cw)	Light	2	**Operation Complexity (Oc)**	Low	1
	Moderately heavy	2.2		Moderate	4.5
	Very heavy	2.4		High	6.5
Requirement of tools (T)	No tools required	1	**Positioning (P)**	No accuracy required	1.2
	Common tools required	2		Some accuracy required	2
	Specialized tools required	3		High accuracy required	5
Accessibility (A)	Shallow and broad fastener recesses	1	**Operation force (Of)**	Low	1
	Deep and narrow fastener recesses	1.6		Moderate	2
	Very deep and very narrow fastener recesses	2		High	4

Then, a procedure is designed to classify and allocate a disassembly operation based on the defined parameters. The flowchart for the introduced procedure is shown in Figure 5.3. First, a disassembly operation is analysed, and its properties and characteristics is identified. Then, based on its disassemblability characteristics and Table 5.1 categorization parameters (p_i), proper scores are assigned and $\sum_{i=1}^{n} p_i$ is calculated, where i = 1, 2, …, 8.

The algorithm is designed in a way that the tasks that are highly complicated or excess the robot's physical limitations, i.e. payload and maximum force and torque,

are assigned to the human, which in Table 5.1, have a higher score. Choosing a higher score for the third category of each parameter is to ensure that the algorithm assigns the task to the human if it is out of robot limitation. For example, if an operation is easy to grasp, light, and with low operation effort, but its complexity is at a high level it is highly likely to be assigned to the human.

Finally, using calculated $\sum p_i$ a proper category is selected, and a disassembly operation is assigned to either robot or human.

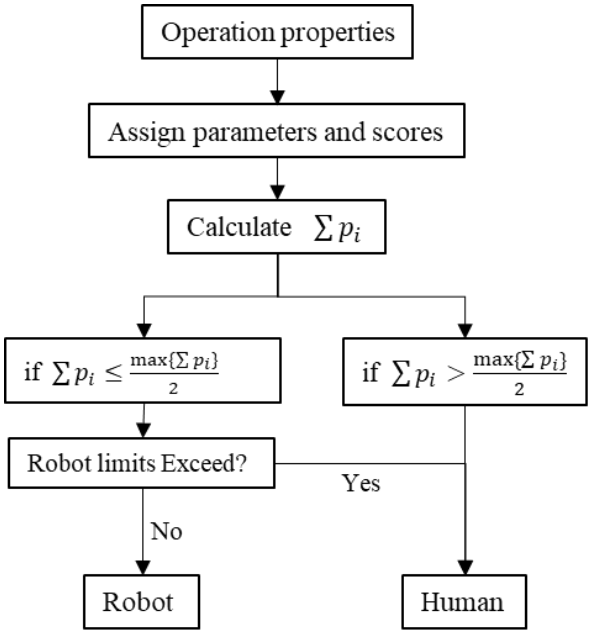


Figure 5.3 The flowchart for classifying and assignment of disassembly operations

5.2.3 Mathematical model and representation

In a collaborative disassembly scenario, it can be more efficient if some disassembly operations are carried out in parallel as actions are assigned to different operators. In other words, in collaborative systems, it is common that sub-assemblies emerge from disassembling the main product with unpredicted characteristics. For instance,

they may require delicate and complex procedure i.e. very hard for automation and should be handled by the human. Therefore, an efficient, robust, and mathematically easy to implement method, is required to represent the disassembly product and as much as possible solutions and scenarios of a human-robot collaborative disassembly system. In this work, the graph-based AND/OR method is used to represent the products and disassembly system. The AND/OR representation method is selected as it is easy to implement and is capable of facilitating the parallel and targeted disassembly planning explicitly.

Precedence relationships and the connections among sub-assemblies and individual components and disassembly operations are mathematically described and encoded using AND/OR method. Based on this method, the AND/OR graph is defined by two sets of nodes as $G = (V, E)$.

In this representation, $V = \{v_1, v_2, \dots, v_n\}$ where $n \in \mathbb{N}$ is the number of all individual components, and v_i are the set of all nodes which components of the product have one-to-one connections. It is notable that a component is considered as a sub-assembly that cannot be disassembled further. In addition, a set of directed edges is defined as $E = \{e_{ij}\}$ where e_{ij} represents a disassembly operation from v_i to v_j as directed edges in AND/OR graph.

An AND/OR representation graph of the case study is shown in Figure 5.11. As it can be seen, each subassembly is represented by a rectangle nude and defined as a combination of alphabetic letters. Each subassembly also is assigned an integer number in parentheses as 1 , 2 , … . The disassembly operations are represented by edge arcs as 1, 2, …, J. n addition, parent and child subassembly are defined such as v_i is the parent of v_j if v_j is created by disassembling v_i and v_j

is called the child. For example, in Figure 5.11 the subassembly [AB] is the parent, and [A] and [B] are the children. A disassembly sequence of operation is considered as a feasible sequence if the following conditions are satisfied.

a) To represent the disassembly operation precedence the Precedence Matrix $Pr = [p_{ij}]$ is defined where:

$$p_{ij} = \begin{cases} 1 & if\ i\ \ can\ be\ carried\ out\ before\ \ j \\ 0 & if\ i\ \ \ cannot\ be\ carried\ out\ before\ \ j \end{cases} \qquad (5.10)$$

To consider a sequence as feasible, the precedence relationship of the operations must be satisfied.

b) Based on the AND/OR graph, an OR relationship among disassembly operations means that different operation paths result in different child sub-assemblies. In this relationship, although two operations can be possible at the same time, however, if one operation is selected the other one cannot happen. For instance, both operations 1 and 2 are feasible and can be selected, but if operation 1 selected and its child sub-assemblies obtained, operation 2 is no more possible cannot be happened. To represent the OR relationship the Conflict Matrix $Ca = [c_{ij}]$ is defined where

$$c_{ij} = \begin{cases} -1 & if\ \ \ i\ conflict\ with\ \ j \\ 0 & if\ i\ \ \ doesn't\ conflict\ with\ \ j \end{cases} \qquad (5.11)$$

Therefore, for operation 1 and operation 2, if $c_{ij} = -1$, based on the OR rule one of them can be carried out, but both together is not feasible.

c) to represent the relationship among operations and sub-assemblies, Incidence Matrix $M = [m_{ij}]$ is defined where:

$$m_{ij} = \begin{cases} 1 \; if \; subassembly \; i \; is \; a \; result \; of \; operation \; j \\ -1 \; subassembly \; i \; is \; disassembled \; via \; operation \; j \\ 0 \quad otherwise \end{cases} \qquad (5.12)$$

Therefore, the following constraints should be satisfied for subassemblies and operation so that a disassembly sequence is considered as a feasible sequence.

$$\sum_{j=1}^{J} x_j \geq 1 \qquad (5.13)$$

$$x_k = \sum_{j=1}^{J} y_{jk} \qquad (5.14)$$

$$0 \leq \sum_{j=0}^{J} g_{jk} x_j \leq 1 \qquad (5.15)$$

$$\sum_{j=1}^{J} y_{jk} \geq \sum_{j=1}^{J} y_{kj} \qquad (5.16)$$

$$\sum_{j=1}^{J} y_{kj} \leq 1 \qquad (8.17)$$

Where $j, k = 1, 2, \ldots, J \;\; and \;\; x_j, y_{kj} \in \{0, 1\}$ and defined as $y_{kj} = 1$ if operation k is after j and $y_{kj} = 0$ otherwise. Also, $x_j = 1$ if operation j is carried out and $x_j = 0$, otherwise.

5.2.4 Disassembly sequence optimization algorithm

The main problem of disassembly planning is to find an optimal sequence of the disassembly operations. In other words, for a product with many individual components and subassemblies, the question is in what order the operations should be carried out and the components are disassembled. Finding an optimum answer to this question will determine the efficiency of the whole process. However, the number of possible solutions rises dramatically with increasing the number of individual components of the product which makes this kind of problem to be considered as NP-hard problem and requires a heuristic method to find a solution.

In addition, a human-robot collaboration system adds extra complexity to the system and makes it even more challenging. In addition, for this problem finding an optimum solution is not guaranteed and usually, a near-optimal solution is produced.

One of the metaheuristics methods that have been used in this field and proven to be efficient is the genetic algorithm (GA). In this research, GA is modified and employed to find a near-optimal solution i.e. a sequence of disassembly operations, for parallel and targeted human-robot collaborative disassembly process. The following sections explain the steps and modifications of the proposed genetic algorithm.

A. Evaluation parameters and fitness function

-non-targeted component index

In a targeted disassembly system, the goal is to disassemble all selected components without disassembling any extra component. However, in a realistic disassembly process it inevitable to disassemble the non-targeted components due to several factors such as accessibility, product geometric constraints, and precedence relationships. To improve the efficiency of the disassembly process and minimize the disassembling unnecessary components non-target component index is defined as Equation 5.18 for all components. This index is defined in a time unit to penalize the operations that disassemble a non-target component.

$$Nt_{ij} = \begin{cases} 1 \ (s) & if\ i\ is\ disassembled\ before\ j \\ 0 \ (s) & otherwise \end{cases} \qquad (5.18)$$

Where i is a non-targeted component and j is a targeted component. This parameter is defined to ensure that the non-essential operations that disassemble the non-target components are placed at the end of the disassembly sequence as much as possible.

-disassembly operation time

The total time of a disassembly operation is a combination of several parameters. These parameters are including basic operation time, preparation time, and travel time. The basic operation time is an average time that takes to perform the operation without preliminary preparation and is different from total operation time. The basic operation time is defined as $tb_{i,seq}^{w}$ where i the operation to disassemble the component i, seq is the place of the operation i in the disassembly sequence and $w \in \{0,1\}$ indicate whether human or robot performs the operation i.e. 0 denotes human and 1 denotes robot. The basic operation time is normalized so that all indices are in the same order and have the same effect on optimization.

The preparation time is the time that takes that the worker i.e. human or robot, prepares the operation preliminaries and includes tool change and waiting time. It is defined as Equation 5.19.

$$tp_i^w = tl_{i-1,i}^w + tw_{i-1,i}^w \qquad (5.19)$$

where i denotes the operation to disassemble the component i and w to indicate the human or robot operator. In addition,

$$tl_{i-1,i}^w = \begin{cases} 1\ (s) & if\ tool\ changes\ from\ operation\ i-1\ to\ i \\ 0\ \ (s) & otherwise \end{cases} \qquad (5.20)$$

$$tw_{i-1,i}^{w} = \begin{cases} 1\ (s)\ \ if\ worker\ waits\ from\ operation\ i-1\ to\ i \\ 0\ (s)\ \ \ otherwise \end{cases} \quad (5.21)$$

Travel time is the time required that robot end effector or human operator move from one to another after finishing operation and calculated as Euclidian distance of the disassembly points divided by travel speed of the operator as Equation 5.22.

$$tt_{i-1,i}^{w} = \frac{\sqrt{(x_{i-1}-x_i)^2+(y_{i-1}-y_i)^2+(z_{i-1}-z_i)^2}}{s^w} \quad (5.22)$$

Where (x_i, y_i, z_i) is the coordinate of the disassembly points and s^w is the travel speed of human or robot. Finally, the total disassembly time index for each operation is calculated using Equation 5.23.

$$T_{i,seq}^{w} = tb_{i,seq}^{w} + tp_{i}^{w} + tt_{i-1,i}^{w} \quad (5.23)$$

- Operator change

To have an optimal disassembly sequence, it is important that minimize the switch between human and robot. In order to consider this parameter, the operator change index is defined as Equation 5.24.

$$oc_{i-1,i}^{w} = \begin{cases} 1\ (s)\ \ if\ operator\ changes\ from\ operation\ i-1\ to\ i \\ 0\ (s)\ \ \ otherwise \end{cases} \quad (5.24)$$

This parameter is defined in the time unit and penalizes the operations that require the operator to change.

B. Encoding the disassembly sequences

To apply the genetic algorithm and search the solution domain for a near-optimal solution, the disassembly sequences should be encoded mathematically based on the optimization parameters, i.e. non-targeted component index, disassembly operation time and operator change. Based on the genetic algorithm method, any possible solution is represented using a chromosome and its smallest element called gene. Any individual parameters of a component or operation e.g. operator change is a gene.

The combination of all genes creates a sequence of all operations for the disassembly process of a product i.e. chromosome. A chromosome is a combination of numbers and other characters and made of different sections equal to the number of optimization variables. In this research, three optimization parameters were defined which their combination obtains the chromosomes. An example of a chromosome for this research can be seen as following:

$$ch_k^g = \{Nt_{12}, \dots Nt_{nm}, ; T_{1,1}^0, \dots, T_{n,m}^1; oc_{1,2}^w, \dots, oc_{n-1,n}^1\} \qquad (5.25)$$

Where k is the number of the chromosome and g is the generation that the chromosome is generated. The above chromosome has three different sections and changed and generated in new generations using different operators which are explained in the next section.

C. genetic algorithm parameters

-initial population

The initial population contains enough number of a randomly selected chromosome to initiate the GA algorithm. The chromosomes should meet the feasibility and precedence relationship condition in order to be eligible to put in the initial population. It is notable that in all steps and generations of the GA the feasibility and precedence relationship conditions are checked. The number of chromosomes in the initial population (np) has a direct effect on the efficiency and calculation time of the GA. Therefore, in this research numerical investigation is carried out to specify np and other GA parameters which are explained in detail in the case study section. It is assumed that the number of chromosomes remain the same from one generation to the next one.

- reproduction

From one generation to the next generation, the chromosomes need to be reproduced so that the GA propagated over the generations until an acceptable solution is achieved. In each generation, a specific number of chromosomes are selected to pass to the next generation and produce the next generation. The selected chromosomes are called parents and produced chromosomes in the next generation are called children.

Children are born using four operations i.e. crossover, mutation, Cut-Paste, and Break-Join. The probability of applying one of these operators on a chromosome are *Pc, Pm, Pcp*, and *Pbj* respectively. Based on the operator's probability it is possible that none of them or a combination of them are applied to a chromosome.

Same as np, these parameters have also direct effect on efficiency and calculation time of the GA, therefore, are investigated and selected numerically in the case study section.

The crossover operator acts on two parents' chromosome and randomly select a gene in one parent to break the chromosome from that point and swap the genes before and after that point with the other parent and produce two children. An example of a crossover operation on two parents to produce two children is shown in Figure 5.4a. It can be seen that the third gene is selected randomly as the breaking point and sub-sequences are swapped to produce child 1 and 2. It is notable that after all reproduction operators the feasibility and precedence relationship conditions are checked, and the new child should meet the conditions.

Mutation operator act on one parent chromosome to generate one child. Different mutation methods were used in researches such as Insert, Inverse, and Swap. In this work, the Swap method is used by which two genes of a chromosome are randomly selected and swapped together. An example is shown in Figure 5.4b.

The Cut-Paste operator is the next reproduction operator that produces a child chromosome from a parent. In this method, one or more genes of a chromosome randomly selected, cut, and then pasted in a randomly selected position in the chromosome. In Figure 5.4c an example of a Cute-Paste operator can be seen.

Break-Join operator is defined to produce a child from a parent chromosome. Based on this operator a breaking point is selected randomly and the chromosome is separated from that point and divided into two sections. Then these two sections are re-joined together in a reverse order to produce a child chromosome, which can be seen in Figure 5.4d.

- Fitness function

A fitness function evaluates the quality of a chromosome, i.e. a sequence of disassembly operations. A fitness function is defined using disassembly process parameters. In this work, the disassembly process parameters are non-targeted component index Nt_{ij}, disassembly operation time $T^{w}_{i,seq}$, and operator change $oc^{w}_{i-1,i}$ which were defined in the previous section. Therefore, the fitness function is defined as per Equation 5.26.

$$f(ch,g) = \alpha \sum_{i=1}^{I} \sum_{j=1}^{J} Nt_{ij} + \beta \sum_{i=1}^{I} \sum_{seq=1}^{SEQ} T^{w}_{i,seq} + \gamma \sum_{i=2}^{I} oc^{w}_{i-1,i} \qquad (5.26)$$

Where ch is the number of the chromosome in the gth generation and $\alpha, \beta, \text{and } \gamma$ are weights that are defined based on the aim and objectives of the disassembly process. The application of these weights is to increase or decrease the effect of one parameter with respect to the others. They are user-defined and adjusted mostly based on the experiential knowledge of an EOL product for disassembly. Depends on the application, GA is used to maximized or minimized the fitness function. In this research the goal is to find a near-optimal solution by minimizing the fitness function, i.e. a smaller fitness of a chromosome means it is a better solution.

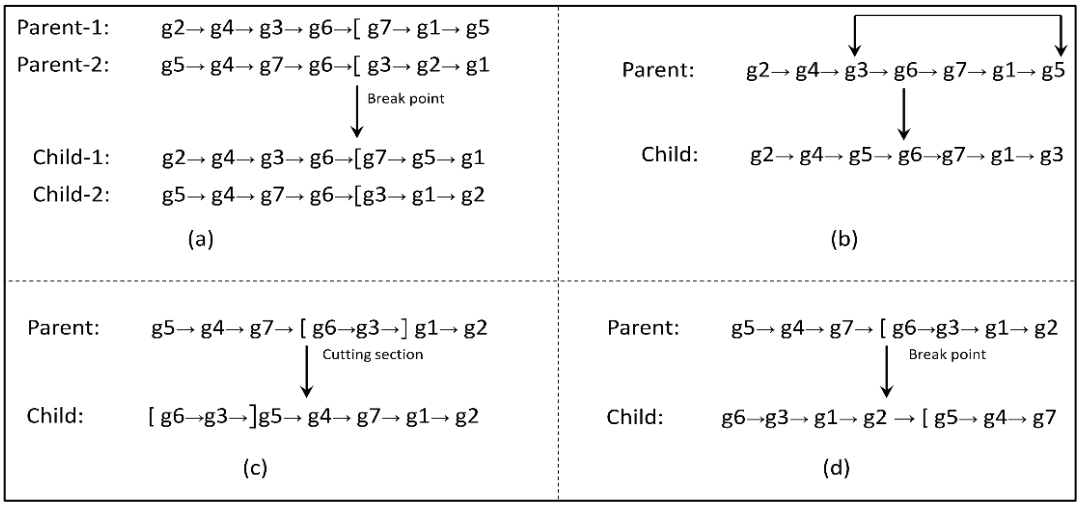


Figure 5.4 Reproduction operator examples, a) Crossover, b) Mutation, c) Cut-Paste, d) Break-Joint

5.3 Experiments and results

5.3.1 Validation of the task classification and allocation

To validate the task classification and allocation, peg-out-hole disassembly operation is selected as a basic and common operation appearing in the disassembly processes. Many disassembly tasks such as removing a pin or pulling a shaft out of a mearing can be represented by this operation. Therefore, this operation was selected to be performed using a robot arm to assess its disassemblability. The properties of the peg and hole are shown in Table 5.2.

Table 5.2 Physical details of the peg and hole.

	Diameter (mm)	Length (mm)	Material	Weight (g)
Peg	30	75	PLA	95
Hole	31	80	PLA	135

The experiment was carried out using a 6-DOF serial manipulator manufactured by TECHMAN. The manipulator model was TM14 with a maximum load of 14 kg and repeatability of ±0.1 mm. The structure of the experimental platform is shown in

Figure 5.5. It is also including a 6-axis force and torque (F/T) sensor and a 2-finger gripper. F/T sensor model is ATI Axia80 which provides ±500 N for force and ±20 Nm for torque with a resolution of ±0.1 N for force and ±0.005 Nm for torque. The 2-finger gripper model is ROBOTIQ 2F with an electric actuator. The sensor is installed between the robot arm and gripper to measure force and torque that apply on end-effector as it contacts the object.

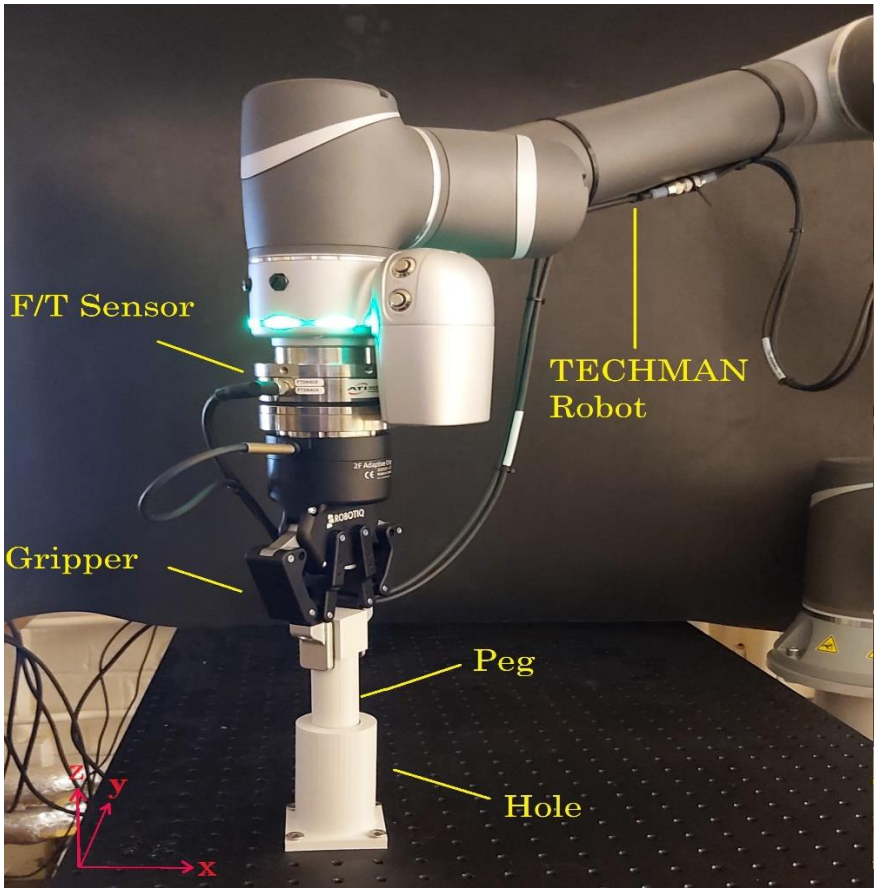


Figure 5.5 Experimental robotic platform for peg-ot-hole disassembly operation.

Based on Table 5.1 and tests using the experiment set up, including the robot's capability, the disassemblability of this operation is assessed and relevant scores are assigned to its classification parameters which can be seen in Table 5.3.

Component size is categorized based on the robot's grasp capability, gripper specification, and peg size. The robot's reliability is ±0.1 mm, the gripper's stroke is 85 mm and the peg's diameter is 30 mm. Therefore, the size is well within the system's specification and it is categorized as "Easy to grasp". Its weight is light compare to the robot's ma i mum payload, therefore categorized as "light", and tool requirement is categorized as "No tool required". There is no restriction to the object, therefore, the accessibility is categorized as "Shallow and broad fastener recesses" and the component shape is "symmetric". The operation complexity is assessed based on the professional expert's knowledge, and for this case, it is considered as "Low". The positioning parameter is assessed based on the robot's accuracy specification and operations accuracy requirement. For this study, with ±0.1 mm repeatability of the robot and 1 mm clearance between peg and hole, it is considered as "Some accuracy required".

Table 5.3 The disassembly operation classification parameters and corresponding scores.

Component size (Cs)	Easily grasped	2	**Component shape (Csh)**	symmetric	0.8
Component weight (Cw)	Light	2	**Operation Complexity (Oc)**	Low	1
Requirement of tools (T)	No tools required	1	**Positioning (P)**	Some accuracy required	2
Accessibility (A)	Shallow and broad fastener recesses	1	**Operation force (Of)**	Moderate	2

For this operation, as the weight of the peg is low, it is expected that the operation force is low. However, there are situations that the uncertainty level is high and peg contacts the hole, and a wedge-like situation occurs. In this case, the forces and torques on the end effector rise dramatically and could result in damage to the equipment or failure of the operation. Therefore, to validate this parameter

experimentally, uncertainty situation simulated to peg and hole contact, and the forces and torques during the operation were recorded using the F/T sensor. The uncertainty introduced using a randomly selected ±1 mm error in xy plane and ±3 degrees peg's tilt from its perpendicular condition on y plane. The e periment repeated 10 times with the introduced situations and the average forces and torques were measures as shown in Figure 5.6. The figure shows that the average torques and forces rise in some directions, however, it is lower than the gripper and robot's limitation. Therefore, the operation force parameter is considered as " oderate".

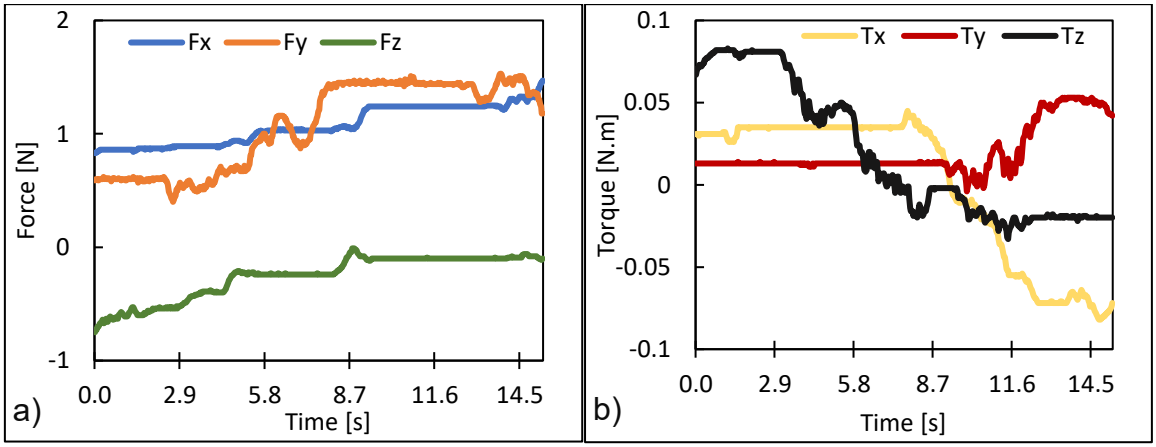


Figure 5.6 Measured a) Forces and b) Torques for peg-out-hole disassembly operation.

5.3.2 case study

To examine the method and validate the hypothesis, the method is tested on an automotive EOL product. A fuel pump was selected as the case study and its CAD model and exploded view are shown in Figures 5.7a and 5.7b respectively. The product has 20 individual components which include 5 fasteners i.e. bolt screws. And individual component is part or subassembly that cannot be disassembled further. It should be noticed that in the figure the fastener, i.e. screws, bolts, etc, are

shown with numbers and other components are shown with alphabetic letters. The property of the components and required operation and tools are summarised in Table 5.4. The table shows different disassembly operations required to disassemble a component. There are five disassembly operation types that may require a tool or disassemble without a tool. There are also five different tools to perform operations. The table also shows the disassembly point and mass for each component.

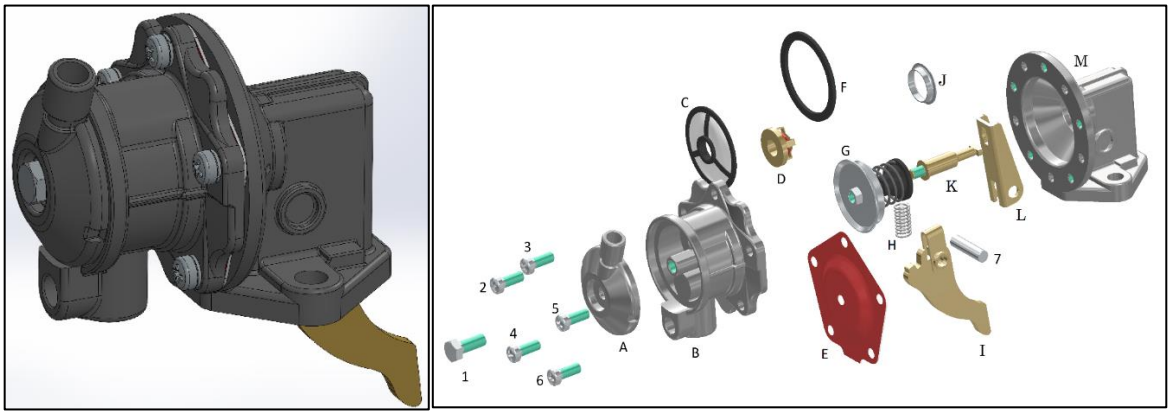


Figure 5.7 a) CAD model and b) exploded view of the fuel pump

Table 5.4 The individual components and properties of the fuel pump

No.	Name	Disassembly Operation	Tool	Disassembly Point (mm)	Mass (g)
1	Bolt	Unscrewing	Spanner	(0, 0,0)	10
2	Screw 1	Unscrewing	Screwdriver	(-50, 0,0)	6
3	Screw 2	Unscrewing	Screwdriver	(0,50,0)	6
4	Screw 3	Unscrewing	Screwdriver	(0,-50,0)	6
5	Screw 4	Unscrewing	Screwdriver	(50,0,0)	6
6	Screw 5	Unscrewing	Screwdriver	(50,50,0)	6
7	Pin	Pulling out	Hammer	(20,-30,80)	25
A	Upper case	Removing	No tool	(0,50,20)	178
B	Chamber	Removing	No tool	(0,50,50)	350
C	Filter	Removing	No tool	(0,50,50)	6
D	Guide kit	Removing	No tool	(0,50,50)	55
E	Gasket	Separation	long-nose pliers	(0,50,50)	7

F	O-ring	Separation	long-nose pliers	(0,50,70)	4
G	Diaphragm	Pulling out	No tool	(0,50,70)	125
H	Spring	Pulling out	pliers	(0,-50,70)	6
I	Handle	Removing	No tool	(0,-80,70)	120
J	Ring	Pulling out	No tool	(0,50,70)	5
K	Shaft	Pulling out	No tool	(0, 0,80)	142
L	Connector	Removing	No tool	(0,-50,90)	65
M	Lower case	Removing	No tool	(0,0,100)	260

Then, the method described in the previous section is employed to find a near-optimal sequence of operation for disassembling the fuel pump using the human-robot collaboration disassembly system. The flowchart of the proposed method is shown in Figure 5.8.

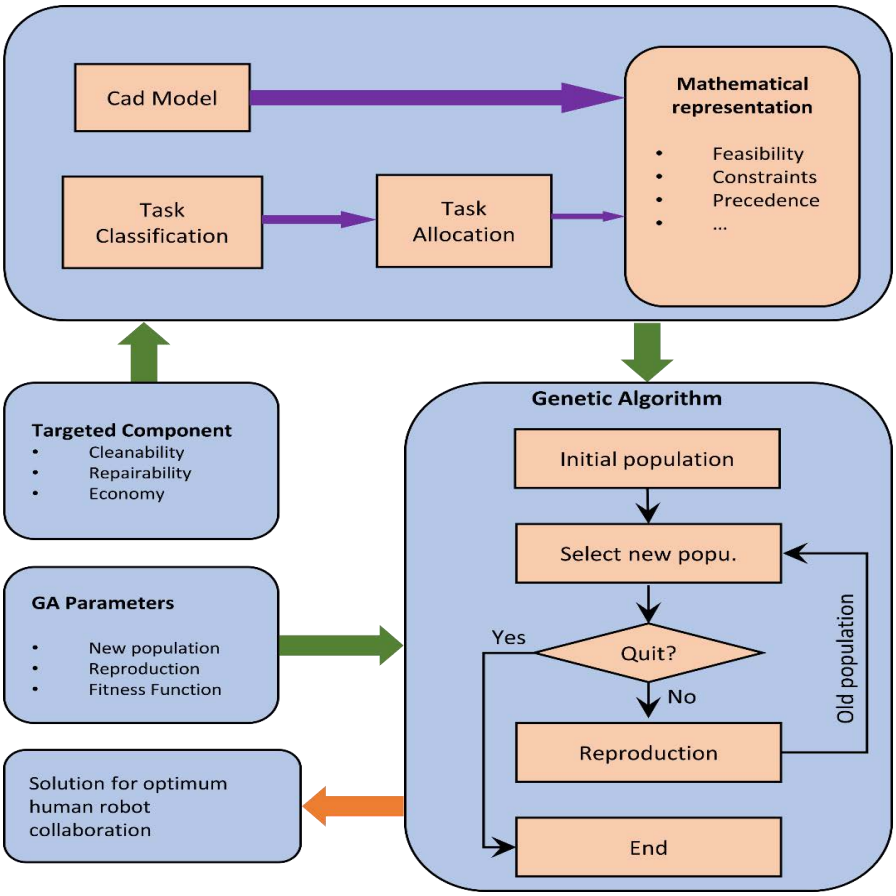


Figure 5.8 Flowchart and structure of the proposed method

5.3.3 Performance analysis

As previously discussed, the performance and efficiency of the GA are highly dependent on the initial parameters such as initial population number (np) and probability factors of the reproduction operators, i.e. Pc, Pm, Pcp, and Pbj. Therefore, extensive computational simulation investigations were carried out and different genetic algorithm parameters were studied. All experiments and computational simulations were carried out on a machine with ntel® Core™ i5 6500 CPU @ 3.2 GHz, 8.00 GB RAM, NVIDIA GeForce GTX 970 and Windows 10 operating system. The GA and other simulation algorithms were programmed on commercial software MATLAB© R2019b.

First, to determine the optimum initial population size (np), different population sizes were selected and performed the algorithm. Then the time and the total number of generations to converge the algorithm were plotted which can be seen in Figures 5.9a and 5.9b. It is notable that each simulation was repeated 5 times and the average time and number of generations were calculated to reduce the computation error. The results show increasing the population number results in achieving the optimal result with a smaller generation. However, further increasing the population number, increases the computation load and time dramatically. Therefore, the results suggest that an initial population number of np=40 is an optimal number for this study.

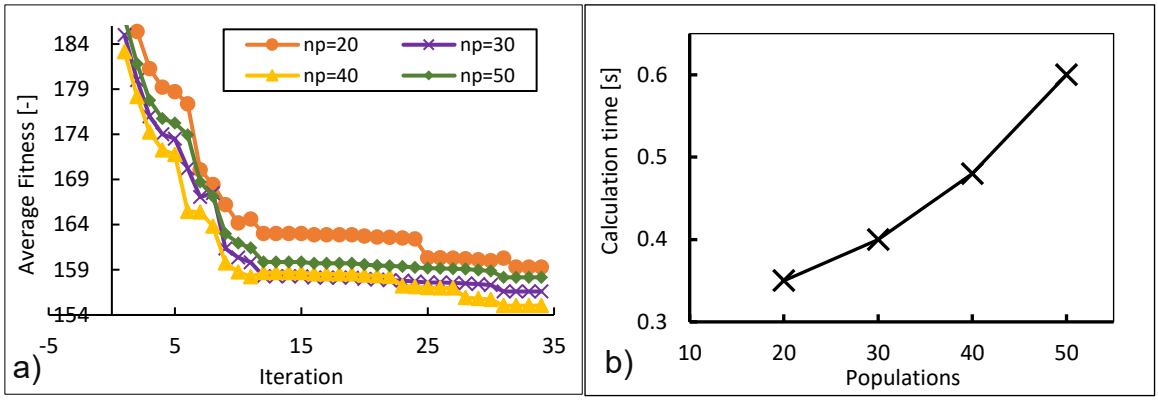


Figure 5.9 a) Total produced generation to convergence for each population, b) Total computation time of algorithm with different population sizes.

The optimum values for other probability factors were determined using a similar approach as for the initial population. The experiments were repeated for different probabilities where $P \in [0,1]$, and results for convergence generation were plot which is shown in Figure 5.10. The result shows that the operation probability has a direct effect on the algorithm efficiency. The trends for all parameters are almost similar; for very small all high probability, the calculation time increases. The optimum values are at the range between 0.05 to 0.25. Table 5.5 summarises the optimum parameters for the GA base on the simulation results.

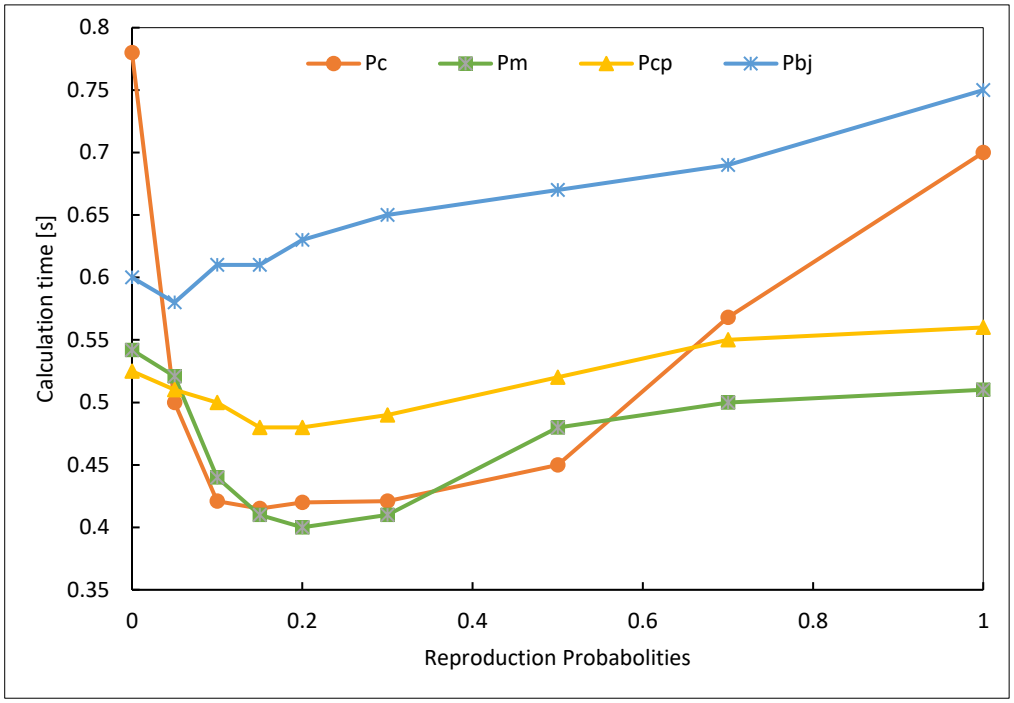


Figure 5.10 Computational calculation time for different reproduction operator probabilities

Table 5.5 Genetic algorithm's optimal parameters

NO	PARAMETER	VALUE
1	*np*	40
2	*Pc*	0.15
3	*Pm*	0.2
4	*Pcp*	0.15
5	*Pbj*	0.05

To represent the disassembly process and precedence relationship mathematically the graph-based AND/OR is employed. The created AND/OR graph for this case study is shown in Figure 5.11. The graph shows all contact, operation sequences, and precedence relationships. The AND/OR graph joined with the feasibility and constraint factors are used to represent the solution domain. It is notable that the AND/OR graph just shows part of the possible operations and subassembly. In this graph, the subassemblies are shown by a rectangular and operations by an ark

joining to directions. Based on this graph there are 30 possible subassemblies and 18 operations.

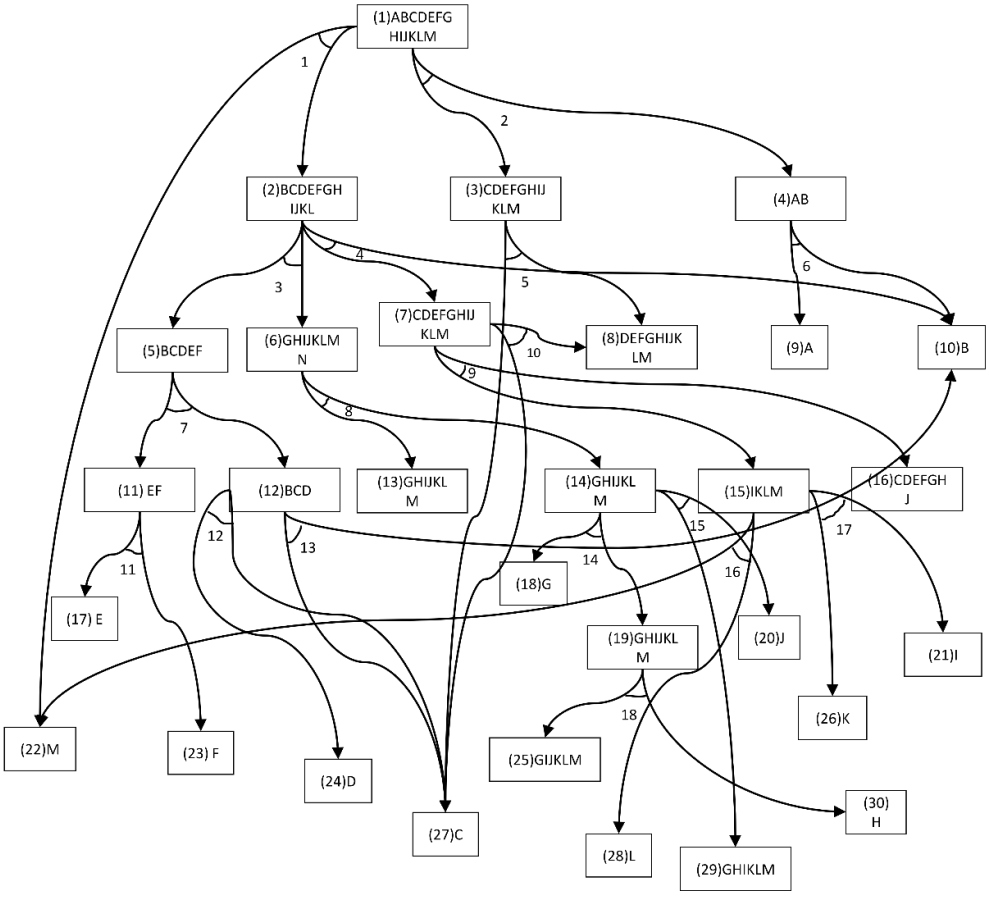


Figure 5.11 AND/OR graph-based disassembly process representation of the fuel pump

After setting the optimum parameters for the algorithm, mathematical representation, and other preliminaries the algorithm was run for the described case study, and results were plotted. The actual fitness value and computational calculation time for each iteration generated by the proposed method are shown in Figures 5.12a and 5.12b. To validate the proposed method and verify its efficiency, the Particle Swarm algorithm (PSA) [66] was used and the results compared. Figure 5.12a demonstrates the fitness values of the solutions while the algorithms are

iterating and solving the problem. The results show about 8.8% improvement in fitness value produced by the proposed method in compare with PSA. Figure 5.12b shows the running time of the algorithms when it is iterating. It can be seen that the calculation time of the proposed method is slightly higher than the PSA method. However, the fitness values of this method are clearly lower than the PSA which means a higher quality solution for disassembly sequence planning.

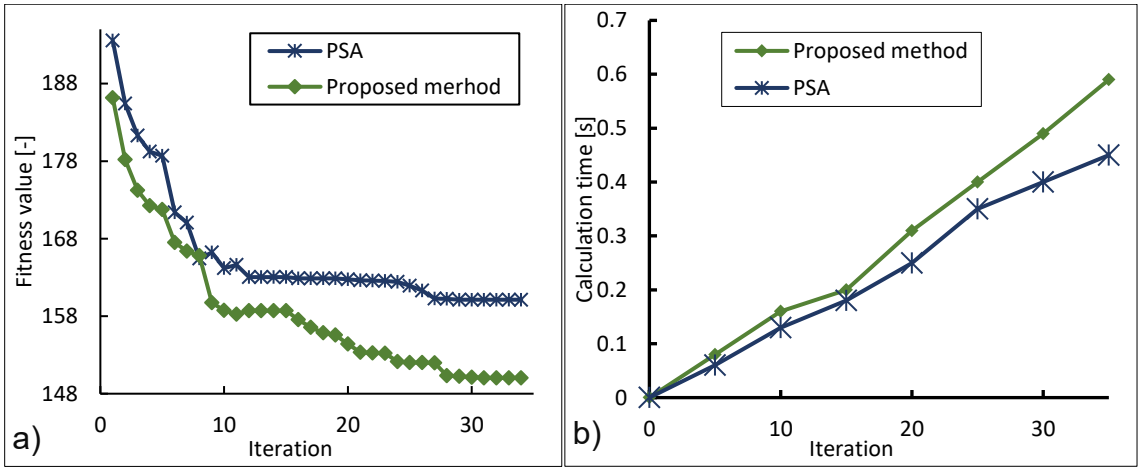


Figure 5.12 a) fitness values of the proposed method in comparison with the PSA method, b) Computational calculation running time of the proposed method and PSA method

As previously discussed, in this kind of problem the challenge is to find a series of near-optimal solutions, and finding an optimum solution is not usually the case. A list of three different near-optimal solutions is presented in Table 5.6. Usually, a decision-maker i.e. artificial intelligence or human decision-maker is required to select a solution based on the requirement of the process. Also, the fitness of each solution is shown in the table. The Gantt chart of the first solution of Table 5.6 is demonstrated in Figure 5.13. The Gantt chart shows the scheduling of the robot and human, the disassembly times and operation sequences of the disassembly

process. It is notable that all requirements and parameters defined previously, such as tool change, operator change, and remanufacturability were considered by algorithm while generating the solution.

Table 5.6 Three near-optimal solutions of disassembly sequences of the case study

Human-robot collaboration solution	fitness
Human: 1→ 2→ 3→ 4→ 5→ 6→ C→ 7→ E→ M→ H→ L→ K→ J Robot: A→ B→ D→ F→ I→ G	**149.3**
Human: 1→ 5→ 4→ 6→ 3→ 2→ C→ 7→ E→ F→ I→ G→ M Robot: A→ H→ L→ B→ D→ K→ J	**149.9**
Human: 1→ 3→ 4→ 5→ 6→ 2→ C→ I→ E→ F→ 7→ G→ M Robot: A→ B→ L→ H→ D→ J→ K	**151.1**

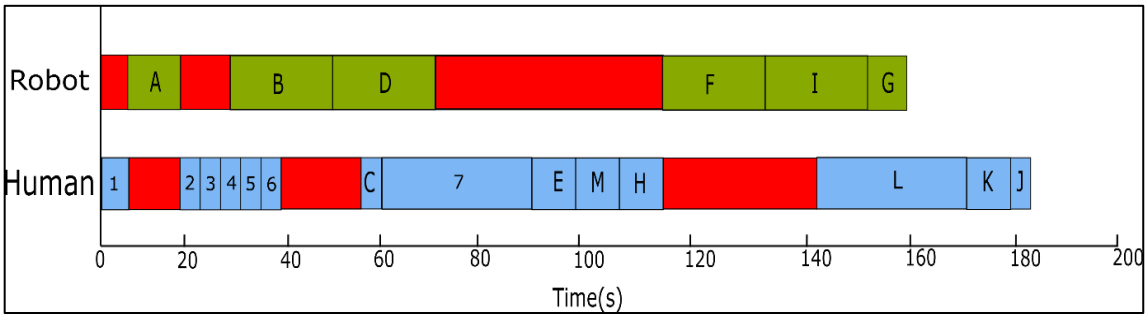


Figure 5.13 The Gantt chart of human-robot collaboration for the first solution.

5.4 Conclusion

The efficiency of the disassembly process as the main step of dealing with EOL products is determinant for the future remanufacturing industry. The manual disassembly is not efficient and is not justified economically. In addition, due to the high level of uncertainty and complex nature of disassembly operation fully autonomous systems are not robust and reliable. Human-robot collaborative systems are being developed and tested and the reports and results are promising.

The main developments and human-robot collaborative system proposals are currently appearing in manufacturing and especially assembly domains, however, there is a lack of fundamental research and proposed methods for remanufacturing and disassembly systems. In this chapter, the fundamental of human-robot collaborative disassembly systems is investigated and the main definitions and characteristics are established. A novel method is proposed for disassembly task classification and allocation based on the requirements of human-robot collaboration. In addition, to enhance the efficiency of the disassembly process, different parameters are adapted to target and select the components for the disassembly process based on the remanufacturability requirements. The genetic algorithm is modified based on newly defined parameters to optimize the process and find a near-optimal solution. To select the optimum parameters for GA, different computational simulations carried out and the best parameters are selected. A 6-DOF TECHMAN robot arm was used to set up experiment rig and validate the classification and allocation hypothesis. The peg-out-hole disassembly operation was selected as a common disassembly operation to test the method. Finally, to validate and verify the efficiency of the proposed method, an automotive EOL product is selected as the case study, and the results are presented. The results demonstrate the efficiency and reliability of the proposed method in comparison with previous methods, therefore, objective 3 is met.

B v

Chapter 6- Conclusions

6.1 Conclusions

This research has presented various methods and techniques to improve the reliability and efficiency of disassembly process of automotive products. The focus of this research was to investigate planning of different disassembly modes, i.e. manual, automated, and collaborative to find an optimised disassembly plan. To consider the previous works and find the outline of existing methods, a thorough literature review was carried out on disassembly process planning. Different areas of disassembly planning studies were investigated, and different methods and approaches were discussed to reveal key barriers and challenges. Based on the analysis, main factors affecting the efficiency of the disassembly process were highlighted to outline the thesis methodology and research direction.

The focus of the first part of this research was to investigate and propose a new method for disassembly sequence based on the new criterion and parameter with focus on manual disassembly operations. For long time many researches have considered the time of the disassembly operation as the main parameter of the finding an optimum solution. In this chapter, new parameters based on the part handling, disassembly task complexity and difficulty, and demand for disassembled component were defined. The method offers effectiveness, reliability, and compatibility with employed state of the art representation and optimisation algorithms, i.e. the hybrid graph method and genetic algorithm. Common automotive products were selected and analysed to test and validate the hypothesis and proposed method. Optimum disassembly sequences for a turbocharger and a water

pump were generated and the disassembly processes based on that sequences were carried out. The results were compared with time-based solution which showed 13% and 10% improvement in disassembly time for turbocharger and water pump respectively. The achievements and validated approaches in this part were used as foundation of the **Objective 3** and toward the thesis main objective i.e. a reliable and efficient disassembly process. The main findings of this chapter are as followings:

- Time-based parameters operation time and robot travel time are not efficient in disassembly sequence planning.
- Using disassemblability characteristics of the components and operation for disassembly planning shows a promising improvement over time-based parameter.
- Experiments on a turbocharger shows 13% improvement in disassembly time using proposed method.
- Experiments on a water pump shows 10% improvement in disassembly time using proposed method.

The aim of the second part of this research was to investigate the fundamentals and science of disassembly operations. In this section, the peg-out-hole disassembly operation was selected as one of the most common disassembly tasks to study. In addition, intelligent based planning strategies were proposed and developed to tackle one of the most challenging aspect of automated disassembly processes. i.e. high-level uncertainty. Based on the literatures, although there are thorough studies on peg-in-hole assembly operation, there is lack of fundamental knowledge on peg-in-hole disassembly operation. Therefore, first, the peg-out-hole disassembly

operation was mathematically modelled and analysed to investigate basic science of the operation, and also identify and analysing the peg and hole contact states. Force/Torque sensor was used to collect data while peg and hole are in contact and build force and torque maps for different contact states. Effective strategies were introduced to improve the maps and classify the peg and hole contact states. To estimate the position and orientation of the peg and hole using force torque information, a novel estimation method was proposed to address uncertainty in disassembly operations toward a reliable and effective robotic disassembly. To obtain force and torque data and validate the hypothesis and proposed method, an experiment using a TM robot arm equipped with a 6-DOF Force/Torque sensor was designed and carried out. Experimental results show the efficiency and reliable accuracy for the proposed pose estimation method. This part fulfilled the **Objective 2** and its results and established knowledge were used to achieve **objective 3**. The main findings of this chapter are summarised as below:

- The depth of the peg is a function of peg and hole diameters.
- Force and torque maps contain information that could be employed to estimate the relative position and orientation of peg and hole.
- Despite useful information, force and torque maps contain redundant information that impact the estimation significantly.
- A map with higher QFM results in higher estimated error.
- Average estimated error using the proposed method is less than 6%.

The final part of this work focused on human-robot collaborative disassembly operations based on the developed methods and from the previous sections. The reliability and ability of human to deal with complex tasks were combined with

accuracy and repeatability of the robot to develop a reliable and efficient disassembly plan. Therefore, first the fundamental of a collaborative human-robot system was analysed and the main characteristics and parameters were identified and established. Disassembly tasks were classified and allocated based on the human-robot collaboration requirements. For this purpose, the difficulty and complexity categorisation system developed in part 1, was modified and employed. To Validate this classification method and test its suitability for robotic disassembly, the proposed experiment in section 2 was employed. Finally, to test the proposed human-robot collaborative disassembly planning method, an automotive EOL product was selected as the case study and hypothesis and strategies were tested. The results proved the efficiency of the proposed method. The main findings of this chapter are as followings:

- Complete disassembly is not an efficient approach for disassembly process in remanufacturing.
- Cleanability, Reparability and Economy as the main remanufacturability parameters can efficiently prioritise and select components for disassembly.
- Score based task allocation is able to efficiently assign disassembly tasks to human or robot.
- Experiments on a fuel pump shows 8.8% improvement in disassembly time provided by proposed method compare with Particle Swarm algorithm.

The achievements and strategies developed and presented in this work, demonstrated novel methods and new techniques toward an efficient and reliable disassembly process. These were achieved by establishing fundamental and basic disassembly operation science and knowledge and developing intelligent planning

strategies enabling efficient and reliable disassembly process. Therefore, the aim of the research has been achieved.

6.2 Contributions

The key contributions of this research are as followings:

- For the first time, optimisation parameters based on the component's handling characteristics and disassembly operation difficulty and complexity were defined and employed. This research has identified potential practicality that these parameters offer over time-based parameters.
- This research has resulted in a practical and effective disassembly planning that directly could be applied for automotive EOL products.
- The research has presented and verified a novel method for contact state estimation of peg-out-hole disassembly operation to tackle high-level uncertainty in such operations. In addition, it has investigated and established new fundamental knowledge and mathematical analysis of this operation for the first time.
- In this thesis, main characteristics and parameters affecting human-robot collaborative disassembly systems have been analysed and established. The effects and importance of these parameters were identified and employed to develop an efficient and reliable disassembly operation.
- This work has presented new strategies and algorithms and developed intelligent disassembly planning employing both human's and robot's capability and strength for an efficient and reliable disassembly process.

6.3 Future Works

In chapter 3, the disassemblability categorisation scores that were used for e a luating the component's handling and operation's comple ity and difficulty could be improved by experimental validations using more EOL product case studies.

Further works can improve the estimation accuracy and explore peg-out-hole with different cross section such as triangle or square in chapter 4. Also, the results of this work can be employed to develop more reliable and efficient automated disassembly systems and provide a model free method. In addition, this method can address the high-level uncertainty in disassembly operations and provide more flexible automated system which is less affected by system or environment errors.

In the chapter 5, peg-out-hole disassembly operation was selected to validate the task classification and allocation. Further disassembly operations such as unscrewing, and component separation could be considered as the basic disassembly tasks.

In addition, some of the relevant future directions are as followings:

- Setting up human-robot collaborative disassembly cell and disassemble the automotive EOL products based on the planning solutions produced by this research methods.
- Investigate different basic disassembly operation such as unscrewing and components separation fundamentally and mathematically to identify relevant characteristics and parameters similar what has been done in this thesis.

- Developing free model method for other disassembly operations using Force/Torque sensor information or vision systems to address high level uncertainty.

References

[1] OECD, Material Resources, “Productivity and the Environment.” Paris: OECD Publishing, 2015.

[2] M. Tennant, “Sustainability and manufacturing.” London: UK Government, Office for Science, Foresight, 2013.

[3] Y.S. Ma. and H.B. Jun, “Disassembly process planning algorithms for end-of-life product recovery and environmentally conscious disposal." International Journal of Production Research, vol. 49, no. 23, pp. 7007-7027, 2007.

[4] J. Manyika, J. Sinclair, et al., Manufacturing the future: The next era of global growth and innovation.” McKinsey Global Institute, 2012.

[5] A. Priyono, W. Ijomah, and U. Bititci, “Disassembly for remanufacturing: A systematic literature review, new model development and future research needs," Journal of Industrial Engineering and Management, vol. 9, no. 4, pp. 899-932, 2016.

[6] D. Parker, K. Riley, S. Robinson, et al., “Remanufacturing market study." Available for download at: https://www.remanufacturing.eu/assets/pdfs/remanufacturing-market-study.pdf. Accessed on 10 April 2020, 2015.

[7] Q. wang Deng, H. lan Liao, B. wen Xu, and X. hui Liu, “The resource benefits evaluation model on remanufacturing processes of end-of-life construction machinery under the uncertainty in recycling price." Sustainability, vol. 9, no. 2, p. 256, 2017.

[8] H. Wang., D. Xiang., et al., “Intelligent disassembly planning: a review on its fundamental methodology." Assembly Automation, vol. 33, no. 1, pp. 78-85, 2013.

[9] Hammond. S. and A. C. Sanderson, “AND/OR graph representation of assembly plans." IEEE Transactions on Robotics and Automation, vol. 6, no. 2, pp. 188-199, 1999.

[10] K. Feldmann, S. Trautner, and O. Meedt, “Innovative disassembly strategies based on flexible partial destructive tools." Annual Reviews in Control, vol. 23, pp. 159 164, 1999.

[11] Y. Tang, M. Zhou, E. Zussman, and R. Caudill, “Disassembly modelling, planning, and application." Journal of Manufacturing Systems, vol. 21, no. 3, pp. 200-217, 2002.

[12] K. Moore, A. Gungor, and S. Gupta, “Petri net approach to disassembly process planning for products with complex and/or precedence relationships." Eur. J. Oper. Res., vol. 135, no. 2, pp. 428-449, 2001.

[13] Y. Tang, M. Zhou, E. Zussman, and R. Caudill, “Disassembly modelling, planning and application: a review." Journal of Manufacturing Systems, vol. 3, pp. 2197- 2202, 2000.

[14] S. Parsa and M. Saadat, “Intelligent selective disassembly planning based on disassemblability characteristics of product components." The International Journal of Advanced Manufacturing Technology, vol. 104, pp. 1769-1783, 2019.

[15] D. Pham, A. Ghanbarzadeh, E. Koc, S. Otri, S. Rahim, and M. Zaidi, “The bees algorithm technical note." Manufacturing Engineering Centre, Cardiff University, UK, p. 1-57, 09 2005.

[16] M. Dorigo, M. Birattari, and T. Stutzle, “Ant colony optimization." IEEE Computational Intelligence Magazine, vol. 1, no. 4, pp. 28-39, 2006. 72

[17] J. Kennedy and R. Eberhart, “Ant colony optimization." Proceedings of ICNN'95 International Conference on Neural Networks, vol. 4, pp. 1942-1948, 1995.

[18] S. Behdad and D. Thurston, “Disassembly process planning trade-offs for product maintenance." Proceedings of ASME International Design Engineering Technical Conference, pp. 427-434, 2010.

[19] Y. Luo, Q. Peng, and P. Gu, “Integrated multi-layer representation and ant colony search for product selective disassembly planning." Computers in Industry, vol. 75, pp. 13-26, 2016.

[20] S. Parsa, M. Saadat, “Intelligent planning using genetic algorithm for automated disassembly." Advances in Manufacturing Technology XXXII, vol. 8, pp. 189-194, 2018.

[21] Z. Zhou, J. Liu, and D. T. Pham., et al., “Disassembly sequence planning: Recent
developments and future trends." Proc IMechE Part B: J Engineering Manufacture, vol. 133, no. 5, pp. 1450-1471, 2019.

[22] Bourjault A., “Contribution to a methodological approach of automated assembly: automatic generation of assembly sequence." PhD Thesis, University of Franche-Comte, Besancon, 1984.

[23] Yeh. WC., “Optimization of the disassembly sequencing problem on the basis of self-adaptive simplified swarm optimization." IEEE T Syst Man Cyb, vol. 42, no. 1, pp. 250-261, 2012.

[24] Song X and Zhou W and Pan X, et al., “Disassembly sequence planning for electro-mechanical products under a partial destructive mode." Assembly Automation, vol. 34, no. 1, pp. 106-114, 2014.

[25] Song X and Pan X, “Electromechanical product disassembly sequence planning based on partial destruction mode." Comput Integr Manuf, vol. 18, no. 5, pp. 927-931, 2012.

[26] A. Lambert, “Disassembly sequencing: a survey," Int. J. Prod. Res., vol. 41, no. 16, p. 3721-3759, 2003.

[27] R. Vigano and G. Gomez, \Automatic assembly sequence exploration without precedence definition." Int. J. Interact. Des. Manuf., vol. 7, p. 79-89, 2013.

[28] J. Li, L. Khoo, and S. Tor, “A novel representation scheme for disassembly sequence planning." Int. J. Adv. Manuf. Technol., vol. 20, no. 8, p. 621-630, 2002.

[29] S. Min, X. Zhu, and X. Zhu, “Mechanical product disassembly and/or graph construction." International Conference on Measuring Technology and Mechatronics Automation, p. 627-631, 2010.

[30] J. Li, L. Khoo, and S. Tor, “An object-oriented intelligent disassembly sequence planner for maintenance." Comput. Ind., vol. 56, no. 7, p. 699-718, 2005.

[31] L. Zhang, Z. Liu, M. Yang, and D. Hu, “Disassembly sequence planning based on interpretative structural model." J. Comput. Aided Des. Comput. Graph., vol. 23, no. 4, p. 667-675, 2011.

[32] T. Cao and A. Sanderson, “Task sequence planning using fuzzy petri nets systems." Man. Cybern., vol. 25, no. 5, p. 755-768, 1995. 73

[33] J. Gao, X. Dong, H. Chen, G. Duan, and J. Wang, “Disassembly and/or graph model for disassembly for recycling." Electron. Environ., vol. 1, p. 54-59, 2003.

[34] H. J. Kim, D. H. Lee, and P. Xirouchakis, “Disassembly scheduling: literature review and future research directions." International Journal of Production Research, vol. 45, no. 18-19, pp. 4465-4484, 2007.

[35] R. JL and C. JA, “Multi-objective partial disassembly optimization based on sequence feasibility." J. Manuf. Syst., vol. 32, no. 1, p. 281-293, 2013.

[36] R. JL and C. JA, “Partial disassembly sequencing considering acquired end-of-life product age distributions." International Journal of Production Research, vol. 52, no. 24, p. 7496-7512, 2014.

[37] Xia K, Gao L, Li WD, et al., “A q-learning based selective disassembly planning service in the cloud based remanufacturing system for WEEE." In: Proceeding of ASME 2014 international manufacturing science and engineering conference, pp. 1-8, 2014.

[38] Kuo. TC, “Waste electronics and electrical equipment disassembly and recycling using petri net analysis: considering the economic value and environmental impacts." Comput Ind Eng, vol. 65, no. 1, pp. 54-64, 2013.

[39] Guo X, Liu S, Zhou MC, et al, “Disassembly sequence optimization for large-scale products with multisource constraints using scatter search and petri nets." IEEE T Cybernetics, vol. 46, no. 11, p. 2435-2446, 2016.

[40] Deng H, Qiang T, Guo X, et al, “Probability evaluation modelling and planning of product disassembly profit." Int J u- e- Serv Sci Technol, vol. 8, no. 9, p. 327-340, 2015.

[41] Dong B and Zhang R, “Disassembly sequence planning based on synchronous net." IEEE Proceeding of the 2013 sixth international symposium on computational intelligence and design, vol. 1, p. 297-300, 2013.

[42] Hsu. HP, “A fuzzy knowledge-based disassembly process planning system based on fuzzy attributed and timed predicate/transition net." IEEE T Syst Man Cy, vol. 47, no. 8, p. 1800-1813, 2017.

[43] Zhao S, Li Y, Fu R, et al., “Fuzzy reasoning petri nets and its application to disassembly sequence decision-making for the end-of-life product recycling and remanufacturing." Int J Comp Integ M, vol. 27, no. 5, p. 415-421, 2014.

[44] Tang Y and Zhou MC, “Learning-embedded disassembly petri net for process planning." Proceeding of the 2006 IEEE international conference on systems, man and cybernetics, vol. 1, p. 80-84, 2006. 74

[45] T. Kuo and M. Wang, “Waste electronics and electrical equipment disassembly and recycling using petri net analysis." The 40th International Conference of Computers and Industrial Engineering, vol. 1, pp. 1-6, 2010.

[46] X. Zha, “An object-oriented knowledge-based petri net approach to intelligent integration of design and assembly planning." Artif. Intell. Eng, vol. 14, no. 1, p. 83-112, 2000.

[47] F. Hsieh, “Robustness analysis of petri nets for assembly/disassembly processes with unreliable resources." Automatica, vol. 42, no. 7, p. 1159-1166, 2006.

[48] F. Giudice, “Disassembly depth distribution for ease of service: a rule-based approach." J. Eng. Des., vol. 21, no. 4, pp. 375-411, 2010.

[49] S. Smith and W. Chen, “Rule-based recursive selective disassembly sequence planning for green design." Adv. Eng. Inf., vol. 25, no. 1, pp. 77-87, 2011.

[50] N. Wu and Q. Peng, “Maintainability evaluation based on the product disassembly analysis." ASME International Design Engineering Technical Conferences and Computers and Information in Engineering Conference, p. 101-109, 2009.

[51] Zhang. CM, “Optimization for disassemble sequence planning of electromechanical products during recycling process based on genetic algorithms." Int J Multim Ubiq Eng, vol. 11, no. 4, pp. 107-114, 2016.

[52] Yang SY, Li JJ, Wen ZJ, et al., “Research on disassembly sequence planning for transfer case of concrete pump." Mach Des Res, vol. 30, no. 5, pp. 106-109, 2014.

[53] X. Song, et al., “Disassembly sequence planning for electro-mechanical products under a partial destructive mode." Assembly Automation, vol. 34, no. 1, pp. 106-114, 2014.

[54] Y. M. Huang and Y. Liao, “Disassembly processes with disassembly matrices and effects of operations." Assembly Automation, vol. 29, no. 4, pp. 348-357, 2009.

[55] Z. Ziqiang, et al., “Research of partial destructive based selective disassembly sequence planning." The Open Mechanical Engineering Journal, vol. 9, pp. 605-612, 2015.

[56] S. Smith and W. Chen, “Multiple-target selective disassembly sequence planning with disassembly sequence structure graphs." Proceedings of the ASME IDETC/CIE, pp. 605-612, 2012.

[57] C. Chung and Q. Peng, “The selection of tools and machines on web-based manufacturing environments." Int. J. Mach. Tools Manuf., vol. 44, no. 2, p. 317-326, 2004. 75

[58] Xia K, Gao L, et al., “A simplified teaching-learning-based optimization algorithm for disassembly sequence planning." Proceeding of the 2013 IEEE 10th international conference on e-business engineering, p. 393-398, 2013.

[59] Xia K, Gao Land et al., “A cloud-based disassembly planning approach towards sustainable management of WEEE." Proceeding of the 2015 IEEE 12th international conference on e-business engineering, p. 203-208, 2015.

[60] Luo Y and Peng Q, “Disassembly sequence planning for product maintenance." Proceeding of the ASME 2012 international design engineering

technical conferences and computers and information in engineering conference, p. 601-609, 2012.

[61] Li HJ, Jiang J and Wang YF, “Disassembly sequence planning based on extended interference matrix and genetic algorithm." Comp Eng Des, vol. 34, no. 3, p. 1064-1068, 2013.

[62] Smith SS and Chen WH, “Rule-based recursive selective disassembly sequence planning for green design." Adv Eng Inform, vol. 25, no. 1, p. 77-87, 2011.

[63] Smith S, Hsu LY and Smith GC, “A novel selective parallel disassembly planning method for green design." J Eng Design, vol. 26, no. 10, p. 283-301, 2015.

[64] Pornsing C. and Watanasungsuit A., “Discrete particle swarm optimization for disassembly sequence planning." IEEE international conference on management of innovation and technology, p. 480-485, 2014.

[65] Lu C and Liu YC, “A disassembly sequence planning approach with an advanced immune algorithm." P I Mech Eng C: J Mec, vol. 226, no. 11, p. 2739-2749, 2012.

[66] W.D. Li, K.Xia, et al, “Selective disassembly planning for waste electrical and electronic equipment with case studies on liquid crystal displays." Robot Cim: Int Manuf, vol. 29, no. 4, p. 248-260, 2013.

[67] Li WD, Xia K, et al, “A distributed service of selective disassembly planning for waste electrical and electronic equipment with case studies on liquid crystal display," Cloud manufacturing distributed computing technologies for global and sustainable manufacturing, p. 23-47, 2013.

[68] Z. C. Chung and Q. Peng, “Evolutionary sequence planning for selective disassembly in de-manufacturing." Int. J. Comput. Integr. Manuf., vol. 19, no. 3, p. 278-286, 2006.

[69] H. Han, J.-M. Yu, and D.-H. Lee, “Mathematical model and solution algorithms for selective disassembly sequencing with multiple target components and sequence dependent setups." Int. J. Prod. Res., vol. 5, no. 16, p. 4997-5010, 2013. 76

[70] P. Pedrazzoli, R. Rinaldi, and C. Boer, “A rule based approach to the gripper selection issue for the assembly process." IEEE International Symposium on Assembly and Task Planning, p. 202-207, 2001.

[71] G. Zhang, K. Deng, Q. Hou, and S. Lai, “Research on assembly modelling and sequence planning based on features." International Technology and Innovation Conference, p. 408-411, 2006.

[72] Wang. H., “Disassembly sequence planning for end-of-life products." Master Thesis, University of Manitoba, Winnipeg, MB, Canada, 2016.

[73] Chen Y. and Chen W., “Product disassembly sequence optimization based on profit probability under uncertain environment." Comput Integr Manuf, vol. 20, no. 4, p. 793-798, 2014.

[74] Zhang Z, Feng Y, et al., “A novel approach for parallel disassembly design based on a hybrid fuzzy-time model." J Zhejiang Univ: Sc A, vol. 16, no. 9, p. 724-736, 2015.

[75] Hui W, Dong X and Duan GH, “A genetic algorithm for product disassembly sequence planning." Neurocomputing, vol. 71, no. 13, p. 2720-2726, 2008.

[76] Pornsing C. and Watanasungsuit A., “Discrete particle swarm optimization for disassembly sequence planning." IEEE international conference on management of innovation and technology, p. 480-485, 2014.

[77] Xing YF, Wang CE and Liu Q, “Disassembly sequence planning based on pareto ant colony algorithm." J Mech Eng, vol. 48, no. 9, p. 186-192, 2012.

[78] Kheder M, Trigui M and Aifaoui N, “Disassembly sequence planning based on a genetic algorithm." P I Mech Eng C: J Mec, vol. 229, no. 12, p. 2281-2290, 2015.

[79] Guo X and Liu S, “A scatter search approach for multi-objective selective disassembly sequence problem." Discrete Dynamics in Nature and Society, vol. 756891, 2014.

[80] Jin G, Li WD et al., “A systematic selective disassembly approach for waste electrical and electronic equipment with case study on liquid crystal display televisions." Proc IMeche, Part B: J Engineering Manufacture, vol. 231, p. 2261-2278, 2017.

[81] Rickli JL and Camelio JA, “Partial disassembly sequencing considering acquired end-of-life product age distributions." Int J Prod Res, vol. 52, no. 24, p. 7496-7512, 2014.

[82] Tian GD, Zhou MC, et al., “Probability evaluation models of product disassembly cost subject to random removal time and different removal labor cost." IEEE T Autom Sci Eng, vol. 9, no. 2, p. 288-295, 2012.

[83] Tian GD, Liu Y, et al., “Evaluation model and algorithm of product disassembly process with stochastic feature." Clean Technol Envir, vol. 14, no. 2, p. 345-356, 2012. 77

[84] Tian GD, Zhou MC and Chu J, “A chance constrained programming approach to determine the optimal disassembly sequence." IEEE T Autom Sci Eng, vol. 10, no. 4, p. 1004-1013, 2013.

[85] A. H. Gandomi, A. Emrouznejad, et al., “Evolutionary Computation in Scheduling.” Hoboken: John Wiley, first ed., 2020.

[86] Kang JG, Lee DH et al., “Parallel disassembly sequencing with sequence dependent operation times." CIRP Ann: Manuf Techn, vol. 50, no. 1, p. 343-346, 2001.

[87] Lambert. AJD, “Optimizing disassembly processes subjected to sequence-dependent cost." Comput Oper Re, vol. 34, no. 2, p. 536-551, 2007.

[88] Gungor A and Gupta SM, “Disassembly sequence plan generation using a branch-and-bound algorithm." Int J Prod Res, vol. 39, no. 3, p. 481-509, 2001.

[89] Kongar E. and Gupta M, “Disassembly sequencing using genetic algorithm." Int J Adv Manuf Technol, vol. 30, pp. 497-506, 2008.

[90] McGovern S and and Gupta M, “alancing method and genetic algorithm for disassembly line balancing." European Journal of Operational Research, vol. 179, no. 3, pp. 692-708, 2007.

[91] Deepak Agrawal, Phani T. et al., “Automated disassembly sequence planning and optimization." Proceedings of the Industrial and Systems Engineering Research Conference, pp. 1-5, 2013.

[92] J. Rocha et al., “Process planning using a genetic algorithm approach." Proceedings of the IEEE International Symposium on Assembly and Task Planning, pp. 1-5, 1999.

[93] J. Mohanta, D. Parhi, and S. Patel, “Path planning strategy for autonomous mobile robot navigation using petri-GA optimization." Comput. Electr. Eng., vol. 37, no. 6, p. 1058-1070, 2011.

[94] Y. Xie, M. Huang, Y. Zhong, and B. Kuang, “Disassembly sequence planning based on the simulated annealing and genetic algorithm." J. Mech. Eng., vol. 1, p. 103-105, 2007.

[95] Chen JZ, Zhang YX and Liao HT, “Disassembly sequence planning based on improved genetic algorithm." Adv Intel Soft Compu, vol. 2, p. 471-476, 2011.

[96] Wu H and Zuo HF, “Using genetic annealing simulated annealing algorithm to solve disassembly sequence planning." J Syst Eng Electron, vol. 20, no. 4, p. 906-912, 2009.

[97] Li J., Tor S. and Khoo L., “A hybrid disassembly sequence planning approach for maintenance." J Comput Inf Sci Eng, vol. 2, no. 1, p. 28-37, 2002. 78

[98] Zhang W, Su Q and Liu P, “Research on virtual maintenance disassembly sequence intelligent planning." J Syst Simu, vol. 25, no. 8, p. 1912-1918, 2013.

[99] Pham DT, Ghanbarzadeh A, et al., The Bees Algorithm Technical Note. Cardiff University: Manufacturing Engineering Centre, first ed., 2005.

[100] Pham D.T. and Castellani M, “The bees algorithm modelling foraging behaviour to solve continuous optimisation problems." Proc. ImechE, Part C, vol. 223, no. 12, pp. 2919-2938, 2009.

[101] Jiayi Liu, Zude Zhou et al., “Robotic disassembly sequence planning using enhanced discrete bees algorithm in remanufacturing." International Journal of Production Research, vol. 59, no. 9, pp. 3134-3151, 2018.

[102] L. Wang, R. Cai, L. Jing, and H. Zhang, “Object-guided ant colony optimization algorithm with enhanced memory for traveling salesman problem." Res. J. Appl. Sci. Eng. Technol., vol. 4, no. 20, p. 3999-4006, 2012.

[103] Liu X, Peng G et al, “Disassembly sequence planning approach for product virtual maintenance based on improved max-min ant system," Int J Adv Manuf Tech, vol. 59, no. 5, p. 829-839, 2012.

[104] Wang JF, Wu X and Fan X, “A two-stage ant colony optimization approach based on a directed graph for process planning." Int J Adv Manuf Tech, vol. 80, p. 839-850, 2015.

[105] Xu J, Zhang SY and Fei SM, “Product remanufacture disassembly planning based on adaptive particle swarm optimization algorithm." J Zhejiang Univ: Sc A, vol. 45, no. 10, p. 1746-1752, 2011.

[106] W. Yeh, “amplified swarm optimization in disassembly sequencing problems with learning effects." Comput. Oper. Res., vol. 39, p. 2168-21772012, 2012.

[107] A. Majkowski, M. Ko lodziej, et al., “Selection of EEG signal features for ERD/ERS classification using genetic algorithms." 18th International Conference on Computational Problems of Electrical Engineering, pp. 1-4, 2017.

[108] Smith S and Hung PY, “A parallel disassembly method for green product design." Proceeding of IEEE international conference on electronics goes green, p. 1-6, 2012.

[109] Smith S, Hsu LY and Smith GC, “Partial disassembly sequence planning based on cost-benefit analysis." J Clean Prod, vol. 139, p. 729-739, 2016.

[110] Ziqiang Z., Guohong D. et al., “Research of partial destructive based selective disassembly sequence planning." The Open Mechanical Engineering Journal, vol. 9, pp. 605-612, 2015.

[111] S. Smith and P. Y. Hung, “A novel selective parallel disassembly planning method for green design." Journal of Engineering Design, vol. 26, p. 283-301, 2015. 79

[112] Kara S., Pornprasitpol. P. and H Kaebernick, “Selective disassembly sequencing: A methodology for the disassembly of end-of-life products." Annals of the CIRP, vol. 55, no. 1, pp. 37-40,2006.

[113] Duflou J. R., Seliger G. et al., “Efficiency and feasibility of product disassembly: a case-based study," CIRP Annals Manufacturing Technology, vol. 57, p. 583-600, 2008.

[114] Renteria A., Alvarez E. et al., “A methodology to optimize the recycling process of WEEE: case of television sets and monitors." International Journal of Advanced Manufacturing Technology, vol. 54, p. 789-800, 2011.

[115] Ryan A., O’Donoghue L. and Lewis H., “Characterising components of liquid crystal displays to facilitate disassembly." Journal of Cleaner Production, vol. 19, p. 1066-1071, 2011.

[116] Sanchez B. and Haas C, “Capital project planning for a circular economy." Journal of Construction Management and Economics, vol. 36, no. 6, p. 303-312, 2018.

[117] Sanchez B. and Haas C, et al., “A selective disassembly multi-objective optimization approach for adaptive reuse of building components." Resources, Conservation and Recycling, vol. 154, p. 104605, 2020.

[118] H. Wang, Q. Peng, et al., “Selective disassembly planning for the end-of-life product," Procedia CIRP, vol. 60, p. 512-517, 2017.

[119] X. Guo, M. Zhou, et al., “Lexicographic multiobjective scatter search for the optimization of sequence-dependent selective disassembly subject to multiresource constraints." IEEE TRANSACTIONS ON CYBERNETICS, vol. 1, pp. 1-11, 2019.

[120] H.-W. Kim, C. Park, and D.H. Lee, “Selective disassembly sequencing with random operation times in parallel disassembly environment." International Journal of Production Research, vol. 56, no. 24, p. 7243-7257, 2018.

[121] ElSayed A., Kongar E., et al, “A robotic-driven disassembly sequence generator for end-of-life electronic products." J Intell Robot Syst, vol. 68, pp. 43-52, 2012.

[122] S. Smith and P.Y. Hung, “A novel selective parallel disassembly planning method for green design." Journal of Engineering Design, vol. 26, no. 10, p. 283-301, 2015.

[123] S. Smith, L.Y. Hsu, and G. C. Smith, “Partial disassembly sequence planning based on cost-benefit analysis." Journal of Cleaner Production, vol. 139, pp. 729-739, 2016.

[124] H. Poschmann, H. B. ggemann, and D. Goldmann, “Disassembly 4.0: A review on using robotics in disassembly tasks as a way of automation." Chem. Ing. Tech, vol. 92, no. 4, p. 341-359, 2020.

[125] S. Yang, et al., “Opportunities for industry 4.0 to support remanufacturing." Appl. Sci., vol. 8, p. 1177, 2018.

[126] J. Li, M. Barwood, and S. Rahimifard, “Robotic disassembly for increased recovery of strategically important materials from electrical vehicles." Robotics and Computer-Integrated Manufacturing, vol. 5, p. 203-212, 2018. 80

[127] R. Knoth, M. Hoffmann, et al., “Intelligent disassembly of electronic equipment." in: Proceedings EcoDesign: Second International Symposium on Environmentally Conscious Design and Inverse Manufacturing, vol. 1, p. 557-561, 2001.

[128] S. Vongbunyong, S. Kara, and M. Pagnucco, “Application of cognitive robotics in disassembly of products." CIRP Ann. Manufact. Technol., vol. 62, no. 1, p. 31-34, 2013.

[129] M. Eugenia, “A generalised approach to the temporal optimisation cycle of an assembly/disassembly mechatronics line served by mobile robot with manipulator." Proceedings of the 33rd Chinese Control Conference, vol. 1, p. 3881-3887, 2014.

[130] C. Kasperzyk, M. koo Kim, et al., “Automated re-prefabrication system for buildings using robotics." Automation in Construction, vol. 83, pp. 184-195, 2017.

[131] F. Torres, P. Gil, et al., “Automatic pc disassembly for component recovery." The International Journal of Advanced Manufacturing Technology, vol. 23, p. 39-46, 2004.

[132] G. Eckerth, T. Honker, et al., “Intelligent disassembly systems for industrial reusing and closed loop economy." IFAC Proceedings Volumes, vol. 31, no. 7, pp. 105-110, 1998.

[133] K. Umeda and A. Tamio, “Three-dimensional vision system for mechanical assembly/disassembly." Advanced Robotics, vol. 11, no. 2, pp. 147-167, 1996.

[134] J. Borras, R. Heudorfer, et al., “The kit swiss knife gripper for disassembly tasks: A multi-functional gripper for bimanual manipulation with a single arm." EEE/RSJ International Conference on Intelligent Robots and Systems (IROS), vol. 1, p. 4590-4597, 2018.

[135] K. Tani, T. Kawamura, and M. Owaki, “Task programming for robots using multimode control - preparation of modes to generate motions for disassembly task." IFAC Proceedings Volumes, vol. 42, no. 16, pp. 143-148, 2019.

[136] Puente S., Torres F. and Díaz C., “Assembly/disassembly strategies for service applications." IFAC Proceedings Volumes, vol. 41, no. 2, pp. 15805-15810, 2008.

[137] I. Aguinaga, D. Borro, and L. Matey, “Path-planning techniques for the simulation of disassembly tasks." Assembly Automation, vol. 27, no. 3, pp. 207-214, 2007.

[138] L. C. Carvalho, “Handbook of Research on Entrepreneurship and Marketing for Global Reach in the Digital Economy.” ABSCA, Hershey: IGI Global, 2019.

[139] H. Levesque and G. Lakemeyer, “Cognitive robotics." Foundations of Artificial Intelligence, vol. 3, pp. 869-886, 2008. 81

[140] S. Sardina., D. Giacomo, and et al., “On ability to autonomously execute agent programs with sensing." The 4th International Workshop on Cognitive Robotics, vol. 1, pp. 1-8, 2004.

[141] Kim BH, Yi BJ, et al., “Stiffness analysis for effective peg-in/out-hole tasks using multi-fingered robot hands." IEEE/RSJ International Conference on Intelligent Robots and Systems, vol. 1, pp. 1-8, 2000.

[142] R. Usubamatov, K. Leong, et al., “Analyses of peg-hole jamming in automatic assembly machines." Assembly Automation, vol. 31, no. 4, pp. 358-362, 2011.

[143] K. Zhang, J. Xu, et al., “Jamming analysis and force control for flexible dual peg-in-hole assembly." IEEE Transactions on Industrial Electronics, vol. 66, no. 3, pp. 358-362, 2011.

[144] Z. Yongquan, L. Hong, et al., “Peg-hole disassembly using active compliance." The Royal Society. Collection, vol. 1, no. 1, 2019.

[145] X. Zhang, Y. Zheng, et al., “Peg-in-hole assembly based on two-phase scheme and F/T sensor for dual-arm robot." Sensors, vol. 17, no. 9, pp. 1-8, 2004.

[146] H. A. ElMaraghy, “Changeable and Reconfigurable Manufacturing Systems.” Springer Series in Advanced Manufacturing, Cardiff: Springer, 2009.

[147] I.W. Kim, D.J. Lim, et al., “Active peg-in-hole of chamferless parts using force/moment sensor." IEEE/RSJ International Conference on Intelligent Robots and Systems, vol. 1, no. 1, 1999.

[148] M. W. Abdullah, H. Roth, et al., “Force/torque data modelling for contact position estimation in peg-in-hole assembling application." MATEC Web of Conferences, vol. 28, no. 1, 2015.

[149] Y. Wang, P. Wang, et al., “Contact force/torque prediction and analysis model for large length-diameter ratio peg-in hole assembly." IEEE International Conference on Robotics and Biomimetics, vol. 1, no. 1, 2018.

[150] T. Tang, H.C. Lin, et al., “Autonomous alignment of peg and hole by force/torque measurement for robotic assembly." IEEE International Conference on Automation Science and Engineering (CASE), vol. 1, no. 1, 2016.

[151] K. Zhang, M. Shi, et al., “Force control for a rigid dual peg-in-hole assembly." Assembly Automation, vol. 37, no. 2, pp. 200-207, 2017.

[152] F. Dietrich, D. Buchholz, et al., “On contact models for assembly tasks: Experimental investigation beyond the peg-in-hole problem on the example of force torque maps." IEEE/RSJ International Conference on Intelligent Robots and Systems, vol. 1, pp. 2313-2318, 2010.

[153] W. Newman, Y. Zhao, and Y.-H. Pao, “Interpretation of force and moment signals for compliant peg-in-hole assembly." IEEE International Conference on Robotics and Automation, vol. 1, p. 571- 576, 2001. 82

[154] F. Dietrich, F. Wobbe, et al., “Enhancements of force-torque map based assembly applied to parallel robots." IEEE International Conference on Industrial Technology, vol. 1, pp. 507-512, 2010.

[155] Jasim I., Plapper P., et al., “Contact-state modelling in force-controlled robotic peg-in-hole assembly processes of flexible objects using optimised gaussian mixtures." Part B: Journal of Engineering Manufacture, vol. 231, no. 8, p. 1448-1463, 2017.

[156] Jasim I., Plapper P., “Contact-state monitoring of force-guided robotic assembly tasks using expectation maximization-based gaussian mixtures models." Int J Adv Manuf Technol, vol. 73, p. 623-633, 2014.

[157] Ren Y, Zhang C, Zhao F, Xiao H, Tian G, “An asynchronous parallel disassembly planning based on genetic algorithm.” Eur J Oper Res 269(2):647–660, 2018.

[158] Zhang XF, Zhang SY, “Product cooperative disassembly sequence planning based on branch-and-bound algorithm.” Int J Adv Manuf Technol 51(9-12):1139–1147, 2010

[159] Oyedepo SO, Olayiwola FR, “A study of implementation of preventive maintenance programme in Nigeria power industry–Egbin thermal power plant, case study.” Energy Power Eng 3(3):207–220, 2011.

[160] Wang L, Yu ZW, Han Q, Guo B, Xiong HL, “Multi-objective optimization based allocation of heterogeneous spatial crowdsourcing tasks.” IEEE Trans Mob Comput 99:1–14, 2017.

[161] Tian, Y., Zhang, X., Liu, Z., Jiang, X., & Xue, J., “Product cooperative disassembly sequence and task planning based on genetic algorithm.” The International Journal of Advanced Manufacturing Technology, 105(5-6), 2103-2120, 2019.

[162] Tsarouchi, Panagiota, Sotiris Makris, and George Chryssolouris, “Human-Robot Interaction Review and Challenges on Task lanning and rogramming.” International Journal of Computer Integrated Manufacturing 29 (8): 916–931, 2016.

[163] alik, A. A., & Bilberg, A., “Comple ity -based task allocation in human-robot collaborati e assembly.” ndustrial ob ot, Vol. 46 o . 4, pp. 471-480, 2019.

[164] Quan Liu, Zhihao Liu, Wenjun Xu, Quan Tang, Zude Zhou & Duc Truong Pham, “Human-robot collaboration in disassembly for sustainable manufacturing.” International Journal of Production Research, 57:12, 4027-4044, 2019.

[165] 157A. Desai and A. Mital, “Evaluation of disassemblability to enable design for disassembly in mass production." International Journal of Industrial Ergonomics, vol. 32, p. 265-281, 2003.

[166] Xuhui Xia, Huixian Zhu, et al., “3D-based multi-objective cooperative disassembly sequence planning method for remanufacturing.” The nternational Journal of Advanced Manufacturing Technology, 106: 4611–4622 2020.

[167] ISO 10218-1: Robots and Robotic Devices - Safety Requirements for Industrial Robots - Part 1: Robots, 2011.

Apendix A. Publications by the author

Peer-reviewed journal papers

1- **S. Parsa** and . Saadat, “ ntelligent selecti e disassembly planning based on disassemblability characteristics of product components." *The International Journal of Advanced Manufacturing Technology,* vol. 104, pp. 1769-1783, 2019.

2- **S. Parsa** and M. Saadat, “Contact States Estimation of Automated Peg-Out-Hole Disassembly Operation Using Force/Torque Sensor.” *IEEE Transactions on Mechatronics,* Under revision.

3- **S. Parsa** and M. Saadat, “Human-robot collaboration disassembly planning for end-of-life product disassembly process.” *Robotics and Computer-Integrated Manufacturing,* Under revision.

Peer-reviewed conference papers

1- **S. Parsa**, . Saadat, “ ntelligent planning using genetic algorithm for automated disassembly." *Advances in Manufacturing Technology XXXII*, vol. 8, pp. 189-194, 2018.